

PhD
Thesis

Investigation of Rut Patterns In Different Terrain Conditions
for Vehicular Movements

Manoj Kumar Kalra

June
2024

INVESTIGATION OF RUT PATTERNS IN DIFFERENT TERRAIN CONDITIONS FOR VEHICULAR MOVEMENTS

A Thesis Submitted
In Partial Fulfillment of the Requirements
for the Degree of

DOCTOR OF PHILOSOPHY
by

MANOJ KUMAR KALRA
(2K16/PHD/CE/01)

Under the Supervision of

Prof. A. Trivedi
Delhi Technological University
DTU, Delhi

Prof. S. K. Shukla
Edith Cowan University
ECU, Australia



Department of Civil Engineering

DELHI TECHNOLOGICAL UNIVERSITY
(Formerly Delhi College of Engineering)
Shahbad Daultapur, Main Bawana Road, Delhi-110042, India
June 2025

DELHI TECHNOLOGICAL UNIVERSITY

(Formerly Delhi College of Engineering)

Shahbad Daulatpur, Main Bawana Road, Delhi-110042, India

CERTIFICATE OF THESIS SUBMISSION FOR EVALUATION

(Submit in Duplicate)

1. Name: ...Manoj Kumar Kalra
2. Roll No.: ...2K16/PHD/CE/01
3. Thesis title: Investigation of Rut Patterns in Different Terrain Conditions for Vehicular Movements
4. Degree for which the thesis is submitted: Doctor of Philosophy (PhD)
5. Faculty of the University to which the thesis is submitted: Faculty of Civil Engineering
6. Thesis Preparation Guide was referred to for preparing the thesis. YES ☒ NO ☐
7. Specifications regarding thesis format have been closely followed. YES ☒ NO ☐
8. The contents of the thesis have been organized based on the guidelines YES ☒ NO ☐
9. The thesis has been prepared without resorting to plagiarism. YES ☒ NO ☐
10. All sources used have been cited appropriately. YES ☒ NO ☐
11. The thesis has not been submitted elsewhere for a degree. YES ☒ NO ☐
12. Submitted 2 spiral bound copies plus one CD. YES ☒ NO ☐

(Signature of Candidate)

Name(s): Manoj Kumar Kalra

Roll No: 2K16/PHD/CE/01

INVESTIGATION OF RUT PATTERNS IN DIFFERENT TERRAIN CONDITIONS FOR VEHICULAR MOVEMENTS

**A Thesis Submitted
In Partial Fulfillment of the Requirements for the
Degree of**

DOCTOR OF PHILOSOPHY

by

**MANOJ KUMAR KALRA
(2K16/PHD/CE/01)**

Under the Supervision of

**Prof. A. Trivedi
Delhi Technological University
DTU, Delhi**

**Prof. S. K. Shukla
Edith Cowan University
ECU, Australia**



Department of Civil Engineering

**DELHI TECHNOLOGICAL UNIVERSITY
(Formerly Delhi College of Engineering)
Shahbad Daultpur, Main Bawana Road, Delhi-110042, India**

June 2025

ACKNOWLEDGEMENT

I would like to express my deepest gratitude to my supervisor, **Prof. Ashutosh Trivedi of DTU, Delhi and Dr Sanjay Kumar Shukla of ECU Australia** for their invaluable support, guidance and encouragement throughout this research work. Their valuable expertise and constructive feedback have been instrumental in shaping the research work presented in this thesis.

I am grateful to Prof. K.C Tiwari, Head of the Civil Engineering Department, DRC Chairman and DRC committee members for their insightful comments, constructive criticism, and dedication for ensuring the coherence of this work.

Heartfelt thanks to express my profound gratitude to all the students of ITS and SD Lab who generously extended all possible support and valuable time.

Deep gratitude is due towards Prof Rohit Kumar of DTU and Ms Upika Mittal of DGRE who spent their valuable time in extending their valuable guidance and support at every moment.

Finally, the unwavering support, encouragement and understanding by my family throughout this journey remained a constant source of motivation and strength for undertaking this research work.

I wholeheartedly acknowledge the support and encouragement by all.



(Manoj Kumar Kalra)



Delhi Technological University
Shahbad Daulatpur, Bawana Road, Delhi-110042

DECLARATION

I, **Manoj Kumar Kalra**, hereby declare that this thesis entitled "**Investigation of Rut Patterns in Different Terrain Conditions for Vehicular Movements**" is entirely my research work except where otherwise acknowledged. The research work has been accomplished under the guidance of Prof. Ashutosh Trivedi and Prof. Sanjay Kumar Shukla. The data, figures, and results presented in this thesis are authentic and accurately represent the findings of my research. The present research work has not been submitted, either in whole or in part, for any other degree or qualification at this or any other institution.

New Delhi

A handwritten signature in blue ink, appearing to read "Manoj K. Kalra", is positioned above the printed name.

Manoj Kumar Kalra
Roll No. 2k16/PhD/CE/01



Delhi Technological University
Shahbad Daulatpur, Bawana Road, Delhi-110042

CERTIFICATE

Certified that **Manoj Kumar Kalra (2K16/PHD/CE/01)** has carried out his research work presented in this thesis entitled **“Investigation of Rut Patterns in Different Terrain Conditions for Vehicular Movements”** for the award of **Doctor of Philosophy** from the Department of Civil Engineering, Delhi Technological University, Delhi, under our supervision. The thesis embodies results of original work, and studies are carried out by the student himself and the contents of the thesis do not form the basis for the award of any other degree to the candidate or to anybody else from this or any other University/Institution.

A blue ink signature of Prof. S.K. Shukla.

(Prof. S.K. Shukla)
ECU, Australia

A blue ink signature of Prof. A. Trivedi.

(Prof. A. Trivedi)
DTU, Delhi

Date: Jun 2025

Investigation of Rut Patterns in Different Terrain Conditions for Vehicular Movements

Manoj Kumar Kalra

ABSTRACT

The movement of vehicles on an unpaved terrain is a common requirement in many fields including agriculture, forestry, automobile, planetary rovers and defence. Other than surface topographical features, the most important parameter to the movement of vehicles is the underlying soil condition. Acquiring the data by conventional methods is laborious and cumbersome task. The alternative means have therefore been explored by various researchers. One of the most effective ways employed for analysing the prevalent soil condition is by monitoring the rut formed by vehicular movement in the area. Many soil parameters like soil condition, its gradation, moisture content, soil strength etc. impact the vehicular rut. Vehicle loading conditions like tyre size, vehicle weight, its speed, curvatures, and repeated passes also influence the rut shapes. Although many parametric studies have been conducted to characterize and model the rut shapes based on all these, yet several aspects are still to be studied.

One aspect of the issues pertains to modelling and evaluation of rut depth. Most of the literature focuses on evaluating the rut depth. Certain issues are however typical in different scenarios which need to be addressed. The rut in desertic terrain has been observed to get filled by the sand pouring from sides. Similarly, the rut profile has been observed to become eccentric on the curves. This aspect demands for mapping the shapes of rut profiles in different terrain-vehicle running conditions. Moreover, with advent of technology, the rut profile measurement tools too have moved from manual to advanced laser-based sensors. The laser profiler on one hand measures the rut profile with precision, however, it needs heavy memory devices for storage and interpretation of data. The optimization aspect of rut profile data needs to be explored for efficient movement decisions. Further, a number of models are developed that try to characterize the influence of different causative factors on rut. While selection of appropriate model is one aspect, the overall impact of all causative factors on the maximum soil distress levels in any area is important to be studied for ascertaining the suitability of the terrain for any emergency movement. Another aspect of rutting research pertains to addressing the issues in wider spatial domain. While evolving suitable spatial models governing trafficability potential is an important aspect, the validation of interpreted information is another important area needing attention. Here, identification of track impressions that look like edges in coarse resolution images can provide useful information about identifying the trafficable zones. Identifying the tracks manually being tedious, alternate means need to be explored. Moreover, the rut tracks formed by the leading vehicle is said to provide useful information for the rut following robotic vehicles,

defence, and forestry. The delineation of track impressions from surrounding terrain and visibility conditions is an important consideration needing attention.

In this research work, rut has been investigated from different perspectives. One aspect focuses on the experimental studies of rut profiles in different fields while the other one tries to address the issue of delineation of rut tracks by collating various image processing techniques. In the field based experimental studies, various shapes of rut profiles on different types of soil and vehicle running conditions were investigated. The rut profile data was captured using both manual and laser-based systems. The most common rut shapes observed in field are identified and grouped in different categories. Attempt was then made to devise better ways for optimal storage of most common rut profiles. By using the proposed mathematical formulations, an additional compression of more than 80% over the conventional compression techniques could be achieved on straight patches and 71% on turnings. In another experimental study, soil distress level was investigated using multiple vehicular passes on varied terrain conditions. This study paves the way for identifying and mapping the unpaved areas suitable for planning emergency support. Another part of study focused on visual enhancement and detection of rut-based track impressions. In order to detect edges like track features in satellite images, various edge detection algorithms are explored. The comparative study of different algorithms revealed that the Canny Edge detection method gives relatively better results. Further studies are however needed for improved detection and delineation of tracks. It is observed that the tracks formed by vehicular rut impressions appear like thin edges in images of coarse-resolution. However, when using the fine resolution images, the same features appear like elongated areas. In such a scenario, the edge detection filters and even the conventional contrast enhancement techniques are able to delineate these features to a limited extent. The role of texture of these tracks that can differentiate these tracks from their surroundings has been explored in this study. Gray level co-occurrence matrix (GLCM) which is a texture measurement technique has been employed here. To compare the effectiveness of various techniques in enhancement of track contrast in a given surrounding, a new quantitative track index (TI) based measure has been proposed in this study. Here, the effectiveness of technique in enhancing the track contrast has been evaluated. Various forms of track indices as proposed in this study have been compared. The proposed track index effectively sorts correctly the contrast images to the level of 88%. The proposed track index-based technique is seen as effective means for sorting the images based on track contrast. This method can bring in improved fidelity of decisions for the sustainable operations. The study was extended further and a new technique based on track index has been developed that is seen as adaptive for enhancing the track contrast in a given surrounding.

The outcome of above research has been presented in various chapters of this thesis. The approach of bringing in optimization in data storage is a step towards making efficient decisions about trafficability condition of the terrain. The evaluation of maximum soil distress level under different dynamic conditions sets another way of identifying and mapping the safe trafficable zones for planning emergency

movement. The image analysis-based improved identification of rut tracks is an important contribution in visual analytics-based systems on-board vehicles. The mobility decisions could be made better and efficient using this track index based technique. The edge detection algorithm could set the way for improved identification of unpaved tracks in satellite images. Further research is however needed for automated delineation of rut tracks for inferring trafficable zones. The machine learning approach could be explored here.

LIST OF PUBLICATIONS

The list of publications along with Journal/Conference details are given below:

1. Kalra, M. K., Trivedi, A. and Shukla, S. K., 2023. Non-Linear Regression Analysis of Rut Profile Data for Optimal Data Storage and Efficient Terrain Condition Analysis. *IEEE Geoscience and Remote Sensing Letters*. <https://doi.org/10.1109/LGRS.2023.3303134> (**SCIE, IF: 4.8**)
2. Kalra, M. K., Shukla, S. K. and Trivedi, A., 2023. Track-Index-Guided Sustainable Off-Road Operations Using Visual Analytics, Image Intelligence and Optimal Delineation of Track Features. *Sustainability*, 15(10), 7914. <https://doi.org/10.3390/su15107914> (**SCIE, IF: 3.9**)
3. Kalra, M. K., Trivedi, A. and Shukla, S. K., 2023. Adaptive Technique for Contrast Enhancement of Leading Vehicle Tracks. *Defence Science Journal*, 73(6). <https://doi.org/10.14429/dsj.73.18765> (**SCI, IF: 0.9**)
4. Kalra, M. K., Trivedi, A. and Shukla, S. K., 2023. Different Edge Detection Algorithms in Identification of Tracks in Images. 4th International Sustainability Conference on Health, Safety, Fire and Environmental Advances (**HSFEA-2023**) organised by UPES Dehradun, India.
5. Kalra, M. K., Trivedi, A. and Shukla, S. K., 2023. Soil Distress Studies in Managing Emergency Support to the Flood Impacted Areas. 6th World Congress on Disaster Management (**WCDM-2023**), organised by Graphic Era University, Dehradun, India

TABLE OF CONTENT

<u>S.</u>	<u>DESCRIPTION</u>	<u>PAGE</u>
	ACKNOWLEDGEMENTS	i
	DECLARATION	ii
	CERTIFICATE	iii
	ABSTRACT	iv
	LIST OF PUBLICATIONS	vii
	TABLE OF CONTENT	viii
	LIST OF TABLES	xi
	LIST OF FIGURES	xii
	LIST OF SYMBOLS	xiv
1.	CHAPTER-1: INTRODUCTION	1
1.1.	General	1
1.2.	Vehicular Movement on Unpaved Terrain	1
1.3.	Relevance of Rut Based Terrain Investigation	2
1.4.	Various Tools and Techniques for Rut Investigations	3
1.5.	Research Gaps in Literature	4
1.6.	Research Methodology to Address the Research Problems	6
1.7.	Objectives of the Proposed Research	8
1.8.	Structure of the Thesis	8
1.9.	Benefits of the Proposed Rut Studies	9
1.10.	References	10
2.	CHAPTER-2: LITERATURE REVIEW	13
2.1.	Modelling the Impact of Various Influencing Factors on Rut	13
2.2.	Various Tools and Techniques Used for Rut Investigations	17
2.3.	Analysis of Spatial Data to Infer Features Influencing Rut	18
2.4.	Various Techniques Used for Enhancement of Features in Images	19
2.5.	Conclusion	22
2.6.	References	22
3.	CHAPTER-3: OPTIMAL DATA STORAGE OF COMMONLY OBSERVED RUT SHAPES USING PROPOSED MATHEMATICAL FORMULATIONS	28
3.1.	Introduction	28
3.2.	Field Observation of Rut Profiles	29
3.3.	Development of Mathematical Formulations for Rut Profile	32
3.4.	Results and Discussion	34

3.5. Conclusion and Suggestions for Further Work	39
3.6. References	40
4. CHAPTER-4: EXPERIMENTAL INVESTIGATION OF SOIL MOISTURE AND NUMBER OF PASSES IN IDENTIFYING THE MAXIMUM SOIL DISTRESS LEVEL FOR EMERGENCY MOVEMENTS	42
4.1. Introduction	42
4.2. Materials and Methods	46
4.3. Study Area	47
4.4. Results and Discussion	47
4.5. Conclusion	49
4.6. References	50
5. CHAPTER-5: INVESTIGATION OF VARIOUS EDGE DETECTION ALGORITHMS IN IDENTIFICATION OF PATHS FORMED BY VEHICLE RUT	53
5.1. Introduction	53
5.2. Objective	56
5.3. Methodology	56
5.4. Result and Discussion	56
5.5. Conclusions	62
5.6. References	63
6. CHAPTER-6: EVALUATING THE POTENTIAL OF DIFFERENT TEXTURE MEASURES IN ENHANCING THE RUT TRACKS	65
6.1. Introduction	65
6.2. Review of Past Works	67
6.3. Tools and Methodology Used	68
6.3.1. Using Some Linear and Non-Linear Transformation Functions	68
6.3.2. Using Spatial Filters	70
6.3.3. Using Texture Measures	71
6.4. Results	72
6.4.1. Quantification of Track Contrast Using Proposed Track Indices	75
6.4.1.1. Based on Difference in Mean Values	77
6.4.1.2. Based on Ratio of Mean Values	77
6.4.1.3. Based on Normalized Difference in Mean Values	77
6.4.1.4. Based on the Ratio of Coefficient of Variance	78
6.4.2. Analysis of Track Contrast Data	79
6.5. Discussion	82
6.6. Conclusions	85

6.7. References	85
7. CHAPTER-7 : AN ADAPTIVE TECHNIQUE TO SELECT THE MOST EFFECTIVE RUT ENHANCEMENT MEASURE IN A GIVEN SURROUNDING	89
7.1. Introduction	89
7.2. Related Work	90
7.3. Methodology Used	91
7.4. Various Edge Enhancement and High-Frequency Filters	91
7.5. Image Texture Measures	92
7.6. Data and Tools Used	94
7.7. Image Analysis and Results	96
7.8. Track Index based Optimal Selection	98
7.9. Discussion	102
7.10. Conclusion	103
7.11. Scope for Future Studies	104
7.12. References	104
8. CHAPTER-8: CONCLUSION, FUTURE SCOPE AND SOCIAL IMPACT	108
8.1. Summary of Work	108
8.2. Conclusions Drawn from Rut Studies	110
8.3. Future Research Trajectories	113
8.4. Social Impact and Contributions to Knowledge	114
9. PLAGIARISM VERIFICATION	117
10. BRIEF PROFILE	119

LIST OF TABLES

Table No.	Description
Table 3.1	Depth to width ratio of rut under different soil and movement conditions
Table 3.2	Regression fit results for rut profile in different test cases
Table 6.1	Computation of track index (TI) for quantifying image contrast using different indices
Table 6.2	Computation of effectiveness of different track indices
Table 7.1	Computation of Track Index (TI) quantifying image contrast

LIST OF FIGURES

Fig. No.	Description
Fig. 3.1	Different shapes of Rut Profiles as observed in the field: a) Shallow rut in alluvial soils of medium consistency b) Deep rectangular rut on soils of low consistency c) Conical rut profile on frictionless soils of deserts d) Asymmetric rut shape created by vehicles on turnings
Fig. 3.2	Shapes of typical rut profile data considered for evaluation of proposed mathematical formulations
Fig. 3.3	Different shapes as generated using proposed mathematical formulations by varying the input parameters to match the commonly observed rut shapes in various terrain types
Fig. 3.4	Typical Regression Fit curves on the rut Profile data of medium consistency soil
Fig. 4.1	The study conducted under varied moisture conditions 1) Dry Area 2) Slightly Moist 3) Moist area and 4) Flooded area
Fig. 4.2	Rut profile created by vehicle on soil a) Along the wheel track b) Across the wheel track
Fig. 4.3	Cone Index variation under different moisture conditions in study area
Fig. 4.4	Rut depth after 1 and 'n' passes on different terrain features
Fig. 5.1	Original Image of the terrain around Chandigarh
Fig. 5.2	Histogram of the image indicating the dynamic range of intensity values
Fig. 5.3	Original image superimposed by Sobel edges
Fig. 5.4	Original image superimposed by Prewitt edges
Fig. 5.5	Original image superimposed by Roberts edges
Fig. 5.6	Original image superimposed by Zerocross edges
Fig. 5.7	Original image superimposed by Canny edges
Fig. 5.8	Original image superimposed by proposed edge filter
Fig. 5.9	Original image compared with Canny Edges

- Fig. 6.1 Multiscale images of roads: (a) original in gray tone indicating coarse-, medium- and fine-scale images (source: Google Earth) enhanced using (b) Sobel edge detection filter, (c) Laplacian filter and (d) high-pass filter. (Images created using SNAP 8.0 software)
- Fig. 6.2 Multiscale images of roads indicating coarse-, medium- and fine-scale images enhanced using (a) homogeneity, (b) energy, (c) contrast and (d) entropy as the texture measures. (Images created using SNAP 8.0 software)
- Fig. 6.3 Effect of different texture measures on tracks in desertic terrain: (a) original gray image and texture images created using filters of (b) energy, (c) entropy, (d) GLCM mean, (e) GLCM variance and (i) homogeneity image. (Images created using SNAP 8.0 software)
- Fig. 6.4 Location of pixels chosen for comparing the contrast in track areas with reference to its surroundings (Image created using SNAP 8.0 software)
- Fig. 6.5 Process flow to generate image with maximum track index outside of using various contrast enhancement measures
- Fig. 6.6 Different contrast enhancement measures of leading vehicle tracks: (a) original gray image of the tracks and images created using (b) Sobel edge detection filter, (c) Laplacian edge filter, (d) non-linear maximum filter and (e) high-pass filter, and using texture measures of (f) energy, (g) entropy, (h) contrast and (i) homogeneity. (Images created using SNAP 8.0 software)
- Fig. 7.1 a) Multi-resolution images of tracks (Source: Google, Maxar Technologies). Result after convolving images b) using Sobel edge detection filter c) using second-order Laplacian filter and d) using the high-pass filter.
- Fig. 7.2 Result of GLCM texture analysis on the multi-resolution images a) Contrast Image b) Entropy Image c) Energy Image and d) Variance
- Fig. 7.3 Field Image of vehicle tracks impressions of leading vehicle
- Fig. 7.4 a) Images of Vehicle Track impressions as observed in vehicle running condition a) In Original Gray tone and Using b) High-Pass filter c) Laplacian Filter d) Sobel Edge detection filter and GLCM measures of e) Dissimilarity f) Contrast g) Entropy h) Correlation i) Mean filter
- Fig. 7.5 Location of pixels chosen for comparing the contrast of track areas with reference to its surroundings

LIST OF SYMBOLS

Symbol	Description
α	Concentration factor that depends on soil homogeneity
β	Angle made by the edge of circular plate with central axis
Γ	Gamma Function sensitive to highlight desired gray levels of image
Δ	Deflection of loaded tire (m)
θ_s	Static contact angle of wheel (deg)
P	Density of the soil (kN/m ³)
σ_h	Stress at vertical depth h_v along centre of the circular plate (kPa)
σ_i	Standard deviation of column i
σ_j	Standard deviation of column j
∇f	Gradient of image $f(x,y)$
$\nabla^2 f$	Laplacian of image $f(x,y)$
*	Convolution- $Conv(w,f)$ of the filter $w(s,t)$ with the image $f(x,y)$
μ_i	Mean value of row i
μ_j	Mean value of column j
a	A multi-pass coefficient
a_i	Coefficient of equation corresponding to i^{th} term ($i=1,n$)
a_n, b_n	n^{th} Constant of equation
b	Breadth of pressure plate/ Unloaded width of tyre (m)
B'	Width of Rut profile
c	coefficient of cohesion of soil (kPa)
C	Compression Ratio
CI	Cone Index of soil (kPa)
CIW_1	Cumulative Impact Width after first pass (m)
CIW_n	Cumulative Impact Width after nth pass (m)
c_s	Scaling constant for output values to be in a desired dynamic range
CV	Coefficient of Variance
d	Tyre unloaded diameter (m)
d'	Rut depth at different locations 'b' across the rut profile
$f(x,y)$	Array of pixels in the original image
f_{max}	Maximum gray values of the image pixels
f_{min}	Minimum gray values of the image pixels
$g(x,y)$	Array of pixels in the transformed image
$GLCM$	Gray level Co-occurrence Marix
g_x	First derivative or gradient of the image $f(x,y)$ in x direction

g_y	First derivative or gradient of the image $f(x,y)$ in y direction
h	Sinkage of wheel / plate (m)
$h(r_k)$	Histogram of image representing number of pixels for different gray levels
$h(\theta)$	Wheel sinkage at an arbitrary wheel angle θ with vertical (m)
h'	Section height of unloaded tyre (m)
h_d	Dynamic sinkage of wheel (m)
h_s	Static sinkage (m)
h_u	Height of unloaded section of tyre (m)
h_v	Depth of the circular plate (m)
k	Soil stiffness constant for sinkage (kN/m^{2+n})
k_c	Cohesive modulus of terrain deformation (kN/m^{n+1})
k_c'	Cohesive modulus of sinkage deformation, dimensionless
k_ϕ	Frictional modulus of terrain deformation (kN/m^{n+2})
k_ϕ'	Frictional modulus of sinkage deformation, dimensionless
L	Quantization level indicating number of gray levels in the image
LOG	Laplacian of Gaussian
n	Exponent of terrain deformation
N	Number of Wheel passes
n_l	Number of selected pixels in the off-track zones to the left of track
n_1	Number of selected pixels in off-track zones to the left of left track
n_2	Number of selected pixels on the track
n_2	Number of selected pixels on the left track
n_3	Number of selected pixels in the off-track zones to the right of track
n_3	Number of selected pixels between the two tracks
n_4	Number of selected pixels on the right track
n_5	Number of selected pixels in off-track zones to the right of right track
N_{CI}	Wheel Numeric
NGP	Nominal Ground Pressure (kPa)
n_k	Number of pixels in the image with a gray level of r_k
p	Vertical average contact pressure (kPa)
$p(h)$	Stress at sinkage level h (kPa)
$p(i,j)$	Probability value recorded for the co-occurrence of cells i,j in GLCM matrix
P_{OT}	Pixels in the off-track
P_T	Pixels on-track
r	Wheel radius (m)
r'	Input pixel values

R^2	Co coefficient of determination / Goodness of fit
RCI	Rating cone index (kPa)
r_k	k^{th} kth gray level in the dynamic range of gray levels
S	Slip of wheel in decimal
s'	Output pixel values
TI	Track Index for comparing the track contrast
$TI(CV)$	Track Index based on ratio of Coefficient of variance
$TI(D)$	Track Index based on difference in mean value of statistical measure
$TI(ND)$	Track Index based on Normalised difference of Mean values
$TI(R)$	Track Index based on Ratio of mean value of statistical measure
TR	Track Ratio for comparing the track contrast
W	Vertical load of wheel in kN
$w(s,t)$	Filter of dimension (s x t)
X	Statistical measure of image texture
X_l	Gray values of selected pixels in the off-track zones to the left of track
x_1	Gray values of selected pixels in off-track zones to the left of left track
X_2	Gray values of selected pixels on the track
x_2	Gray values of selected pixels on the left track
X_3	Gray values of selected pixels in the off-track zones to the right of track
x_3	Gray values of selected pixels between the two tracks
x_4	Gray values of selected pixels on the right track
x_5	Gray values of selected pixels in off-track zones to the right of right track
x^i	i^{th} Degree of polynomial variable in x
X_{max}	Minimum value of selected pixels for the given statistical measure
X_{min}	Minimum value of selected pixels for the given statistical measure
y	Rut depth at point 'x' across the rut profile
Y	Normalized value of Statistical measure X
z	Sinkage Distance into the soil (mtr)
Z_1	Sinkage after one loading (m)
Z_n	Sinkage after n loadings (m)
Z_{n-1}	Wheel Sinkage after n-1 loadings (m)

CHAPTER - 1

INTRODUCTION

This chapter introduces to the literature relevant to highlight the importance of rut studies for vehicular movements over unpaved terrain. It also highlights the gaps in the study, the research problems, the proposed research methodology and the objectives set for this research work. The structure and organisation of the thesis, the benefits to practitioners, researchers and society in general are also given in this chapter.

1.1 General

The movement of vehicles on an unpaved terrain is a common requirement in many industrial applications. During world war II, in 1945 the poor performance of army vehicles led to beginning the detailed studies at Waterways Experiment Station (WES) by US army for evaluating the trafficability potential of different areas. (Willoughby and Turnage, 1988). Today, it has been the subject matter for evaluation by many researchers in agriculture, forestry, automobile industry, robotics, planetary explorations and defence (Borges et al., 2022).

1.2 Vehicular Movement on Unpaved Terrain

In forestry, timber logging operations are quite common and soil disturbance is an unavoidable in such operations. The severity of disturbance impacting the soil conditions for growth of plants in these areas varies as per prevalent conditions. Good planning and practices of soil-vehicle matching can limit such damages (Ares et al., 2005). The studies related regarding devising such means and models are therefore continued for better understanding of soil wheel interaction. Marra et al., 2022 studied the impact of wood extraction on soil compaction and rutting caused by skidding and forwarding operations. Regular attempts are made in the agriculture industry for devise precision agricultural practices. Efforts are made in a number of fields including planetary exploration, all-terrain vehicles, mining, and agricultural vehicles to devise systems that perceive the environment and make on-board decisions for travelling with limited supervision. The knowledge of terrain is beneficial for any vehicle to work with its environment in a better way. Reina et al., 2017 presented one such system wherein, three sets namely color, geometric and soil-wheel interaction features are considered to characterize a given terrain. The

studies continue to develop better understanding of terrain-vehicle interaction behavior for devising improved farm machinery and practices.

With advancement of technology, these days many autonomous systems are coming up for different applications. For instance, Kitić et al., 2022 described about an autonomous robotic system for collection of soil samples in field and its analysis in real time. The process is fully autonomous and the samples are geo-referenced and a map is created for precision needs of fertilization. Considering the issues of undesired soil compaction, the system has been designed to be lightweight. A survey on terrain trafficability analysis for planetary rovers is presented by Chhaniyara et al., 2012. The paper describes the relevance of autonomy and mobility on soft and unstructured terrain for the success of future surface exploration robotic missions. The methodology for terrain characterisation using different techniques has been described to trade-off the technique for improved mobility of planetary rovers. These studies reveal that the successful operations using such systems are dependent upon understanding the soil- vehicle interaction behavior under varied movement conditions, which is a subject of continued study in this field.

1.3 Relevance of Rut Based Terrain Investigation

The movement characteristic of a given vehicle depends upon various terrain related factors that include surfacial topographic features and subsurface variables comprising primarily the response of soil. There are a number of soil variables which have spatial and temporal variation impacting the movement characteristics of vehicles. Characterization of vehicular movement on an unpaved terrain is a challenging task. Acquiring the spatially and temporally varying soil data by conventional methods is laborious and cumbersome task. The alternative methods are therefore evolved by researchers.

The movement of vehicles on unpaved soils leads to exerting its load and other forces on the soil. When the loading exceeds the bearing capacity of the soil, the soil begins to deform and cause rutting on the soil. The rut formed on the soil surface is reflective of different soil-vehicle movement conditions. The information about vehicle mobility in an area has been correlated with the rut impressions on the ground. Vehicle immobilization is said to be there when the rut depth exceeds the ground clearance of vehicles (Affleck, 2005). This information forms the basis for deciding different mobility corridors and the suitable vehicles for a given terrain (Herl, 2005). The information of about rut formation is important consideration for protecting the environment (Liu, 2009). The rut formed by wheels on soil which is manifestation of various soil and vehicle running conditions is highly correlated with the soil strength of the terrain (Vennik et al., 2017). Various soil properties and vehicle parameters influence the rut characteristics. Some of the soil parameters that influence the rut include soil moisture, organic matter content, soil- texture and compaction level of soil. The influencing vehicle parameters include its load, tyre

inflation pressure, its size and the number of passes among others.

On the natural terrain, the rut depth is not uniform. The rut depth is not same across the cross-section in situations like turning. The rut based analysis typically considers measurement of rut only at a few points. There is also a problem in synchronizing the rut depth with other measurements. Identifying such issues, Botha et al., 2019 presented a study to measure 3D profile of rut to assist in real time measurements of changed mobility condition using cameras. Based on the tests conducted on variety of terrain features, the research also brought out that rut depth can be used as useful tool to determine the vehicular mobility in changing off-road conditions. The technique demonstrates the potential of rut study to support the driver in making decisions related to mobility and safety. There are a number of associated aspects which are investigated by various researchers to define the underlying soil in a better way.

1.4 Various Tools and Techniques for Rut Investigations

In recent years, many innovative tools have emerged for assessing soil surface disturbances. The rut measurement tools have moved from manual measurements (Jester and Klik 2005) to the advanced innovative techniques like ultrasonic techniques (Lisein et al., 2013), laser profiling (Koreň et al. 2015) or by using photogrammetry techniques (Pierzchała et al. 2016). Each of these techniques has its own merits and de-merits. A sizeable knowledge gaps associated with the use and efficacy of these new tools have also come to surface in extending the benefits of these tools for the successful and efficient missions (Marra et al. 2018). One such issue is that when using the laser based systems, the huge point cloud demands for heavy resources for data storage, retrieval and its analysis. The attempts for optimal storage and efficient solutions are therefore the need of time. The effectiveness of various sensors in extreme environmental conditions of dust and moisture is a matter of further study.

It is noteworthy that the rut which forms after passage of vehicles is different from sinkage which accounts for both elastic and plastic deformation of the terrain. A rheological soil model with the elasto-plastic behavior to measure sinkage has been described by Bolling, 1987. The elastic behavior of the soil is especially important for issues like evaluation of rolling resistance and available draw-bar pull for movement of vehicle. The relevant techniques for measurement of ground response need to consider this effect.

The rut due to movement of vehicles is formed primarily by two factor. One relates to static sinkage which is caused by vertical load of the wheel. The other factor relates to dynamic sinkage caused by the slip associated with wheel rotation (Ishigami, 2008). The rut depth is also investigated by various other causative factors

including multiple wheel passes, size of wheel, loading conditions and different soil parameters (Crossley, 2001; Saarilahti, 2002). The studies continue to improve the understanding of soil behavior under various loading conditions. The cumulative rut on the terrain is important to be considered for overall impact analysis on the soil.

Although parametric studies are there to quantify the prevalent conditions of ground, however, the most common factor that is considered in Terramechanics studies is cone index based approach for its simplicity in determining the performance of vehicles. Jones and Arp, 2017 presented a model for depicting variation in Cone Index on the three different forest locations in New Brunswick based on daily records of snow, temperature and rain. The cone index based studies have also been advanced further by various researchers to correlate the vehicle mobility and evolve solution in variety of situations.

Research has also moved to explore the use of satellite imagery and aerial platforms to study the rut and track impressions for different applications. On one hand the track impressions on the soil are useful for surveillance purpose while on other hand they reveal useful information about the soil. Bhatnagar et al., 2022 worked on drone based imagery for wheel rut investigation using deep learning techniques. In such image based studies, the delineation of rut impressions is an important consideration. The surrounding terrain features influence the track contrast. Different image processing techniques including terrain texture have been explored by various researchers for improved identification of rut and vehicle tracks. The studies are continued further to improved image interpretation for better delineation of rut and track profiles.

1.5 Research Gaps in Literature

Although research is continued on investigation of rut from different perspectives yet there are a number of issues which if addressed can bring improved and efficient solution to vehicle mobility problems. The following issues present the research gaps whose solution needs to be explored further:

a) The rut in desertic terrain gets filled back by the sand pouring from sides. This can lead to incorrect interpretations when using ultrasonic or laser sensors to measure the rut profile. Suitable corrections are needed.

b) The vehicles get immobilized either by the excessive sinkage or by poor traction. There are models that infer the sinkage and rut and also the effect of slippage on draw-bar pull and net traction, etc. The models explaining the threshold limits in various kinds of soils and terrain surfaces under different conditions need to be studied.

c) Effect of plate size on the sinkage estimation has been observed as an important aspect. The rut profile obtained for various vehicles need to be explored further from this perspective.

d) In view of the sudden and momentary loadings by vehicular movements on unpaved terrain, the rheological behavior of elasto-plastic nature of soil needs to be studied further.

e) Impact of various landform features on rut formation is an important input that needs attention from movement planning. Suitable models integrating the effect of various influencing parameters need to be investigated further.

f) The technological advances need to be utilized as per the terrain conditions. For instance, advanced laser techniques may not work in extreme dust environment while ultrasonic sensors may not work well for vehicles moving at higher speeds. The solution to such scenarios needs to be devised further.

g) Interpretation of remoulding index that is dependent upon the soil characteristics has been explored using time consuming tests. The possibility of simpler means needs to be explored for better utilization in on-the-go interpretation.

Based on the gaps as identified from the literature review, the following broad research studies are considered important:

1. Investigation of rut patterns on soils of different terrain/landform features
2. To undertake a parametric study of rut on a given terrain feature by studying the changes in rut pattern to identify significant causative factors in that terrain
3. Examining the suitability of various rut measurement techniques
4. Examining different terrain investigative tools considering elasto-plastic behavior of the soils
5. Modelling rut for cumulative influence of different causative factors in spatial domain
6. Improving the terrain classification based on texture study, including terrain properties and vehicle parameters

1.6 Research Methodology to Address the Research Problems

Based on the literature review, identified gaps and the broad research problems, critical evaluation was carried out to plan further research work. Various aspects that are considered for deciding the research methodology and planning further the experimental and analytical studies are given below:

1. The rut in desertic terrain has been observed to get filled by the sand pouring from sides. Similarly, the rut profile has been observed to become eccentric on the curves having higher depth on the outer edge and lesser on the inner one. The shape of the rut profile which is characteristic of given terrain type, the soil, and vehicle running conditions has been observed as more important than merely the rut depth as referred in most of the literature.

2. In view of the sudden and momentary loadings by vehicular movements on unpaved terrain, the rheological behavior of elasto-plastic nature of soil is an important consideration for correct interpretation. Therefore, monitoring the soil-wheel sinkage during vehicle loading on soil and the rut after its passage are two different considerations. The first one i.e. sinkage is considered important for computing the overall resistance to the movement of vehicle while the second one i.e. rut is observed as better while using systems to measure the post effect of vehicular movement on the soils. This aspect is important for placement of monitoring systems on-board vehicle.

There are a number of tools that can be used for mapping the rut profile. Manual rut profiler being simpler, portable for inaccessible areas and not needing any computational environment or power backup was used for close monitoring of rut shapes. The laser profiler on the other hand is an advanced tool to measure the rut profile with precision for better inferences. These tools however need heavy memory devices for storage of data. The systems for inferring movement decisions on-board vehicle need to optimize the memory for efficient decision.

The vehicles get immobilized either by the excessive sinkage or by poor traction. There are models that infer the sinkage of wheel which has been a measure of static sinkage due to loading conditions. The movement of wheel on slippery surfaces gives rise to additional sinkage called dynamic sinkage which increases by increase in wheel slip. Moreover, the sinkage level on the soil is also influenced by the plate size and also the vehicle tyre or track configuration. In other influencing parameters, the effect of multiple loadings is also there on overall sinkage and the rut. The influence of soil type evaluated using the remoulding index of soil is also important. The dynamically changing parameters like compaction level and soil moisture also influence the rut. The cumulative effect of all such parameters on maximum soil distress levels in any area can give important insight about the

suitability of any unpaved terrain for planning the vehicular movement during emergencies. The identification of safe and trafficable zones considering the cumulative effect on maximum possible soil distress by vehicular movement is one such research aspect for bringing simpler decisions about movement. Specific studies in this regard may bring out better insight and utility of rut studies for different operational needs.

3. Impact of various landform features on the rut formation is important consideration that needs attention from movement perspective. Various modelling techniques have been developed for classifying the terrain as per the trafficability potential. While evolving suitable models is an important aspect, the validation of interpreted information is another important aspect needing attention. A lot of vital information about the suitability of terrain can get revealed by studying the rut impressions in the area forming vehicle tracks on the unpaved terrain. On one hand satellite and aerial images can be utilized to capture the rut impressions while on the other hand optical cameras could be utilized manually or on-board vehicle. In the coarse resolution images, these tracks appear like edges. There are many edge-enhancement measures whose suitability needs to be explored from track detection perspective.

4. One aspect that has been considered important in the study of rut impressions in the images is the relative size of the rut. The rut and the tracks impressions which look like thin edges in the low-resolution images appear like elongated areas in the high-resolution images. These track impressions get highlighted as per the surrounding terrain features. The conventional tone-based image processing techniques can highlight these tracks to a limited extent. The role of texture becomes important here as it can distinguish the features by considering a group of pixels having distinguishing features.

5. There are different measures based on tone and texture of the features which try to enhance the rut impressions in any area. The effectiveness of enhancement of these features could vary as per the surrounding terrain. In such a case, the technique that is adaptive to the given surroundings also needs to be explored to assist in efficient movement decision.

The above aspects are considered for planning further research work to fill the gaps by considering two broad areas. One aspect of the study was planned was to focus on rut studies based on ground-based experimentation while the other aspect focused on the image analysis for improved delineation of rut impressions formed by vehicular movement.

1.7 Objectives of the Proposed Research

Based on the above analysis, the following objectives are planned for further detailed investigations in this research:

- 1) To study the shapes of rut profiles in different terrain-vehicle running conditions.
- 2) To study the optimization aspects of rut profile data for efficient movement decisions.
- 3) To identify the key factors influencing the rut depth and study their impact on the soil distress levels in the area for ascertaining the suitability of the terrain for any emergency movement.
- 4) To explore various edge enhancement measures for their effectiveness in enhancing the track features.
- 5) To study the effect of image texture in enhancing the track features
- 6) To explore the possibility of evolving some technique for most optimal enhancement of rut shape in a given surrounding terrain

1.8 Structure of the Thesis

The following points give brief about these studies presented in different Chapters of this thesis.

Chapter 1: This chapter introduces to the literature relevant to highlight the importance of rut studies for vehicular movements over unpaved terrain. It also highlights the gaps in the study, the research problems, the proposed research methodology and the objectives set for this research work. The structure and organisation of the thesis, the benefits to practitioners, researchers and society in general are also given in this chapter.

Chapter 2: In this chapter, the relevant literature has been collated to reflect the existing and current practices in the relevant research areas. The literature also forms the basis for further investigation of rut from different perspectives.

Chapter 3: In this chapter, rut shapes as investigated from different perspectives have been presented. The common types of rut shapes have been identified and then represented using different mathematical formulations. The effectiveness of these equations in achieving optimisation in storage of rut profile data has been discussed.

Chapter 4: The experimental studies have been conducted for understanding the effect of soil moisture and the number of vehicle passes on soil distress levels. The utility of the study has been explored for identifying the maximum soil distress level in the area to plan emergency movement on the unpaved terrain.

Chapter 5: The study about the path formed by vehicle rut appearing as edges in the course resolution images has been presented. Various edge detection algorithms have been explored and compared for identifying the most suitable one for studying the rut and track features in the images.

Chapter 6: The role of texture that becomes important in fine resolution images has been explored here. Specific studies have been conducted to evaluate the potential of different texture measures in enhancing the rut tracks.

Chapter 7: The suitable rut enhancement measures have been observed to vary as per the surrounding terrain. An adaptive technique has been explored that can select the most effective rut enhancement measure in a given surrounding.

Chapter 8: The important conclusions drawn from this research work have been presented in this chapter. The future aspects of the current study and its social impact have also been presented in detail.

The above studies have been presented in this research work.

1.9 Benefits of the Proposed Rut Studies

The analysis of trafficability potential of any unpaved area is a common requirement for varied fields. The vehicles in industries like forestry, agriculture, and in defence frequently need to evaluate the potential of unpaved terrain for planning movement. Further, in many operations like firefighting, emergency response during peak traffic, alternate unpaved tracks are followed. In all these applications, the proposed rut study brings a better insight of the prevailing terrain conditions.

The proposed technique for optimized storage of data captured by on-board laser scanners can make the on-board mobility evaluation systems more efficient. The studies related to maximum soil distress under different dynamic

conditions can be the basis for creating maps for planning emergency movement in the safe areas.

The proposed visual analytics based techniques could assist the decision-makers for improved decisions while encountering low-contrast areas and make such operations sustainable. This study can have application in different industries like autonomous ground vehicle movement, robotic vehicles, defence, and night safari, etc. where the track impressions of previous vehicles can extend a vital support particularly in low contrast areas.

The outcome from study on all these studies can pave way for making on-board mobility decisions more useful and efficient.

1.10 References

Affleck R. T. (2005). Disturbance measurements from off-road vehicles on seasonal terrain. ERDC/CRREL TR-05e12. US Army Corps of Engineers. Engineer Research and Development Center.

Ares, A., Terry, T. A., Miller, R. E., Anderson, H. W., & Flaming, B. L. (2005). Ground-based forest harvesting effects on soil physical properties and Douglas- Fir growth. *Soil Science Society of America Journal*, 69(6), 1822-1832.

Bhatnagar, S., Puliti, S., Talbot, B., Heppelmann, J. B., Breidenbach, J., & Astrup, R. (2022). Mapping wheel-ruts from timber harvesting operations using deep learning techniques in drone imagery. *Forestry*, 95(5), 698-710.

Bolling I. (1987). Bodenverdichtung und Triebkraftverhalten bei Reifen - Neue Meß- und Rechenmethoden. Dissertation, TU M"unchen, 1987

Borges, P., Peynot, T., Liang, S., Arain, B., Wildie, M., Minareci, M., Lichman, S., Samvedi, G., Sa, I., Hudson, N., Milford, M., Moghdam P., & Corke P. (2022). A survey on terrain traversability analysis for autonomous ground vehicles: Methods, sensors, and challenges. *Field Robot*, 2(1), pp.1567-1627.

Botha, T., Johnson, D., Els, S., & Shoop, S. (2019). Real time rut profile measurement in varying terrain types using digital image correlation. *Journal of Terramechanics*, 82, 53-61.

Chhaniyara, S., Brunskill, C., Yeomans, B., Matthews, M. C., Saaj, C., Ransom, S., & Richter, L. (2012). Terrain trafficability analysis and soil mechanical property identification for planetary rovers: A survey. *Journal of Terramechanics*, 49(2), 115-128.

Herl, B. K., Doe W. W., & Jones D. S. (2005). Use of military training doctrine to

predict patterns of maneuver disturbance on the landscape. I. Theory and methodology. *Journal of Terramechanics*, 42, 353-371.

Ishigami, G., Miwa, A., Nagatani, K., & Yoshida, K. (2007). Terramechanics-based model for steering maneuver of planetary exploration rovers on loose soil. *Journal of Field robotics*, 24(3), 233-250.

Jester W., & Klik A. (2005) Soil surface roughness measurement—methods, applicability, and surface representation. *CATENA* 64:174–192.

Jones M.F. & Arp P.A. (2017). Relating Cone Penetration and Rutting Resistance to Variations in Forest Soil Properties and Daily Moisture Fluctuations. *Open Journal of Soil Science*, 7, 149-171. <https://doi.org/10.4236/ojss.2017.77012>

Kitić, G., Krklješ, D., Panić, M., Petes, C., Birgermajer, S., & Crnojević, V. (2022). Agrobot Lala—An autonomous robotic system for real-time, in-field soil sampling, and analysis of nitrates. *Sensors*, 22(11), 4207.

Koreň M., Slančík M., Suchomel J., & Dubina J. (2015). Use of terrestrial laser scanning to evaluate the spatial distribution of soil disturbance by skidding operations. *Iforest* 8:386–393

Lisein J., Pierrot-Deseilligny M., Bonnet S., & Lejeune P. (2013). A Photogrammetric Workflow for the Creation of a Forest Canopy Height Model from Small Unmanned Aerial System Imagery. *Forests* 2013, 4, 922–944

Liu K. (2009). Influence of Turning on Military Vehicle Induced Rut Formation. PhD diss., University of Tennessee. Available at http://trace.tennessee.edu/utk_graddiss/620.

Marra, E., Cambi, M., Fernandez-Lacruz, R., Giannetti, F., Marchi, E., & Nordfjell, T. (2018). Photogrammetric estimation of wheel rut dimensions and soil compaction after increasing numbers of forwarder passes. *Scandinavian Journal of Forest Research*, 33(6), 613-620.

Marra, E., Laschi, A., Fabiano, F., Foderi, C., Neri, F., Mastrolonardo, G., Nordfjell T., & Marchi, E. (2022). Impacts of wood extraction on soil: Assessing rutting and soil compaction caused by skidding and forwarding by means of traditional and innovative methods. *European Journal of Forest Research*, 1-16.

Pierzchała M., Talbot B., & Astrup R. (2016). Measuring wheel ruts with close-range photogrammetry. *Forestry* 89:383–391.

Reina, G., Milella, A., & Galati, R. (2017). Terrain assessment for precision agriculture using vehicle dynamic modelling. *Biosystems engineering*, 162, 124-139.

Saarilahti, M. (2002). Soil interaction model. *Quality of Life and Management of*

Living Resources Contract, No. QLK5-1999-00991. Department of Forest Resource management, University of Helsinki.

Vennik K., Keller T., Kukk P., Krebstein K. & Reintam E. (2017). Soil rut depth prediction based on soil strength measurements on typical Estonian soils. Elsevier Journal of Bio systems engineering 163 (2017)78-86

Willoughby W. E., & Turnage G. W. (1990). Review of a procedure for predicting rut depth. Unpublished memo

CHAPTER - 2

LITERATURE REVIEW

In this chapter, the relevant literature has been collated to reflect the existing and current practices in the relevant research areas. The literature also forms the basis for further investigation of rut from different perspectives.

The rut formed by movement of vehicles on unpaved terrain has been the subject matter of study in various fields. It has been investigated from different perspectives. The following paragraphs give the relevant research conducted in this regard.

The rut formed by wheels on soil which is manifestation of various soil and vehicle running conditions. Various soil properties and vehicle parameters influence the rut characteristics. Some of the soil parameters that influence the rut include soil moisture, organic matter content, soil- texture and compaction level of soil. The influencing vehicle parameters include its load, tyre inflation pressure, its size and the number of passes among others. The rut has been studied by various researchers from different perspectives which include exploring the relevant terrain properties (Bekker, 1960; Saarilahti, 2002; Raper, 2005; Botta et al., 2006), modeling the effect of various influencing factors like turning (Liu et.al, 2009) and in using various tools (Suvinen, 2006, Jones, 2017, Mohtashami, 2022) for characterizing the rut. An overview of studies conducted from different perspectives has been given here.

2.1 Modelling the Impact of Various Influencing Factors on Rut

The rut that is formed after passage of vehicles is different from sinkage which accounts for both elastic and plastic deformation of the terrain. The rut due to movement of vehicles is the plastic deformation and is caused primarily by two factors viz the static caused by vehicle load and dynamic factors. The rut due to movement of vehicles is formed primarily by two factors. One relates to static sinkage which is caused by vertical load of the wheel. The other factor relates to dynamic sinkage caused by the slip associated with wheel rotation. In order to assess the static sinkage, the load sinkage studies reveals important insight about the terrain.

Based on the early descriptions of such behaviour as has been reported by Bernstein, 1913 and also by Goriatchkin, 1937 (as cited by Bekker, 1956). The equation proposed for wheel sinkage is described as,

$$p = kz^n \quad (2.1)$$

Here, p is average vertical contact pressure, k is stiffness constant of soil sinkage, z is the sinkage depth into the soil and exponent n is a soil constant indicating exponent of terrain deformation. The variation of soil stiffness constant k with size of loading object revealed the main deficiency associated with this equation. It was also observed that sinkage of a rectangular plate also depends upon the width of the rectangle plate (Taylor, 1948). Bekker, 1956 combined these two concepts and suggested the pressure-sinkage relationship as,

$$p = (k_c / b + k_\phi) z^n = kz^n \quad (2.2)$$

where, k_c and k_ϕ are the soil stiffness constants, which are said to be independent of plate size. The above equation when tested in laboratory and field was found to be reasonably accurate. Bekker, 1960 also found that the radius of the disks is the more appropriate measure to associate with b , whereas b is the smaller dimension when using the rectangular plate.

Wong, 1978 mentions that the equation by Bekker as above is essentially an empirical equation. Further, understanding the limitation that the moduli k_c and k_ϕ are not dimensionless, Reece, 1965-66 proposed a new equation for the pressure-sinkage relation as,

$$p(h) = (ck'_c + \rho b k'_\phi) \left(\frac{h}{b}\right)^n \quad (2.3)$$

Also, k'_c and k'_ϕ are cohesive and frictional moduli of soil deformation, and n is the exponent of terrain deformation. ρ is the weight density of terrain here and c is cohesion of soil. Here, h indicates Sinkage of wheel / plate and b indicates the breadth of pressure plate/ unloaded width of tyre. Note that, for frictionless soil, the term k_ϕ to be negligible. Similarly, for the dry cohesion-less sand, the term k_c to be negligible. If $n = 1$, both these equations become equivalent equations, since $c.k'_c = k_c$ and $\rho.k'_\phi = k_\phi$.

Rutting research has also been observed as important in the field of robotics. Various principles of terramechanics are applied for modelling the wheel-soil interface and the associated rut formation and movement characteristics of various planetary rovers. Based on the classical equations as above, the stresses exerted by rovers are evaluated further by many researchers (Ishigami, 2008; Senatore and Iagnemma, 2014). By employing the equation for a wheel, the following formulae has been derived; First, at an arbitrary wheel angle θ , the wheel sinkage at $h(\theta)$ is evaluated as,

$$h(\theta) = r(\cos \theta - \cos \theta_s) \quad (2.4)$$

where, θ_s is the static contact angle. Subsequently, the stress $p(h)$ at sinkage ' h ' is evaluated as,

$$p(h) = (ck'_c + \rho b k'_\phi) \left(\frac{r}{b}\right)^n (\cos \theta - \cos \theta_s)^n \quad (2.5)$$

The angle θ_s is numerically computed by solving this equation. Finally, the static sinkage h_s can be derived as,

$$h_s = r(1 - \cos \theta_s) \quad (2.6)$$

On the other hand, the dynamic sinkage is a complex function which depends upon the wheel slip ratio, its surface pattern, together with the soil characteristics. It is relatively complex to obtain dynamic wheel sinkage using an analytical solution, however it can be calculated numerically. Total wheel sinkage ' h ' is then defined as,

$$h = h_s + h_d \quad (2.7)$$

here, h_s is the static sinkage while h_d is the dynamic sinkage resulting from the vehicular movement on the soil. The studies are advanced further by considering other aspects too, e.g. the effect of number of vehicle passes, multi-tire vehicles, etc., making the evaluation complex. Researchers have thus developed various empirical approaches to address the issues with simpler techniques.

Although parametric studies are there to define the soil deformation in a better way, yet for simplicity impricial relations are also devised. The cone index (CI) based models are widely used to correlate it with vehicle performance (Ciobotaru, 2009). The cone index based approach has been taken further by computing the mobility numerics associated with vehicle performance. Many forms of wheel numerics are proposed by various researchers (Taheri et al., 2015) some of which are directly related to wheel sinkage.

Maclaurin, 1990 proposed a wheel sinkage model for measurement of (z/d) for fine-grained soils using the wheel Numeric (NCI) as the underlying basis which as per Turnage, 1972 has been given as,

$$N_{CI} = \frac{CIbd}{W} \sqrt{\frac{\delta}{h_u}} \cdot \frac{1}{1 + \left(\frac{b}{2d}\right)} \quad (2.8)$$

where, CI is the cone index, b is the unloaded width of tire, d is the its unloaded diameter, δ is the tire deflection and h_u is the tire unloaded section height. The effect of multi-pass is carried by various researchers. Multi-pass models were suggested by Scholander, 1974 and Abebe et al., 1984. The general form of the models has been given as,

$$Z_n = Z_1 \cdot N^{\frac{1}{a}} \quad (2.9)$$

where, Z_1 is the sinkage after one loading and Z_n is the sinkage after N loadings, N indicates the number of passes, and a here indicates multi-pass coefficient which is dependent on soil properties and the load intensity. Abebe et al., 1989 suggested the value of a as 2 for softer soil subjected to low load; and 3-4 in case of medium bearing soil subjected to medium load. The same for heavily loaded soils having higher bearing capacity, it takes the value of a as 4 or 5 (Saarilahti, 2002). The sinkage model of Maclaurin, 1990 was used for computing the sinkage after first pass, and the rut depth after every single wheel has then been calculated as,

$$Z_n = (Z_{n-1}^a + Z_1^a)^{\frac{1}{a}} \quad (2.10)$$

where, a is the calculated multi-pass coefficient, and Z_n is the wheel sinkage after N passes. Multi-pass effect of vehicular movements has been studied by Kane, 2010. The effect of number of passes on the Cumulative Impact Width (CIW) has been evaluated as,

$$CIW_n = CIW_1 \cdot N^{\frac{1}{a}} \quad (2.11)$$

where, CIW_1 and CIW_n indicate the Cumulative Impact Width after 1 and N passes respectively; N here is the number of passes, and a is the multi-pass coefficient.

Vehicle maneuver patterns impacts the terrain to a great extent. Ayers, 1994; Affleck et al., 2004; and Althoff and Thien, 2005 brought out that the soil disturbance increases with the decrease in turning radius. Liu, 2009 studied the impact of turning of military vehicles on the rut formation and quantified it using rut depth, its width and the rut index as the indicators.

Among other soil parameters, the soil stiffness estimation reveals important information about the underlying strata influencing the observed rut. The homogeneity of soil strata is another important factor influencing the stress distribution and associated rut that needs attention. The pressure distribution under a circular plate loaded by pressure p follows the equation by Boussinesq (Helenelund, 1974) and is given as,

$$\sigma_h = p \cdot (1 - \cos^\alpha \beta) \quad (2.12)$$

where, β is the angle made by the edge of circular plate with central axis at depth h of the circular plate and α is concentration factor that is governed by soil

homogeneity.

Soil shearing strength has been reported as a major property of soil that influences trafficability. A study reported by Ayers, 1987 shows that both the soil cohesion and its friction angle tend to increase with increase in the density of soil. Moreover, as per McKyes, 1989, the soil moisture influences the trafficability of a cohesive soil to much higher extent than the friction soils. In another study by Smith and Dickson, 1990, it was observed that higher loads result in more compaction in soil at greater depth than near the surface of soil. Usually, different types of vehicles have different severity levels of terrain impact. As per Janzen, 1990, using tracked vehicles, one can manage better the compaction and have better yield over that by a wheeled vehicle.

Based on the study of four military vehicles on unpaved terrain under different conditions, Liu et al., 2010 identified some important vehicle and soil parameters that influence the rut formation.

Smith, 2014 conducted a study over different frequency and amplitude of sinusoidal terrain surfaces. It was observed that the vehicles tend to move flat on the high frequency undulating surface and travel along the geometry when encountering low frequency terrain surfaces.

Mohtashami et al., 2017 carried out a study of rut formation on logging sites in Sweden to understand the influence of soil type, cartographic depth-to-water (DTW), traffic intensity and the road reinforcement during the logging operations. In this study, the soil type and traffic intensity have been observed to be more influencing than DTW and slash reinforcement. Vennik et al., 2017 conducted studies over typical Estonian soils for the rut depth changes after repeated number of military vehicles.

It has also been reported that when soil moisture content rises above the critical level, the plastic deformation replaces the elastic response of soil. The soil is observed to get displaced and form rut by the extra applied stress (Horn et al. 2007; Mohtashami, 2022).

2.2 Various Tools and Techniques Used for Rut Investigations

The evaluation of rut profile accurately is vital to development of terrain-interactive models. Various researchers have developed different techniques that are suited to certain given environmental conditions. Rut depth measurement using a manual profilometer has been reported by Affleck, 2005.

The manual profilometer is easy to operate however it is time consuming and is not suitable when the continuous measurements are the requirement. The requirement of frequent and continuous measurement of sinkage and rut has been there in unmanned ground vehicles, forestry, measurement of rut on the pavements, movement of robots and various planetary rovers. A number of techniques for rut measurement are developed suiting various terrain and environmental conditions.

Different technologies that are used for rut measurement are highlighted by Mallela and Wang, 2006. These include ultrasonic sensors, point lasers, scanning lasers and optical sensors.

Lisein et al., 2013 presented details about use of ultrasonic sensors which is cost effective but the speed of measurement is limited. The system in ROMDAS and ARAN (automated road analyser) as shown is based on ultrasonic sensors.

Pierzchała et al., 2014, 2016 and Haas et al., 2016 presented the potential of photogrammetric techniques over images captured by camera on the forest machinery to collect the stereo images. These images are used for obtaining highly accurate 3D point cloud data of terrain surface, identify and measure the wheel rut alongwith its dimension. The photogrammetric technique is however useful when the light conditions are favorable. Light Detection and Ranging (LiDAR) can therefore provide a better alternative. A ground-based terrestrial laser scanner is employed by Koreň et al., 2015 to evaluate the soil disturbance and vehicle rut caused by the skidding operations. Salmivaara et al., 2018 investigated rut based on a vehicle-mounted LiDAR system. In this study the reliability and efficiency of forest machine mounted LiDAR sensor has been reported. LiDAR scanners are however suitable for rut measurements at closure intervals but they have issues in working in measurements in water logged areas and in dust environment.

The associated soil properties are also important to be studied. The soil properties vary spatially from point to point and for application to wider areas, simpler means like cone penetrometer depicting soil strength are used. The cone penetrometer uses the penetration resistance profile of soil, computes the cone index for quick estimation of trafficability. (Eid and Stark, 1998; Lowery and Morrison, 2002).

2.3 Analysis of Spatial Data to Infer Features Influencing Rut

Remote sensing data is useful in mapping a number of soil properties that include soil minerals, its salinity, moisture, texture, and organic content among others. A review is presented about successful use of space borne, airborne and in situ measurements systems in mapping the soil properties and terrain (Mulder et al., 2011). Later, Singh, 2016 also presented a review of the use of remote sensing data

in different bands including optical, microwave and hyper spectral bands. Remote sensing data assists in improving the incomplete spatial information of the existing regional and global database of soil.

The soil moisture is the key parameter that alters the rut depth. In one of the studies presented by Drusch et al., 2004, captured well the temporal evaluation of soil moisture by using ERA40 product and the surface soil moisture data set derived from ERS scatterometer.

Sadiya et al., 2017 described a GIS and remote sensing based approach for military terrain trafficability analysis of North-East Nigeria. This research is indicative of the potential of various satellite images and digital elevation model (DEM) in getting the information about various terrain features by using various Geographic Information Systems (GIS). The same can be utilized for collating and analyzing the associated terrain data for evaluating the trafficability potential of an area.

In order to infer the soil properties on wider domain, geospatial data together with hydrologic and other weather conditions are there at large. However, the data about soil-bearing capacity for calibration and validation of models are still missing (Salmivaara, et.al., 2018). The important information that spatial data resources reveal trafficable passes quite easily is the location of tracks on the unpaved terrain. Zhang, 2009 worked on using the remote sensing and other technology for monitoring the condition of unpaved roads.

Each terrain can be defined uniquely by a combination of parameters that differ for the kind of terrain. There are a number of parameters of the terrain like slope, soil type, moisture condition, surface cover, etc. that influence the formation of the rut depth with varying degree. In order to compute the cumulative effect, weighted overlays analysis has been commonly employed in different applications (Çalışkan and Atahan, 2023).

2.4 Various Techniques Used for Enhancement of Features in Images

The path formed by vehicle rut is observed like an edge on course resolution images. Delineation of these features in varied surroundings is an important aspect. Many edge detection techniques are developed by various researchers. These techniques preserve the structural features and the high-frequency components belong to either of the two groups based on the derivatives (Marque, 2011). The first one computes the Gradient or the first-order derivative of an image. The second one, based on the second-order derivative is a Laplacian operator. Both these filters highlight sharp changes or discontinuities in the picture. However, the gradient-based filters emphasize the prominent edges while Laplacian filters enhance

the finer details (Gupta and Porwal, 2016). Based on these, researchers brought out several edge detection algorithms. Shrivakshan and Chandasekar, 2012 compared the prominent edge detection algorithms covering Sobel, Robert's cross gradient, Prewitt, Canny, Laplacian of Gaussian (LoG), etc. The goodness of edge detection algorithms depends upon measures such as the accuracy of edge detection, the localization of edges, and the minimal response. Canny's edge detection has been shown as a computationally more expensive algorithm. It has performed better than other operators under varied kinds of scenarios (Narendar and Hareesh, 2011).

Nowadays many applications are coming up where the vehicles need to follow the rut tracks left over by the leading vehicle. For instance, the details for rut following robotic operations in off-road terrain are presented by Ordonez et al., 2011. During strategic missions, vehicles move on unpaved terrain in low contrast dark conditions. In such a scenario, the delineation of tracks or the rut impressions by leading vehicles plays an important role.

The track features that appear like an edge in the coarse-resolution images take the shape of elongated areas in fine-resolution images. In such a scenario, the high pass and edge detection filters give limited information to delineate these tracks passing through diverse surroundings.

These days, many vehicular operations make use of vision-based systems. Caraffi et al., 2007 used decision networks and the stereo vision technique for detecting the off-road path and obstacles. Howard and Seraji, 2001 used a vision system-based mobile robot and applied Artificial Neural Network (ANN) for real-time characterization of terrain. Ordonez et al., 2011 investigated the movement of robotic vehicles by tracking the rut in unpaved areas. Chowdhury et al., 2017 introduced an algorithm for a line-following robot to follow the straight-line path autonomously.

Various digital image processing techniques are employed to enhance the features of interest (Gonzalez et al., 2004). Janani et al., 2015 made a compilation of different image enhancement techniques. Babu et al., 2015 presented a framework for contrast enhancement. However, the techniques the tonal variations based techniques that primarily employ filters and histogram stretching extend limited aid for delineating the tracks. The pattern and texture of these tracks over tonal variation are some appropriate measures to distinguish better these tracks. The statistical measures of the GLCM-based texture analysis technique have shown reasonably good results in a wide range of applications (Mohaniah et al., 2013). Fauji et al., 2020 presented one such study for improving the robustness of detection of road surfaces in varied environmental conditions using a combination of GLCM measures and local binary pattern (LBP).

Various approaches are developed that describe the texture in an image. Bharti et al., 2004 compared different approaches to describe the texture. Humeau-Heurtier, 2019 presented a survey of various methods of texture feature extraction. GLCM-based texture analysis could delineate well the road boundaries (Gravoc and Goma, 2012). Measures like energy, homogeneity, entropy, contrast, etc. define the texture using this approach. The most suitable texture measure that can distinguish the track area more prominently depends upon the surrounding.

Several applications employ texture for extracting the required features. Content-based image retrieval was attempted by Zhang et al., 2008 and Alsmadi, 2020 by combining edge detection and properties of a co-occurrence matrix. Pradhan et al., 2014 demonstrated the extraction of flooded areas using a GLCM-based texture analysis based program over TerraSAR- X satellite image. Micheal and Vani, 2015 employed texture features for automatic mountain detection using DTM data of lunar images. Doycheva et al., 2019 used texture features for evaluating road distress conditions in real-time. Sudha and Aji, 2019 used GLCM texture features as the descriptors of features for image retrieval in varied applications. Liu et al., 2020 employed the local second-order entropy to characterize the variation in the grayscale. Winarno et al., 2021 applied edge detection with GLCM for fingerprint recognition even though the edges are predominant in such images. Here, the authors have used edge detection for preprocessing. Feature extraction based on the GLCM using measures like energy, contrast, homogeneity, and correlation has been decided to improve the results further. Singh et al., 2022 employed features of GLCM on Sentinel-2 imagery for the identification of avalanche debris areas. Kar and Banerjee, 2022 used GLCM texture features to evaluate the intensity of tropical cyclones.

This study used GLCM-based measures as a good descriptor of texture features. Haralick et al., 1973 proposed the GLCM-based concept of measuring texture by computing different texture measures. He introduced 14 features to represent the texture of an image. Subsequently, Connors and Harlow, 1980 presented that out of 14 parameters, only five are good enough to describe texture. These parameters include Energy, homogeneity, entropy, correlation, and contrast.

Clausi, 2002 provided details about the computational complexity using the GLCM method, which is proportional to $O(G^2)$. Suitable selection of displacement value in GLCM has been a significant consideration as the large values result in missing the details of textural information (Gadkari, 2004).

Many machine learning techniques including the advanced deep learning techniques too are evolving that try to delineate the rut and tracks from the surroundings. In the study of microcirculation images, the limitations of deep learning are reported and a hybrid model to strike a balance between accuracy and speed by combining traditional computer vision algorithms and CNN has been

proposed (Helmy et al., 2022). Thus one needs to explore various conventional image processing techniques too that could suitably enhance the rut and vehicle tracks.

2.5 Conclusion

The literature review as above formed the basis for undertaking the research work to meet the set objectives. Various aspects of the study led to devising suitable research methodology and plan further the experimental and analytical studies.

Accordingly, research has been pursued further considering two broad areas. One aspect of the study has been planned to focus on rut studies based on ground-based experimentation wherein the data of rut is to be collected and analysed under different terrain-vehicle running conditions. The other aspect is focused on image analysis wherein, the role of image processing techniques is to be explored further for improved delineation of rut impressions formed by vehicular movement.

The details of above studies have been given in the subsequent chapters.

2.6 References

1. Abele, G., Brown, J., & Brewer, M. C. (1984). Long-term effects of off-road vehicle traffic on tundra terrain. *Journal of Terramechanics*, 21(3), 283-294.
2. Alsmadi, M.K. (2020). Content-based image retrieval using color, shape and texture descriptors and features. *Arabian Journal for Science and Engineering*, 45(4), pp.3317-3330.
3. Althoff, P.S., & Thien, S.J. (2005). Impact of M1A1 main battle tank disturbance on soil quality, invertebrates, and vegetation characteristics. *J Terramechanics* 2005; 42(3-4):159-176.
4. Affleck, R., Shoop S., Simmons K., & Ayers P. (2004). Disturbance from off-road vehicle during spring thaw. *12th ASCE conference*. Edmonton, Canada
5. Ayers, P.D. (1994). Environmental damage from tracked vehicle operation. *J Terramechanics* 1994; 31(3): 173-183.
6. Babu, P., Rajamani, V., & Balasubramanian, K. (2015). Multipeak mean based optimized histogram modification framework using swarm intelligence for image contrast enhancement. *Mathematical Problems in Engineering*, 2015.
7. Barbu, T. (2021). Mixed noise removal framework using a nonlinear fourth-order PDE-based model. *Applied Mathematics & Optimization*, 84(Suppl 2), pp.1865-1876.

8. Bekker, M.G. (1956). Theory of land locomotion - the mechanics of vehicle mobility. Univ. of Michigan Press, Ann Arbor, M I : 522 pp.
9. Bekker, M. G. (1960). Off-the-road locomotion, research and development in terramechanics. University of Michigan Press, Ann Arbor. 220 s.
10. Bernstein, R. (1913). Probleme zur experimentellen Motorpflugmechanik. Der Motorwagen, Vol.16: pp. 199-227.
11. Bharati, M.H., Liu, J.J., & MacGregor, J.F. (2004). Image texture analysis: methods and comparisons. Chemometrics and intelligent laboratory systems, 72(1), pp.57-71.
12. Botta, G. F., Jorajuria, D., Rosatto, H. & Ferrero, C. (2006). Light tractor traffic frequency on soil compaction in the Rolling Pampa region of Argentina. Soil & Tillage Research, 86, 14e19.
13. Çalışkan, B., & Atahan, A.O. (2023). Cartographic Modelling and Multi-Criteria Analysis (CMCA) for Rail Transit Suitability. Urban Rail Transit, 9(1), pp.1-18.
14. Caraffi, C., Cattani, S. & Grisleri, P. (2007). Off-road path and obstacle detection using -decision networks and stereo vision. IEEE Transactions on Intelligent Transportation Systems, 8(4), pp.607-618.
15. Chowdhury, N.H., Khushib, D., & Rashidc, M.M. (2017). Algorithm for line follower robots to follow critical paths with minimum number of sensors. *International Journal of Computer*, 24(1), pp.13-22
16. Ciobotaru, T. (2009). Semi-empiric algorithm for assessment of the vehicle mobility. Leonardo electronic journal of practices and technologies, 8(15), 19-30.
17. Clausi, D.A. (2002). An analysis of co-occurrence texture statistics as a function of grey level quantization. Canadian Journal of remote sensing, 28(1), pp.45-62.
18. Connors, R.W., & Harlow, C.A. (1980). A theoretical comparison of texture algorithms. IEEE transactions on pattern analysis and machine intelligence, (3), pp.204-222.
19. Doycheva, K., Koch, C., & König, M. (2019). Implementing textural features on GPUs for improved real-time pavement distress detection. Journal of Real-Time Image Processing, 16, pp.1383-1394.
20. Drusch, M., Wood, E.F., Gao, H., & Thiele, A. (2004). Soil moisture retrieval during the Southern Great Plains Hydrology Experiment 1999: A comparison between experimental remote sensing data and operational products. Water Resources Research, 40(2).
21. Eid, H.T., & Stark, T.D. (1998). Undrained Shear Strength for Cone Penetration Tests. In: Robertson and Mayne, Eds., Geotechnical Site Characterization, Balkema, Rotterdam.
22. Fauzi, A.A., Utaminingrum, F., & Ramdani, F. (2020). Road surface classification based on LBP and GLCM features using kNN classifier. Bulletin of Electrical Engineering and Informatics, 9(4), pp.1446-1453.
23. Gadkari, D. (2004). Image quality analysis using GLCM. University of Central

- Florida, Orlando, FL. (MS thesis) <https://stars.library.ucf.edu/etd/187> [Accessed on 30 Jul 2022]
24. Gonzalez, R.C., Woods, R.E., & Eddins, S.L. (2004). Digital image processing using MATLAB. Pearson Education India.
 25. Goriatchkin, V.P. (1937). Kolesa zhatvennih mashin. Sob. Soch., Vol. II and V, Moscow.
 26. Graovac, S., & Goma, A. (2012). Detection of road image borders based on texture classification. *International Journal of Advanced Robotic Systems*, 9(6), p.242.
 27. Gupta, S., & Porwal, R. (2016). Combining laplacian and sobel gradient for greater sharpening. *IJIVP*, 6, pp.1239-1243.
 28. Haas, J., Ellhöft, K.H., Schack-Kirchner, H., & Lang, F. (2016). Using photogrammetry to assess rutting caused by a forwarder—a comparison of different tires and bogie tracks. *Soil Tillage Res.* 163:14–20.
 29. Haralick, R.M., Shanmugam, K., & Dinstein, I.H. (1973). Textural features for image classification. *IEEE Transactions on systems, man, and cybernetics*, (6), pp.610-621.
 30. Helenelund, K. V. (1974). Maarakennusmekaniikka. 137. Teknillisen korkeakoulun ylioppilaskunta, Otakustantamo, Otaniemi. 278 p. ISBN 951-671-060-3
 31. Helmy, M., Truong, T.T., Jul, E., & Ferreira, P. (2023). Deep learning and computer vision techniques for microcirculation analysis: A review. *Patterns*, 4(1).
 32. Howard, A., & Seraji, H. (2001). Vision-based terrain characterization and traversability assessment. *Journal of Robotic Systems*, 18(10), pp.577-587.
 33. Humeau-Heurtier, A. (2019). Texture feature extraction methods: A survey. *IEEE access*, 7, pp.8975-9000.
 34. Ishigami, G. (2008). Terramechanics based Analysis and Control for Lunar/Planetary Exploration Robots. PhD thesis submitted in Tohoku University, Japan.
 35. Janani, P., Premaladha, J., & Ravichandran, K.S. (2015). Image enhancement techniques: A study. *Indian Journal of Science and Technology*, 8(22), pp.1-12.
 36. Kane, J.R. (2010). Terrain Impacts from Vehicle Operations across Multiple Passes. Master's Thesis, University of Tennessee, 2010. http://trace.tennessee.edu/utk_gradthes/811
 37. Kar, C., & Banerjee, S. (2022). Tropical cyclones intensity estimation by feature fusion and random forest classifier using satellite images. *Journal of the Indian Society of Remote Sensing*, 50(4), pp.689-700.
 38. Koreň, M., Slančík, M., Suchomel, J., & Dubina, J. (2015). Use of terrestrial laser scanning to evaluate the spatial distribution of soil disturbance by skidding operations. *iForest*. 8:386–393.

39. Liu, C., Xu, A., Hu, C., Zhang, F., Yan, F., & Cai, S. (2020). A New Texture Feature Based on GLCM and Its Application on Edge-detection. In IOP Conference Series: Materials Science and Engineering (Vol. 780, No. 3, p. 032042). IOP Publishing.
40. Liu, K. (2009). Influence of Turning on Military Vehicle Induced Rut Formation. PhD diss., University of Tennessee. Available at http://trace.tennessee.edu/utk_graddiss/620.
41. Liu, K., Ayers, P., Howard, H., & Anderson, A. (2010). Influence of soil and water parameters on soil rut formation. *Journal of Terramechanics* 47(3): 143–150. <https://doi.org/10.1016/j.jterra.2009.09.001>.
42. Lowery, B., & Morrison, J.E. (2002). Soil Penetrometers and Penetrability. In: *Methods of Soil Analysis*, Part 4. Physical Methods, Soil Science Society of America, Inc., Madison, WI, 363-385.
43. Maclaurin E., B. (1990). The use of mobility numbers to describe the in-field tractive performance of pneumatic tyres. *Proceedings of the 10th International ISTVS Conference, Kobe, Japan, August 20-24, 1990*. I: 177-186.
44. Mallela, R., & Wang, H. (2006). Harmonising automated rut depth measurements - Stage 2. Land Transport New Zealand Research Report 277. ISBN 0-478-25388-5, ISSN 1177-0600.
45. Marques, O. (2011). *Practical image and video processing using MATLAB*. John Wiley & Sons.
46. McKyes, E. (1989). *Agricultural engineering soil mechanics*. ELSEVIER, Amsterdam-Oxford-New York-Tokyo.
47. Marques, O. (2011). *Practical image and video processing using MATLAB*. John Wiley & Sons.
48. Micheal, A.A., & Vani, K. (2015). Automatic mountain detection in lunar images using texture of DTM data. *Computers & Geosciences*, 82, pp.130-138.
49. Mohanaiah, P., Sathyanarayana, P., & GuruKumar, L. (2013). Image texture feature extraction using GLCM approach. *International journal of scientific and research publications*, 3(5), pp.1-5. <http://www.ijsrp.org/research-paper-0513/ijsrp-p1750.pdf> [Accessed on 20 Jul 2022]
50. Mohtashami, S., Eliasson, L., Jansson, G., & Sonesson, J. (2017). Influence of soil type, cartographic depth-to-water, road reinforcement and traffic intensity on rut formation in logging operations: a survey study in Sweden. *Silva Fennica* vol. 51 no. 5 article id 2018. 14 p. <https://doi.org/10.14214/sf.2018>
51. Mohtashami, S. (2022). GIS-based decision support systems to minimise soil impacts in logging operations. *Swedish University of Agricultural Sciences. Suvinen A. A GIS-based simulation model for terrain tractability. Journal of Terramechanics*. 2006 Oct 1;43(4):427-49.
52. Mulder, V.L., De Bruin, S., Schaepman, M.E., & Mayr, T.R. (2011). The use of remote sensing in soil and terrain mapping—A review. *Geoderma*, 162(1-2),

pp.1-19.

53. Narendra, V.G., & Hareesha, K.S. (2011). Study and comparison of various image edge detection techniques used in quality inspection and evaluation of agricultural and food products by computer vision. *International Journal of Agricultural & Biological Engineering*, 4(2), pp.83-90.
54. Orhei, C., Bogdan, V., Bonchis, C., & Vasiu, R. (2021). Dilated filters for edge-detection algorithms. *Applied Sciences*, 11(22), p.10716.
55. Pierzchała, M., Talbot, B., & Astrup, R. (2014). Estimating soil displacement from timber extraction trails in steep terrain: Application of an unmanned aircraft for 3D modelling. *Forests* 2014, 5, 1212–1223.
56. Pierzchała, M., Talbot, B., & Astrup, R. (2016). Measuring wheel ruts with close-range photogrammetry. *Forestry: An International Journal of Forest Research*, 89(4), pp.383-391.
57. Pradhan, B., Hagemann, U., Tehrany, M.S., & Prechtel, N. (2014). An easy to use ArcMap based texture analysis program for extraction of flooded areas from TerraSAR-X satellite image. *Computers & geosciences*, 63, pp.34-43.
58. Raper, R. L. (2005). Agricultural traffic impacts on soil. *Journal of Terramechanics*, 42, 259e280.
59. Sadiya, T.B., Eta, J., Oladiti, I., James, G.K., Shaba, H.A., Mamfe, V., Muhammad, S.O., Xu, M., Sha, J., & Sanusi M. (2017). Military Terrain Trafficability Analysis for North-East Nigeria: A GIS and Remote Sensing-Based Approach. *IOSR Journal of Mobile Computing & Application (IOSR-JMCA)* e-ISSN: 2394-0050, P-ISSN: 2394-0042. Volume 4, Issue I (Jan. - Feb. 2017), PP 34-46.
60. Salmivaara, A., Miettinen, M., Finér, L., Launiainen, S., Korpunen, H., Tuominen, S., Heikkonen, J., Nevalainen, P., Sirén, M., Ala-Ilomäki, J., & Uusitalo, J. (2018). Wheel rut measurements by forest machine-mounted LiDAR sensors—accuracy and potential for operational applications?. *International Journal of Forest Engineering*, 29(1), pp.41-52.
61. Scholander, J. (1974). Bearing capacity of some forest soils for wheeled vehicles. Some technical aspects and consequences. *Skogsmarks bärighet för hjulfordon. Några tekniska aspekter och konsekvenser. Specialnotiser från SFM Nr 14*. 97 p.
62. Sen, D., & Pal, S.K. (2010). Gradient histogram: Thresholding in a region of interest for edge detection. *Image and Vision Computing*, 28(4), pp.677-695.
63. Senatore, C., & Iagnemma, K. (2014). Analysis of stress distributions under lightweight wheeled vehicles. *Journal of Terramechanics*, Volume 51, February 2014, Pages 1-17, ISSN 0022-4898.
64. Shrivakshan, G.T., & Chandrasekar, C. (2012). A comparison of various edge detection techniques used in image processing. *International Journal of Computer Science Issues (IJCSI)*, 9(5), p.269.
65. Singh, K.K., Singh, D.K., Thakur, N.K., Dewali, S.K., Negi, H.S., Snehmani, &

- Mishra, V.D. (2022). Detection and mapping of snow avalanche debris from Western Himalaya, India using remote sensing satellite images. *Geocarto International*, 37(9), pp.2561-2579.
66. Singh, S. (2016). Remote sensing applications in soil survey and mapping: A Review *International Journal Of Geomatics And Geosciences* Volume 7, No 2, 2016
 67. Sion, B.D., Shoop, S.A., & McDonald, E.V. (2022). Evaluation of in-situ relationships between variable soil moisture and soil strength using a plot-scale experimental design. *Journal of Terramechanics*, 103, pp.33-51
 68. Smith, W.C. (2014). Modeling of Wheel-Soil Interaction for Small Ground Vehicles Operating on Granular Soil. A dissertation submitted in partial fulfillment of the requirements for the degree of Doctor of Philosophy (Mechanical Engineering) in The University of Michigan
 69. Smith, D.L.O., & Dickson, J.W. (1990). Contributions of vehicle weight and ground pressure to soil compaction, *Journal of Agricultural Engineering Research*, Volume 46,1990, Pages 13-29, ISSN 0021-8634.
 70. Sudha, S.K., & Aji, S. (2019). A review on recent advances in remote sensing image retrieval techniques. *Journal of the Indian Society of Remote Sensing*, 47, pp.2129-2139.
 71. Taheri, S., Sandu, C., Taheri, S., Pinto, E., & Gorsich, D. (2015). A technical survey of Terramechanics models for tire-terrain interaction used in modeling and simulation of wheeled vehicles. *Journal of Terramechanics*, 57, 1e22.
 72. Taylor, D.W. (1948). *Fundamentals of soil mechanics*. John Wiley & Sons, New York: 700 pp.
 73. Turnage, G. W. (1972). Tire selection and performance prediction for off-road wheeled vehicle operations. In *Proceedings of the 4th international ISTVS conference*. Stockholm, Sweden.
 74. Vennik, K., Keller, T., Kuk, P., Krebstein, K., & Reintam, E. (2017). Soil rut depth prediction based on soil strength measurements on typical Estonian soils. *Elsevier Journal of Bio systems engineering* 163 (2017)78-86
 75. Winarno, E., Hadikurniawati, W., Wibisono, S., Septiarini, A. (2021). Edge detection and grey level co-occurrence matrix (glcm) algorithms for fingerprint identification. In *2021 2nd International Conference on Innovative and Creative Information Technology (ICITech)* (pp. 30-34). IEEE.
 76. Wong, J.Y. (1978). *Theory of ground vehicles*. John Wiley & Sons, New York: 330 pp.
 77. Zhang, C. (2009) Monitoring the condition of unpaved roads with remote sensing and other technology. US DOT DTPH56-06-BAA-0002
 78. Zhang, J., Li, G.L., & He, S.W. (2008). Texture-based image retrieval by edge detection matching GLCM. In *2008 10th IEEE International Conference on High Performance Computing and Communications* (pp. 782-786). IEEE.

CHAPTER - 3

OPTIMAL DATA STORAGE OF COMMONLY OBSERVED RUT SHAPES USING PROPOSED MATHEMATICAL FORMULATIONS

In this chapter, rut shapes as investigated from different perspectives have been presented. The common types of rut shapes have been identified and then represented using different mathematical formulations. The effectiveness of these equations in achieving optimisation in storage of rut profile data has been discussed.

3.1 Introduction

The poor performance of military vehicles during World War II led to the beginning of research in trafficability at the Waterways Experiment Station (WES) in 1945 by U.S. Army Engineer (Willoughby and Turnag, 1988). The characterization of vehicular movement on different unpaved terrain features is a challenging task. The possibility of vehicular movement depends upon the surface topographical features and the condition of the underlying soil. Wong, 1978, Saarilahti, 2002 and others considered the effect of these obstacles both empirically and mathematically.

The soil is a dynamic material by nature, and parameters like density, moisture, constituents, etc. influence its state. Evaluating these parameters and their effect by conventional geotechnical instruments is laborious and time-consuming. ASAE standard EP542 give the procedure for estimating the strength of the soil using a cone penetrometer. However, this tool is suitable for a limited area only and is not convenient to map large areas. Various authors made attempts to explore alternate means for evaluating the soil condition. One such way is to observe the rut profile formed by the movement of vehicles on the unpaved ground. As strength decreases, the rut depth increases. Vehicle immobilization condition occurs when the rut depth is larger than the height of vehicle clearance (Affleck, 2005).

However, the rut profile is considered a better measure for mapping the influence of terrain on turnings and conditions like sandy terrain. A study is made on the changes in rut volume by vehicular movements on turnings (Liu, 2009). The equipment for mapping rut profiles varies from manual profilometers (Affleck, 2005) to several advanced profilers (Malella and Wang, 2006). Different technologies in use for rut measurement include ultrasonic sensors, point lasers, scanning lasers, and optical sensors. The manual profilometer is employed to collect data for point locations however, it is not suitable for continuous measurements of changes in terrain properties.

Photogrammetric methods, UAV, and drone platforms are employed to map the rut profiles of the soil (Nevalainen et al., 2017; Marra et al., 2018; 2021 and 2022). A forest machine-based LiDAR sensor is used by Salmivaara et al., 2018 to demonstrate it as a reliable and efficient way of collection of data pertaining to rut depth. The use of mobile laser profilometry for detecting forest road damage and its quantification is presented (Ferencík et al., 2019). The profiler used in this study had eight scanner units, which could cover the whole width of the road with 1000–5000 profiles per sec.

Thus, it is evident how much point cloud data processing is required to create a profile and do further analysis. The importance of rut measurement for applications like controller design and implementation is highlighted by Sandu et al., 2019. Applications of LiDAR have been advancing to mobile-based platforms. An iPhone-12 is used to present LiDAR-derived snow depth estimation (King et al., 2022). This work which used a lightweight LiDAR system brings out the need for research on reducing the computational load for efficient decisions.

The data collected by such scanners is vast. It needs heavy resources for storage, retrieval, and processing. Limited attempts are there to make use of the rut shape mathematically. In the study on the rut following robot, Ordonez, 2009 modeled the previously formed rut shape using a second-order polynomial.

Defining the shape of the deformed geometry is attempted in other applications too. A general equation for the deformed geometry of geosynthetic is given by Shukla and Sivakugan, 2009 that combines the two shapes to compute strain. A regression-based solution for estimating the settlement of reinforced soil foundation is attempted by Khosrojerdi, 2019.

This work presents a comparative analysis of some suitably selected mathematical formulations that could fit the typical shapes of ruts profiles. Nonlinear regression analysis is attempted on the observed data to identify the most suitable equation representing the rut profile in different conditions.

The suitability of these mathematical formulations for depicting rut profiles in different scenarios to achieve optimal data storage is discussed here.

3.2 Field Observation of Rut Profiles

The shape of the rut profile is typical of different terrain features, soil conditions, and vehicle running conditions. A manual rut profiler is used for this study to collect rut profile data in different kinds of terrain scenarios. This profiler consists of rods placed at intervals of 5 cm. The color marking of width 1 cm each is

made on each rod to facilitate the measurement of rut depth. Observation of rut impressions by movement of vehicles was made at a number of locations in open terrain of northern part of India. The representative sites for detailed studies were then identified in alluvial terrain of Chandigarh, Roorkee and the desertic terrain of Suratgarh. The sites in alluvial terrain having low to medium compaction level were identified in the agriculture fields whereas the sites having loose uncompacted sandy soil were identified in the desertic terrain. The rut profiles created in different unpaved terrain conditions of deserts and alluvial terrain in both dry and wet seasons were observed. This data is used for further analysis as given in this chapter.

As illustrated in Fig. 3.1, the shallow rut profile gets formed on alluvial soils of medium consistency. However, a deeper rut gets formed as the consistency of soil decreases.

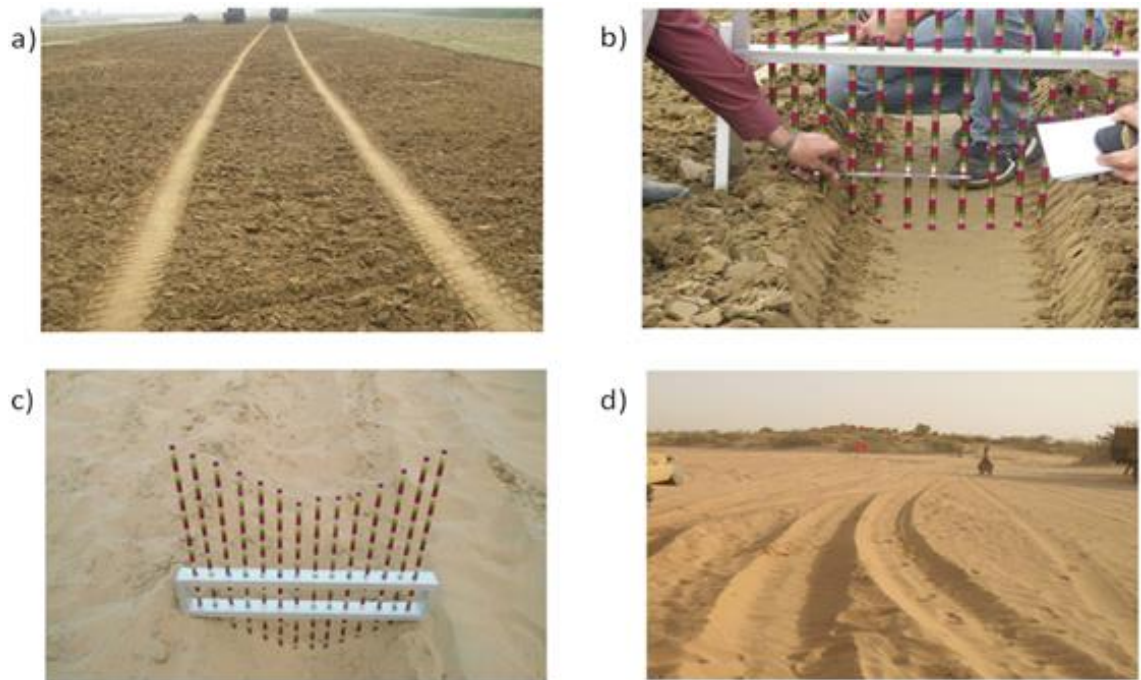


Fig. 3.1 Different shapes of Rut Profiles as observed in the field: a) Shallow rut in alluvial soils of medium consistency b) Deep rectangular rut on soils of low consistency c) Conical rut profile on frictionless soils of deserts d) Asymmetric rut shape created by vehicles on turnings

The rut profile in loose sandy dunal soils of deserts takes a conical shape as the sand from the edges pours in as the rut profile. Further, when the vehicle turns on curves, the rut shape becomes asymmetric due to lateral loads. There are other possible shapes too, but the following typical cases of rut shapes being most common during the movement in different off-road scenarios are considered here:

Case 1: Shallow rectangular shape rut in soils of medium consistency

Case 2: Deep rectangular/ trapezoidal shape rut in alluvial soils of low consistency

Case 3: Conical shape rut on the desert soils

Case 4: Asymmetric rut profile in soils on turnings by vehicle

The typical cases depicted in Fig. 3.2 are considered in this study to explore the optimal representation of these profiles using some mathematical formulations.

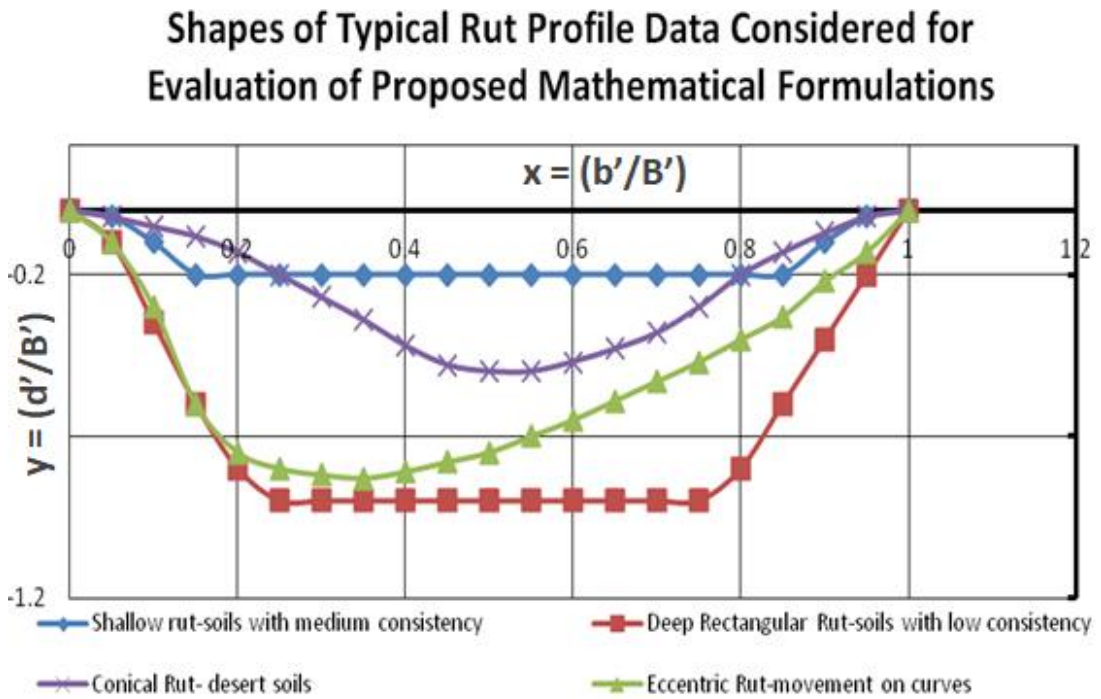


Fig. 3.2 Shapes of typical rut profile data considered for evaluation of proposed mathematical formulations

The authors normalized the cross-sectional rut profile to account for the variation of the rut profile at different places. Thus the depth y representing d'/B' at different sections x across the profile representing b'/B' is used. Here d' is the rut depth at different locations b' across the profile, and B' represents the total rut width. The consolidated rut profile data taken for study for all four cases are given in Table 3.1.

Table 3.1 Depth to width ratio of rut under different soil and movement conditions

Relative track width	Rut profiles by vehicles in different soil and movement conditions			
	On straight Paths		On Turnings by vehicles	
	Alluvial soil-medium consistency	Alluvial soil-low consistency	Desert soil-sand dunes	
b'/B' x	d'/B' y1	d'/B' y2	d'/B' y3	d'/B' y4
0	0	0	0	0
0.05	-0.02	-0.1	-0.1	-0.02
0.1	-0.1	-0.35	-0.3	-0.05
0.15	-0.2	-0.6	-0.6	-0.08
0.2	-0.2	-0.8	-0.75	-0.13
0.25	-0.2	-0.9	-0.8	-0.2
0.3	-0.2	-0.9	-0.82	-0.27
0.35	-0.2	-0.9	-0.83	-0.34
0.4	-0.2	-0.9	-0.81	-0.42
0.45	-0.2	-0.9	-0.78	-0.48
0.5	-0.2	-0.9	-0.75	-0.5
0.55	-0.2	-0.9	-0.7	-0.5
0.6	-0.2	-0.9	-0.65	-0.47
0.65	-0.2	-0.9	-0.59	-0.43
0.7	-0.2	-0.9	-0.53	-0.38
0.75	-0.2	-0.9	-0.47	-0.3
0.8	-0.2	-0.8	-0.4	-0.2
0.85	-0.2	-0.6	-0.33	-0.13
0.9	-0.1	-0.4	-0.22	-0.07
0.95	-0.02	-0.2	-0.13	-0.02
1	0	0	0	0

3.3 Development of Mathematical Formulations for Rut Profile

The authors explored many possible mathematical equations to develop a suitable mathematical formulation that explains rut profiles in varied scenarios. Based on the possibility of generating the most common types of shapes by changing the parameters, the authors chose the mathematical formulations. The equations thus chosen include polynomial equations of varying degrees, a generalized Gaussian shape equation, Fourier transformation, and a modified Bell-shaped equation.

As a common approach, the polynomial fit of different degrees is resorted for defining the rut shape. The polynomial equation thus chosen is:

$$y = f(x) = \sum_{i=0}^n a_i x^i \quad (3.1)$$

The degree of the polynomial equation improves the curve fitting for the most common shapes. As such, regression fit used polynomial equations starting with a quadratic equation and going up to the fourth degree to define the rut shapes. The rut shape in frictionless soils resembles an inverted shape of the Gaussian distribution of probability function. The generalized form of the equation for the Gaussian shape curve is therefore included and given as:

$$f(x) = a_1 . e^{-\left(\frac{x-a_2}{a_3}\right)^2} \quad (3.2)$$

Another way of describing the rut shape is similar to converting any harmonic function using Fourier transformation. This method approximates the curve by using a combination of various sine and cosine curves of different frequencies, as given below:

$$f(x) = \frac{a_0}{2} + \sum_{n=1}^{\infty} a_n \cos\left(\frac{nx}{L}\right) + \sum_{n=1}^{\infty} b_n \sin\left(\frac{nx}{L}\right) \quad (3.3)$$

Here, the coefficients are:

$$a_0 = \frac{1}{L} \cdot \int_{-L}^L f(x) dx \quad (3.4)$$

$$a_n = \frac{1}{L} \cdot \int_{-L}^L f(x) \cos\left(\frac{nx}{L}\right) dx \quad (3.5)$$

$$b_n = \frac{1}{\pi} \cdot \int_{-L}^L f(x) \sin\left(\frac{nx}{L}\right) dx \quad (3.6)$$

The function combines various frequencies and amplitudes of the sine and cosine curves. In the present case, different shapes of rut are represented by considering up to three terms (n) of the above equation. The rut shapes on soils of different consistency also resemble the shape of a bell function, and accordingly, the bell shape function is thus chosen and given as:

$$f(x) = \frac{a_1}{1 + \left| \frac{x - a_2}{a_3} \right|^{a_4}} \quad (3.7)$$

Here, the coefficient a_1 impacts the variation in rut width and depth. The coefficient a_2 determines the center, a_3 represents the rut width, and a_4 the side slope of the membership function curve. Therefore, the use of a modified form of the generalized bell equation, which combines variation in the side slopes, is considered and is given below:

$$f(x) = \frac{a_1}{1 + \left| \frac{x - a_2}{a_3} \right|^{a_4} + \left| \frac{x - a_2}{a_5} \right|^{a_6}} \quad (3.8)$$

All these equations use the normalized rut shapes. They represent the dimensionless ratio of rut depth to its width at various relative locations across the rut profiles. The parameters $a_0, a_1, a_2, a_3, a_4, a_5$ and a_6 are the coefficients of the proposed equations.

3.4 Results and Discussion

The suitability of proposed equations is first analyzed based on regression fit on rut data observed in different scenarios. As a general observation, by taking typical values of the variables, one can generate different shapes using any of the proposed mathematical formulations. Fig. 3.3 illustrates the shapes of curves as obtained using mathematical formulations.

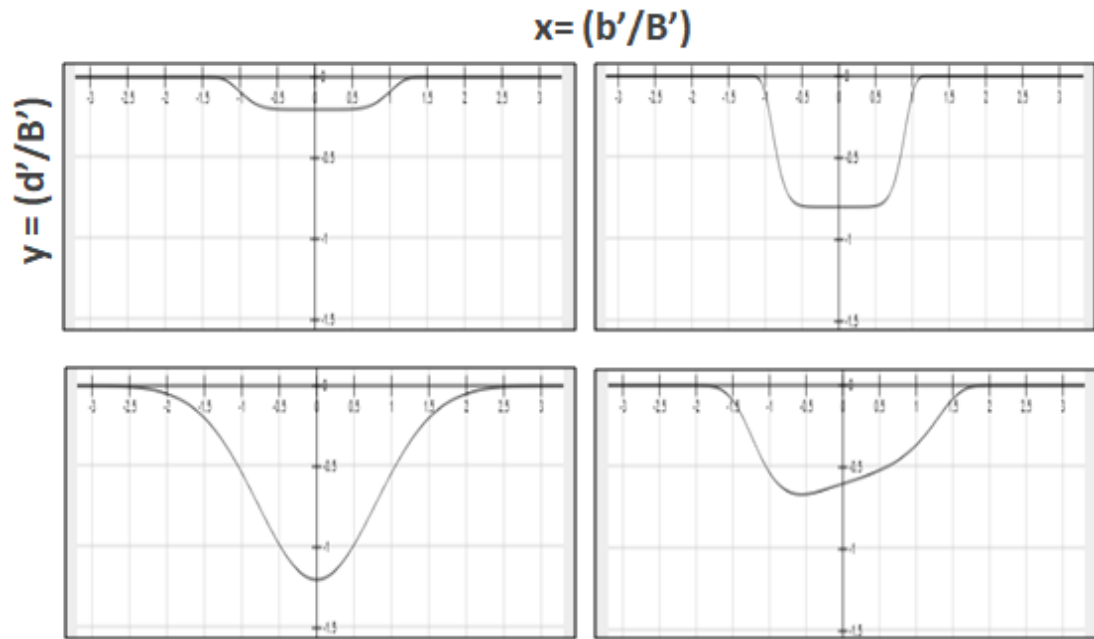


Fig. 3.3 Different shapes as generated using proposed mathematical formulations by varying the input parameters to match the commonly observed rut shapes in various terrain types

It indicates that using any of the proposed mathematical formulations, one can generate the shape of rut profiles in scenarios observed in the field. It also leads to the inference that the selected equations are reasonable and logical. These equations can thus be used as an alternate to represent the rut profiles data. The potential use could be to achieve the optimal data storage requirements as it becomes mandatory in systems using point cloud as given by Ferencík, 2019.

Further, to evaluate the effectiveness of different proposed mathematical formulations, authors employed non-linear regression analysis. The online desmos graphing tool facilitated the computation of regression coefficients and the degree of fit. Table 3.2 displays the result of regression analysis representing the efficacy of different mathematical formulations in various conditions.

Table 3.2 Regression fit results for rut profile in different test cases

S No.	Type of Curve	Regression fit result for various types of curves							R ²	C
		a ₀	a ₁	a ₂	a ₃	a ₄	a ₅	a ₆		
Case1: Rut profile in alluvial soils of medium consistency										
1	Polynomial curve of 2nd degree	-0.022	-0.834	0.8338	-	-	-	-	0.806	7.0
2	Polynomial curve of 3rd degree	0.022	-0.834	0.8338	1E-15	-	-	-	0.806	5.25
3	Polynomial curve of 4th degree	0.026	-2.074	6.7335	-9.32	4.66	-	-	0.924	4.2
4	Generalised Gaussian shape equation	-	-0.202	0.5	-0.414	14.23	-	-	0.991	5.25
5	Fourier Series equation	-0.006	-0.225	0	-0.064	0	0.021	0	0.941	3.0
6	Generalised Bell shape equation	-	-0.201	0.5	0.401	22.58			0.998	5.25
7	Modified Generalised bell shaped Equation	-	-0.201	0.5	5	30	-0.401	22.58	0.998	3.5
Case2: Rut profile in alluvial soils of low consistency										
1	Polynomial curve of 2nd degree	-0.027	-3.894	3.8599	-	-	-	-	0.934	7.0
2	Polynomial curve of 3rd degree	-0.02	-3.991	4.1095	-0.166	-	-	-	0.934	5.25
3	Polynomial curve of 4th degree	0.095	-6.933	18.109	-22.28	11.06	-	-	0.970	4.2
4	Generalised Gaussian shape equation	-	-0.907	0.5046	-0.407	6.495	-	-	0.996	5.25
5	Fourier Series equation	-0.868	0.4301	0.0156	-0.447	-3E-04	0.879	0.018	0.994	3.0
6	Generalised Bell shape equation	-	-0.9	0.5039	0.38	9.645	-	-	0.993	5.25
7	Modified Generalised bell shaped Equation	-	-0.906	-2.806	-3.692	85.57	2.928	-79.45	0.996	3.5
Case 3: Rut profile on sand dunes of desert soil										
1	Polynomial curve of 2nd degree	0.118	-2.118	2.0596	-	-	-	-	0.887	7.0
2	Polynomial curve of 3rd degree	0.072	-1.488	0.4453	1.076				0.903	5.25
3	Polynomial curve of 4th degree	-0.028	1.0727	-11.74	20.33	-9.625			0.993	4.2

S No.	Type of Curve Regression Coefficients	Regression fit result for various types of curves							R ²	C
		a ₀	a ₁	a ₂	a ₃	a ₄	a ₅	a ₆		
4	Generalised Gaussian shape equation	-	-0.497	0.5286	-0.285	2.369			0.997	5.25
5	Fourier Series equation	-0.119	-0.219	0.0108	0.042	0.023	0.119	-0.026	0.999	3.0
6	Generalised Bell shape equation	-	-0.48	0.53	0.243	3.82	-	-	0.990	5.25
7	Modified Generalised bell shaped Equation	-	-0.572	1.2327	0.476	-5.815	-0.924	11.45	0.998	3.5
Case 4: Rut profile on turnings in soils										
1	Polynomial curve of 2nd degree	-0.117	-2.903	3.1181	-	-	-	-	0.887	7.0
2	Polynomial curve of 3rd degree	0.043	-5.087	8.7144	-3.731	-	-	-	0.970	5.25
3	Polynomial curve of 4th degree	0.089	-6.286	14.419	-12.74	4.506	-	-	0.978	4.2
4	Generalised Gaussian shape equation	-	-0.768	0.4547	-0.381	3.884	-	-	0.912	5.25
5	Fourier Series equation	-0.334	-0.244	-0.167	-0.192	0.023	0.345	0.007	0.989	3.0
6	Generalised Bell shape equation	-	-0.758	0.4503	0.341	5.755	-	-	0.911	5.25
7	Modified Generalised Bell shaped Equation	-	1.1156	1.0156	0.324	-1.368	-0.881	24.06	0.996	3.5

Here, the compression ratio C represents the storage efficiency. It is the ratio of the number of original datasets to the number of parameters needed to represent the profile using mathematical formulation. The value of C in Table 2 indicates that one can achieve significant levels of data compression over conventional techniques by using the proposed mathematical models. The most optimal mathematical formulation is the one which represents the rut profile using least number of variables to achieve the desired goodness of fit. In the currently used manual observation of profiles, the compression ratio for the straight patches is 5.25. The %age of data compression calculated as $(1-1/C)*100$ indicates that one can achieve more than 80% compression on the straight patches. The value computes for areas on turning is 71%, while the accuracy level is maintained better than 99% in both cases. This additional data compression could pave the way for efficient data storage and set the basis for an onboard decision aid. The computational aspects will depend upon the selected mathematical formulation, regression type, algorithm design, parallel processing, multithreading aspects, etc. Here, the purpose is to

explore the potential of mathematical formulations in defining rut shapes to address the issues related to real-time applications. The Fig. 3.4 shows typical regression fit curves on the rut profile data of medium-consistency soils. The figure shows the relative comparison of various mathematical formulations on the observed data.

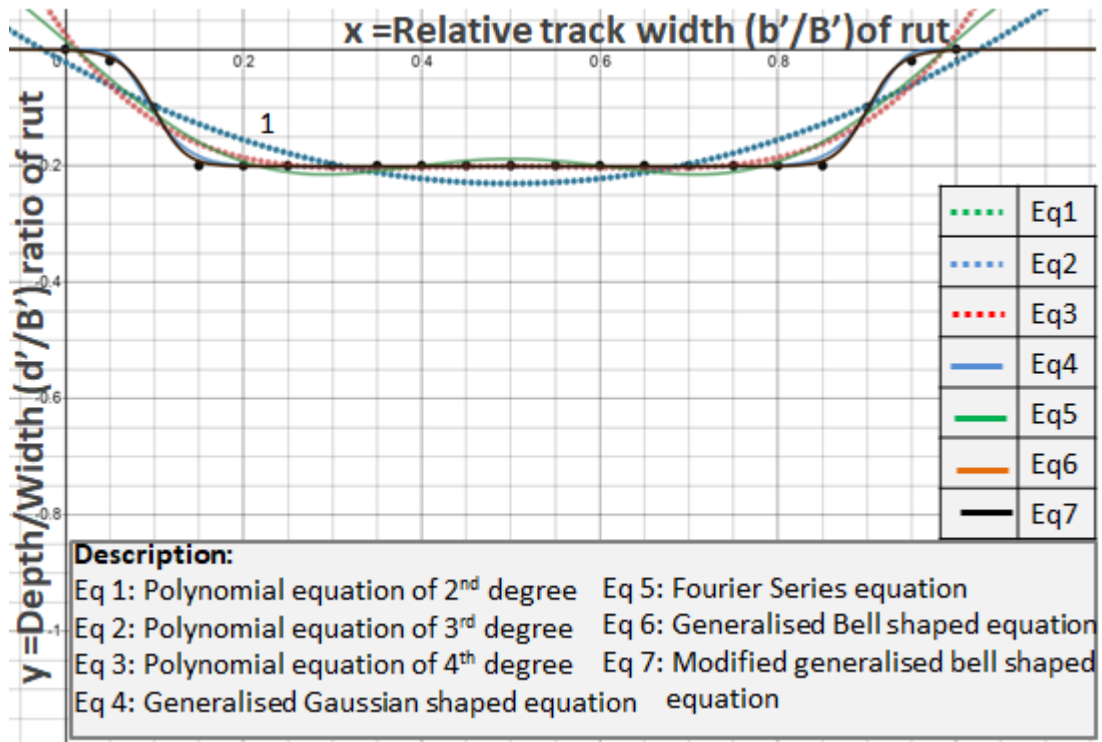


Fig. 3.4 Typical Regression Fit curves on the rut Profile data of medium consistency soil

The graph containing the data and different regression curves indicate that the curves using the proposed mathematical formulations follow the observed data for almost all the test cases. However, for identifying the most suitable predictive equation of the rut profile, the comparative analysis reveals further detail. The analysis of the regression fit shown in the table also indicates that in almost all the cases, the regression fit improves with the increased degree of the polynomial. One can plan to improve the utility of rut profiles by representing better the rut shape as given by Ordonez, 2009. The study also brings out an analysis of an equivalent number of variables used in the regression curves. The comparison given for the third-degree polynomial fit with other mathematical formulations reveals valuable inferences. A considerable improvement is there in the generalized Gaussian shape function than the polynomial equations when movement is on the straight patches.

The goodness of fit is relatively less along the curves. The higher degree equations are, therefore, employed for a better fit. The analysis of regression fit results also indicates that while using the proposed modified generalized bell shape

equation, the results are much better in almost all the scenarios. However, the function needs six input parameters to represent the rut shape.

From the above analysis, some useful inferences are drawn. The generalized Gaussian form or Bell shape function may be advantageous for obtaining precision and optimal storage on straight patches. However, the modified generalized bell-shaped equation is more accurate on the curves.

3.5 Conclusion and Suggestions for Further Work

Results suggest that one can employ mathematical formulations to represent the rut shapes for optimal data storage. Various mathematical formulations are analyzed, and non-linear regression analysis is attempted on the commonly observed rut shapes. One can employ a generalized Gaussian or bell shape equation to represent the rut profile on the straight patches. However, on turnings, the proposed modified bell-shaped equation leads to better precision and optimization.

By using the proposed modified bell-shaped function on these common shapes, the R^2 value moved above 0.98. It could fetch an additional compression of over 80% on straight patches and 71% on turnings. Although complex scenarios could be dealt with separately, an optimal representation of the most common rut shapes can aid the development of an efficient decision support system.

An interesting analysis would be to explore some complex cases in the future. For instance, one may encounter a class wherein two separate rut profiles are blended to create a single rut class. Here some additional mathematical representations may make the profile representation more generic and can address some more rut classes.

In situations where complexity in rut morphologies is there, such as on crossings and different pathways, efforts need to be there to represent the rut profile in a better way. The present work focuses on the new ways to represent optimally the rut profile in different terrain conditions using mathematical equations. It will be a step towards developing an efficient onboard system to store and infer different rut profile-based properties. The categorization of rut profiles, mapping and characterizing the spatial variation of soil type and its condition, and inference about the trafficable state of terrain in near real-time mode are some directly related benefits. In future activities, one can explore the machine learning approach to train the system with rut profile data of varied field scenarios. It can make predictive analysis about various terrain properties and classes in different field running conditions.

The standard cases given in this study are observed prominently in actual off-road conditions. The proposed method indicates the utility of representing the rut shapes mathematically to achieve optimization. This study is a step towards bringing efficiency in addressing various issues of vehicular mobility during operational needs.

3.6 References

- [1] Willoughby, W. E., & Turnage, G. W. (1988). Review of a procedure for predicting rut depth, Unpublished memo.
- [2] Wong, J.Y. (1978). "Theory of ground vehicles," John Wiley & Sons, New York.
- [3] Saarilahti, M. (2002b). Soil Interaction Model- Development of a Protocol for Ecoefficient Wood Harvesting on Sensitive Sites (Ecowood)," Appendix No. 8 Forest Soil Properties.
- [4] EP542, A. S. A. E. (1999). Procedures for using and reporting data obtained with the soil cone penetrometer. St. Joseph, MI.
- [5] Affleck, R. T. (2005). Disturbance measurements from off-road vehicles on seasonal terrain. US Army Corps of Engineers. Engineer Research and Development Center, 2005, ERDC/CRREL TR-05e12. <http://hdl.handle.net/11681/5315> [Accessed on 11 May 2021].
- [6] Liu, K. (2009). Influence of Turning on Military Vehicle Induced Rut Formation," PhD diss., University of Tennessee. Available at http://trace.tennessee.edu/utk_graddiss/620.
- [7] Mallela, R., & Wang, H. (2006). Harmonising automated rut depth measurements: Stage 2 (No. 277). Land Transport New Zealand.
- [8] Nevalainen, P., Salmivaara, A., Ala-Ilomäki, J., Launiainen, S., Hiedanpää, J., Finér, L., & Heikkonen, J. (2017). Estimating the rut depth by UAV photogrammetry. *Remote Sensing*, 9(12), 1279.
- [9] Marra, E., Cambi, M., Fernandez-Lacruz, R., Giannetti, F., Marchi, E., & Nordfjell, T. (2018). Photogrammetric estimation of wheel rut dimensions and soil compaction after increasing numbers of forwarder passes. *Scandinavian Journal of Forest Research*, 33(6), 613-620.
- [10] Marra, E., Wictorsson, R., Bohlin, J., Marchi, E., & Nordfjell, T. (2021). Remote measuring of the depth of wheel ruts in forest terrain using a drone. *International Journal of Forest Engineering*, 32(3), 224-234.
- [11] Marra, E., Laschi, A., Fabiano, F., Foderi, C., Neri, F., Mastrolonardo, G., ... & Marchi, E. (2022). Impacts of wood extraction on soil: Assessing rutting and soil compaction caused by skidding and forwarding by means of traditional and innovative methods. *European Journal of Forest Research*, 1-16.
- [12] Salmivaara, A., Miettinen, M., Finér, L., Launiainen, S., Korpunen, H., Tuominen, S., Heikkonen, J., Nevalainen, P., Sirén, M., Ala-Ilomäki, J. &

- Uusitalo, J. (2018). Wheel rut measurements by forest machine-mounted LiDAR sensors—accuracy and potential for operational applications?. *International Journal of Forest Engineering*, 29(1), 41-52.
- [13] Ferencík, M., Kardoš, M., Allman, M., & Slatkovská, Z. (2019). Detection of forest road damage using mobile laser profilometry. *Computers and Electronics in Agriculture*, 166, 105010.
- [14] He, R., Sandu, C., Khan, A. K., Guthrie, A. G., Els, P. S., & Hamersma, H. A. (2019). Review of terramechanics models and their applicability to real-time applications. *Journal of Terramechanics*, 81, 3-22.
- [15] King, F., Kelly, R., & Fletcher, C. G. (2022). Evaluation of LiDAR-derived snow depth estimates from the iPhone 12 Pro. *IEEE Geoscience and Remote Sensing Letters*, 19, 1-5.
- [16] Ordonez, C., Chuy, O. Y., Collins, E. G., & Liu, X. (2009, October). Rut tracking and steering control for autonomous rut following. In 2009 IEEE International Conference on Systems, Man and Cybernetics (pp. 2775-2781). IEEE.
- [17] Shukla, S. K., & Sivakugan, N. (2009). A general expression for geosynthetic strain due to deflection. *Geosynthetics International*, 16(5), 402-407.
- [18] Khosrojerdi, M., Xiao, M., Qiu, T., & Nicks, J. (2019). Nonlinear equation for predicting the settlement of reinforced soil foundations. *Journal of Geotechnical and Geoenvironmental Engineering*, 145(5), 04019013.

CHAPTER - 4

EXPERIMENTAL INVESTIGATION OF SOIL MOISTURE AND NUMBER OF PASSES IN IDENTIFYING THE MAXIMUM SOIL DISTRESS LEVEL FOR EMERGENCY MOVEMENTS

The experimental studies have been conducted for understanding the effect of soil moisture and the number of vehicle passes on soil distress levels. *The utility of the study has been explored for identifying the maximum soil distress level in the area to plan emergency movement on the unpaved terrain.*

4.1 Introduction

The communication network is the lifeline for any area. The flooding situation can arise in plains, the foothills or any place in mountains wherein the excessive rainfall can disrupt the conventional routes. In such situations, in order to access the areas for the essential services, the unpaved off-road routes are followed. These routes can provide vital links to access these areas impacted by such disasters. The soil conditions in such situations are not always convenient for movement of vehicles. The trafficability analysis of any area is a topic of research for varied fields.

The vehicles in industries like forestry, agriculture, and in Defence frequently use the unpaved terrain for movement. Moreover, in many operations like firefighting, emergency response, alternate routes during peak etc., the unpaved tracks are followed. The surface features together with the existing state of ground, govern the trafficability of such areas. The movement of vehicles in such unpaved areas leads to soil distress. Conventional method for evaluation of soil condition impacting trafficability is time consuming and complex. The alternate means are therefore studied by various researchers. The rut depth caused by vehicular movement on the unpaved terrain reflecting the prevalent state of soil is used to evaluate mobility of vehicles. Fragkos et al., 2019 described about use of clustering and autonomous operations in planning evacuation strategy in disaster struck areas.

Tremendous research continues to study the relevance of rut formed by vehicular movement. The improved state of soil on the earlier vehicle tracks is used for applications like robotics-based operations and for night safari due to better stability (Ordóñez, 2009). Singh et al., 2022 studied the improvement aspects of utilizing the geosynthetic reinforcement on unpaved road. Kalra et al., 2023 proposed using a non-linear regression model for achieving optimal storage of rut profile data for efficient decisions. Detection of rut impressions is of significance in different

strategic missions too particularly for operations in dark conditions posing low contrast. Kalra et al., 2023 suggested various alternate indices that account for tone and texture of rut improving the contrast.

Primarily, the vehicle immobilisation condition occurs when the rut depth by movement of vehicle is greater than the height of clearance under the vehicles (Affleck, 2005). When studied for different dynamic and seasonal changes, it reveals the max distress condition that prevailed in the area. There could be many virgin areas which may not be bearing the signature of vehicular movement. In such a scenario, the study of rut under different dynamic conditions may reveal vital inputs about the likely soil distress level and the possible trafficability condition in any area.

The wheel sinkage and rut depth are although similar but for all practical purposes, one may ignore the difference. The wheel sinkage comprises of two parts i.e. static and dynamic sinkage. The static sinkage is dependent upon the vertical load on wheel, while the wheel rotation governs the dynamic sinkage. Bekker, 1960 gave the following equation to determine static sinkage:

$$p(h) = \left(\frac{k_c}{b} + k_\phi \right) h^n \quad (4.1)$$

where, $p(h)$ represents the static stress under a plate, h the sinkage and b represents the smaller width of the plat. The coefficients k_c and k_ϕ represent cohesive modulus and frictional modulus of deformation respectively, while n here refers to exponent of deformation. These values of k_c , k_ϕ and n are computed using plate-sinkage tests. Further improvements in this model are made by Reece, 1965. Numerical solution is attempted by Ishigami et al., 2007 for understanding the wheel rotation based dynamic sinkage.

The factors affecting soil disturbance, its compaction and the associated trafficability are presented as review for timber harvesting in the forests (Rab et al., 2005). Raper, 2005 brought out that maximum compaction results when the loading is applied at soil moisture conditions near to its field capacity. Liu et al., 2010 presented the vehicle rut is impacted by type of military vehicle, the moisture and texture of soil.

Various models have been suggested to predict the rut depth. Willoughby and Turnage, 1988 gave following equation for the multi-pass effect of wheeled vehicles:

$$z = \frac{5d\sqrt{N}}{\left(\frac{RCI \cdot b \cdot d}{W \left(1 - \frac{\delta}{h}\right)^{\frac{3}{2}} S^{\frac{1}{5}}} \right)^{\frac{5}{3}}} \quad (4.2)$$

where, z is the sinkage in mtr, RCI is the rating cone index in kPa d is the unloaded tyre diameter in mtr, b is the unloaded tyre width in mtr, W is the vertical load of wheel in kN, δ is the deflection of loaded tyre in mtr, h is the section height of unloaded tyre in mtr, N is the number of Wheel passes, and S is the Slip of wheel in decimal. A very relevant study carried out by Yokel et al., 1980 in regard to identifying the soil properties that determine the stability of excavations against cave-in. The study also gives details about the associated simple field and laboratory tests which can help in determining the soil likely under distress considering its collapse potential. Kogure et al., 1985 made a cone index based study of soils in the critical layer influencing trafficability.

Another common approach is there in Terramechanics that utilizes the values of CI or RCI for computing a dimensionless number, called as wheel or the mobility Numerics. Maclaurin, 1990 proposed the following model for sinkage in the fine-grained soils:

$$z = d \cdot \frac{0.224}{N_{CI}^{1.25}} \quad (4.3)$$

Here, N_{CI} is the wheel Numeric given by Turnage, 1972 as below:

$$N_{CI} = \frac{CI \cdot b \cdot d}{W} \sqrt{\frac{\delta}{h}} \cdot \frac{1}{1 + \frac{b}{2d}} \quad (4.4)$$

where CI is the cone index in kPa, δ is the tyre loaded deflection in mtr. Scholander, 1974 described about the general equation of settlement under repetitive loading as,

$$Z_n = Z_1 \cdot N^{\frac{1}{a}} \quad (4.5)$$

where, Z_1 is the sinkage after one loading, Z_n is sinkage after N loadings or the number of passes. The parameter a is the multi-pass coefficient which is dependent

upon the soil properties and the loading condition. Hatchell et al., 1970 in their study brought out that only four passes of a tractor could achieve 90% of the maximum level of density in Atlantic Coastal Plain soils in USA. Abebe et al., 1989 in the study of effect on soil compaction by the multiple passes of a rigid wheel brought out that most of the compaction by the loaded wheel occurs during the first three passes only. The value of a is suggested as 2 for the softer soil that is loaded with small loads; 3-4 for the medium strength soil under medium loads and is recommended as 4-5 for the heavily loaded soils with higher bearing capacity (Saarilahti, 2002). The change in the rut volume by turning of vehicles is studied using profile by Liu, 2009. Vennik et al., 2017 presented the impact of multiple passes of the military vehicles.

Various authors employ the Nominal Ground Pressure (NGP) as the indicator of ground pressure by different vehicles. It is computed by the equation proposed by Owende et al., 2002 as:

$$NGP = \frac{W}{r.b} \quad (4.6)$$

where, W is the wheel load in kN, r is the wheel radius in mtr and b is the tyre width in mtr. The typical NGP ranges depend upon the vehicle configuration and for forest machinery, it ranges from 30 -70 kPa. In order to minimise the impact of movement on soil surface, the NGP and the soil bearing capacity should be matched. A relationship between rut depth and CI/NGP has been given to decide about the operational limit wherein CI/NGP ratio lies between 3 to 7. Among various ways to predict trafficability of terrain, a review of various mobility matrices is given by Wong et al., 2020.

In this work, attempt is made to use the information about soil distress levels to predict the suitability of terrain for different emergency scenarios. In general, the random and unplanned movement on the unpaved areas, creates soil distress condition as per the prevalent state. The low-lying pockets, the agricultural fields etc. which are prone to water logging are impacted highly during the rainy seasons.

In the current study, rut based study is conducted for ascertaining the suitability of areas for mobility of vehicles during different emergencies. The rut depth reflecting soil distress level and having strong correlation with trafficability condition is studied under different dynamic conditions. The multi-pass effect on the rut depth was also carried out to understand the maximum possible soil distress in the area impacting vehicular movement.

4.2 Materials and Methods

In order to address the issue of soil distress, the prevalent soil strength is measured under different dynamic conditions using handheld cone penetrometer. In order to map the behavior of different soil, an ALS vehicle, 4x4 is used for the study. The vehicle had unladed weight of 7750 kg and its wheel diameter was 1.26 m. The soil distress level is observed after repeated movement of vehicle on the same track. The rut measurement due to vehicular movement is carried out using manual rut profilometer.

To evaluate the maximum distress level of soil, the trial site was chosen in an area where the water logging occurred in the past due to rains. The trials were conducted and observations were made in different locations of the area where the moisture levels varied from dry to slightly moist to moist and wet or fully saturated as shown in Fig. 4.1.

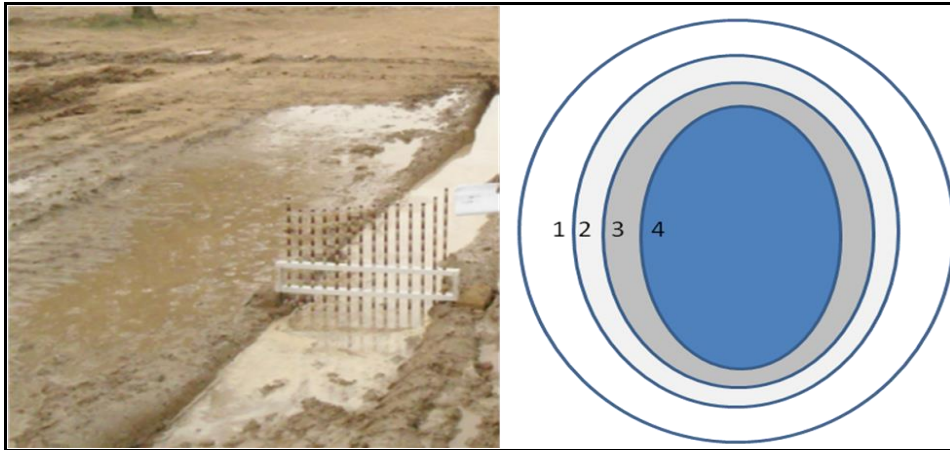


Fig. 4.1 The study conducted under varied moisture conditions 1) Dry Area 2) Slightly Moist 3) Moist area and 4) Flooded area

The vehicle was made to move on the same track in forward and reverse direction and the effect on the rut profile was monitored as per details indicated in the above Fig. 4.2. The rut profile was measured after 1, 10 and 25 passes on different terrain conditions.

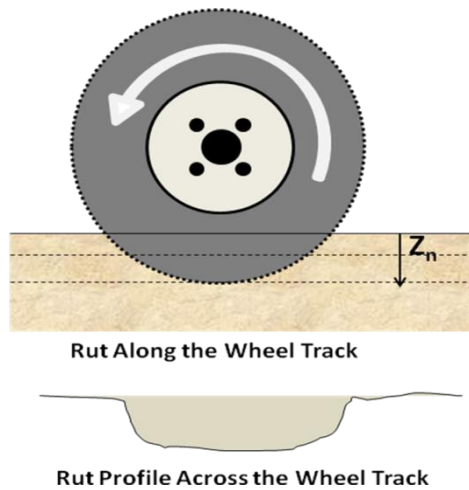


Fig. 4.2 Rut profile created by vehicle on soil a) Along the wheel track b) Across the wheel track

The maximum level of average rut depth indicating the soil distress was noted for each case. The prevalent soil strength condition in the area was also measured using the cone penetrometer to study the influence on soil distress levels.

4.3 Study Area

The study was carried out on the semi-arid region of Hisar, Haryana. The selected site was an open unpaved patch that was devoid of vegetation. There had been rainfall event in the area that led to formation of water logged condition in some pockets.

4.4 Results and Discussion

The soil strength being the prime factor determining the distress level of the soil, the study was made to measure the same under different dynamic conditions of soil. The soil strength along the depth at different places with varied moisture conditions was measured using cone penetrometer. The results of soil strength profile as observed in field are consolidated as given in Fig. 4.3.

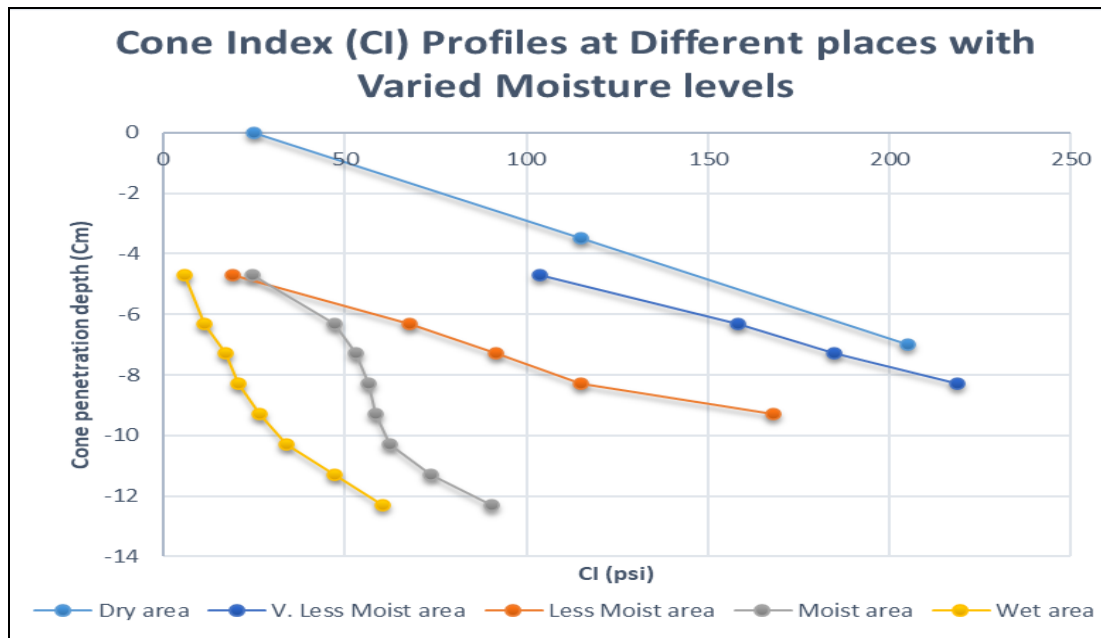


Fig. 4.3 Cone Index variations under different moisture conditions in study area

The high level of soil strength variation indicates the impact of soil moisture on the strength properties of the soil. The associated disturbance level is also monitored as shown in Fig. 4.4. Here the soil rut depth variation is indicated with number of vehicle passes on different portions of the tracks. The plot indicates that the initial level of soil distress occurs as per the initial strength of soil wherein the changes are brought in by the soil moisture and density after ploughing.

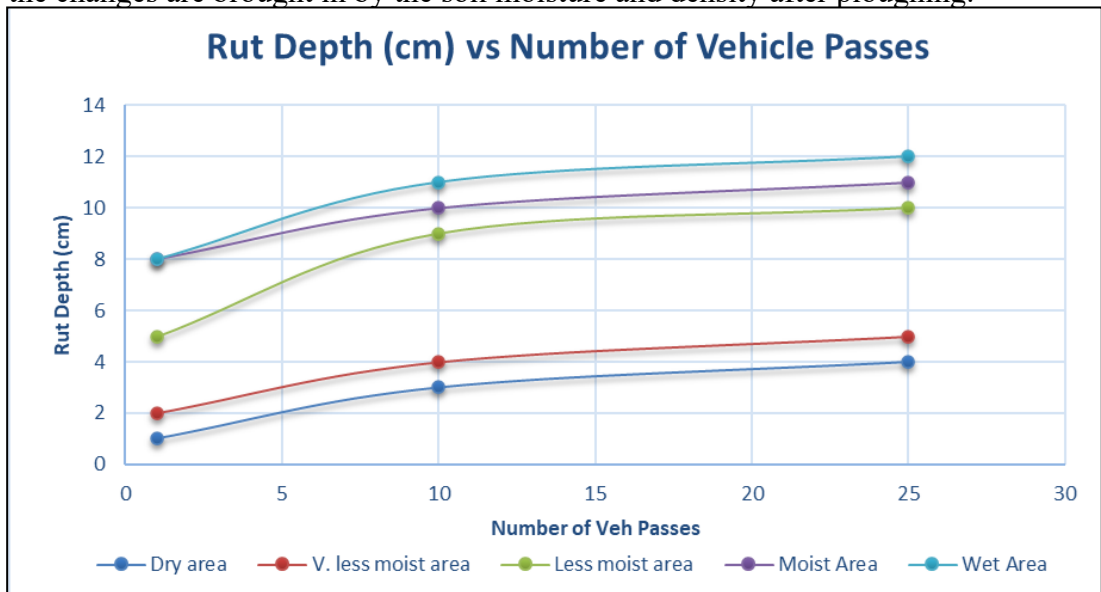


Fig. 4.4 Rut depth after 1 and 'n' passes on different terrain features

The plot indicates that after initial levels of rut, the rate of changes in rut seems to be consistent for different levels of soil moisture and also for ploughed area. The cone index profile as in Fig. 4.3 also indicates that the underlying strata are mostly intact although the top layer is influenced by water accumulation. The water logged condition continued for days in this area reflects a string and impermeable strata below top depth. The effect of tillage practices was there but upto limited depth. The findings are in conformity with the views given by Hatchell et al. (1970) who opined that 90% of maximum level of density could be achieved after just four passes of a tractor.

The maximum value of average rut depth as shown in each case in Fig. 4.4 also indicates the maximum distress level in the area. At one of the locations in wet areas, excessive wheel slip was observed, indicating that these kind of areas when remained water logged, could lead to immobilisation. Similar studies could be extended further to map the dynamics of other areas too. This can become a useful tool for identifying the areas as per the maximum soil distress level.

Another study was conducted to understand the limiting condition for movement. The tyres of vehicles observed excessive slip when passing through the flooded condition. The analysis was carried out by computing the Nominal Ground Pressure (NGP) value for the trial site which in this case arrived at 20.52 psi. The ratio of observed cone index at 6 cm level reaches from 8 in dry condition to approx. 1 in wet condition. The lower strata here indicate stronger conditions, while the top weaker strata caused slippery condition and trafficability issue. The soil strata in critical layer as given by Kogure et al., 1985 needs further detailed study to infer precisely the role in differentiating better the measures influencing different kinds of trafficability issues. Nevertheless, its manifestation in causing excessive rut to limits which restrain the movement of vehicles is important to be considered here from the perspective of vehicular movement planning during emergencies.

4.5 Conclusion

Some key conclusions drawn from the study are:

1. The rut depth caused by movement of vehicles can provide a vital input about the suitability of the area for movement in case of emergencies. The soil distress level measured through rut depth by the vehicular movement in the area can provide useful information about the limit about vehicular mobility in the area.
2. The rut depth increased as the soil moisture level increased. It reached maximum level when flooded.

3. If the flooding continues for days in the depressions or low lying areas, it is indicative of impermeable and compact strata could be there below certain level. The effect of moisture on maximum distress level remained similar.

4. The maximum soil distress level and rut depth that could be expected in the area determines mobility potential in such areas. The initial level of soil distress occurs as per the initial condition of the soil whereas further changes in distress level could be brought in by the soil moisture and altered compaction level after ploughing etc.

5. The present studies are conducted on semi-arid terrain. The soil distress level could be higher when the fine grain or organic soils are there. Studies on similar approach by monitoring dynamic variation of soil under different moisture conditions may be conducted in these areas where the possibility of off-road vehicular movement exists.

6. Depending upon the expected maximum soil distress level, the preventive steps could be decided. As the water level in the area is the major contributing factor, the pockets could be identified which have relatively higher elevation in the area. The unpaved track passing through such areas may be pre-marked and if possible pre-compacted to allow safe movement in the area during emergencies.

The above study indicates the role of mapping the maximum soil distress level for planning movement in such flood impacted areas as part of managing the emergency support.

4.6 References

1. Abebe, A. T., Tanaka, T., & Yamazaki, M. (1989). Soil compaction by multiple passes of a rigid wheel relevant for optimization of traffic. *Journal of Terramechanics*, 26(2), 139-148.
2. Affleck, R. T. (2005). Disturbance measurements from off-road vehicles on seasonal terrain. US Army Corps of Engineers. Engineer Research and Development Center, 2005, ERDC/CRREL TR-05e12. <http://hdl.handle.net/11681/5315> [Accessed on 11 May 2021].
3. Bekker, M. G. (1960). Off-the-road locomotion. Research and development in terramechanics. University of Michigan Press, Ann Arbor. 220 s.
4. Fragkos, G., Apostolopoulos, P. A., & Tsiropoulou, E. E. (2019). ESCAPE: Evacuation strategy through clustering and autonomous operation in public safety systems. *Future Internet*, 11(1), 20. <https://doi.org/10.3390/fi11010020>
5. Hatchell, G. E., Ralston, C. W., & Foil, R. R. (1970). Soil disturbances in

- logging. *Journal of Forestry*, 68(12), 772-775.
6. Ishigami, G., Miwa, A., Nagatani, K., & Yoshida, K. (2007). Terramechanics-based model for steering maneuver of planetary exploration rovers on loose soil. *Journal of Field robotics*, 24(3), 233-250.
 7. Kalra, M. K., Shukla, S. K., & Trivedi, A. (2023). Track-Index-Guided Sustainable Off-Road Operations Using Visual Analytics, Image Intelligence and Optimal Delineation of Track Features. *Sustainability*, 15(10), 7914. <https://doi.org/10.3390/su15107914>
 8. Kalra, M. K., Trivedi, A., & Shukla, S. K. (2023). Non-Linear Regression Analysis of Rut Profile Data for Optimal Data Storage and Efficient Terrain Condition Analysis. *IEEE Geoscience and Remote Sensing Letters.*, vol. 20, pp. 1-5, 2023, Art no. 6501305. doi: 10.1109/LGRS.2023.3303134.
 9. Kogure, K., Ohira, Y. & Yamaguchi, H. (1985). Basic study of probabilistic approach to prediction of soil trafficability — Statistical characteristics of cone index. *Journal of Terramechanics*, 22(3), 147–156. doi:10.1016/0022-4898(85)90049-7
 10. Liu, Kun, "Influence of Turning on Military Vehicle Induced Rut Formation. " PhD diss., University of Tennessee, 2009. Available at http://trace.tennessee.edu/utk_graddiss/620.
 11. Liu, K., Ayers, P., Howard, H., & Anderson, A. (2010). *Influence of soil and vehicle parameters on soil rut formation. Journal of Terramechanics*, 47(3), 143–150. doi:10.1016/j.jterra.2009.09.001
 12. Maclaurin, E. B. (1990). The use of mobility numbers to describe the in-field tractive performance of pneumatic tyres. In *Proceedings of the 10th International ISTVS Conference, Kobe, Japan (Vol. 1, pp. 177-186)*.
 13. Ordonez, C., Chuy, O. Y., Collins, E. G. & Liu X. (2009) Rut tracking and steering control for autonomous rut following. *IEEE International Conference on Systems, Man and Cybernetics*, San Antonio, TX, pp. 2775-2781.
 14. Owende, P. M. O., Lyons, J., Haarlaa, R., Peltola, A., Spinelli, R., Molano, J., & Ward, S. M. (2002). Operations protocol for eco-efficient wood harvesting on sensitive sites (p. 74). Ecowood. <http://www.ucd.ie/foresteng>
 15. Rab, M.A., Bradshaw, J., Campbell, R. & Murphy, S. (2005). Review of factors affecting disturbance, compaction and traffic ability of soils with particular reference to timber harvesting in the forests of South-West western Australia. Department of Conservation and Land Management SFM Technical Report 2. 160 p
 16. Raper RL(2005). Agricultural traffic impacts on soil. *J Terramechanics*, 42(3-4):259-280.
 17. Reece, A. R. (1965). Principles of Soil-Vehicle Mechanics. *Proceedings of the Institution of Mechanical Engineers: Automobile Division*, 180(1), 45–66. doi:10.1243/pime_auto_1965_180_009_02

18. Saarilahti, M. (2002). Soil interaction model. Quality of Life and Management of Living Resources Contract, No. QLK5-1999-00991. Department of Forest Resource management, University of Helsinki.
19. Scholander, J. (1974). Bearing capacity of some forest soils for wheeled vehicles. Some technical aspects and consequences. Skogsmarks bärighet för hjulfordon. Några tekniska aspekter och konsekvenser. Specialnotiser från SFM Nr 14. 97 p.
20. Singh, M., Trivedi, A., & Shukla, S. K. (2022). Evaluation of geosynthetic reinforcement in unpaved road using moving wheel load test. *Geotextiles and Geomembranes*, 50(4), 581-589.
21. Turnage G W. (1972). Using dimensionless prediction terms to describe off-road wheel vehicle performance. ASAE Paper No. 72-634.
22. Vennik, K., Keller, T., Kukk, P., Krebstein, K., & Reintam, E. (2017). Soil rut depth prediction based on soil strength measurements on typical Estonian soils. *Biosystems Engineering*, 163, 78-86. doi:10.1016/j.biosystemseng.2017.08.016
23. Willoughby, W. E., & Turnage, G. W. (1988) Review of a procedure for predicting rut depth, Technical Report.
24. Wong, J.Y. (1989) *Terramechanics and Off-Road Vehicles*, Elsevier, Amsterdam.
25. Yokel, F. Y., Tucker, R. L., & Reese, L. C. (1980). Soil classification for construction practice in shallow trenching (Vol. 121). US Department of Commerce, National Bureau of Standards.

CHAPTER - 5

INVESTIGATION OF VARIOUS EDGE DETECTION ALGORITHMS IN IDENTIFICATION OF PATHS FORMED BY VEHICLE RUT

The study about the path formed by vehicle rut appearing as edges in the course resolution images has been presented. Various edge detection algorithms have been explored and compared for identifying the most suitable one for studying the rut and track features in the images.

5.1 Introduction

Edge detection is an image processing technique that is used to identify the points on the boundaries of an object having discontinuities, or sharp changes in the image intensity values. It is an important part of computer vision and is commonly used for image segmentation, pattern recognition, object identification and motion analysis among various applications. Edges in the image assist the visual processing based systems which form an essential branch of computer vision and machine vision systems. It is one of the first steps for applications such as face detection, object detection and their recognition like for thumb impressions, image segmentation etc.

In the current study, edge detection is explored for identification of tracks both paved and unpaved which are relatively linear features. The edge detection helps in better delineation of tracks for creation of data base using digitization and also to assist in development of automated detection. The edges also help in delineation of rut tracks formed on unpaved terrain by vehicular movement. These tracks provide wealth of information about terrain strength, ground distress level, preferred routes for futuristic developments. Kalra et al., 2023 proposed using non-linear regression analysis for optimal storage of rut profile data related to prevalent soil condition for efficient decisions. These tracks in the soft ground terrain are also used by rut following robotic vehicle for better stability (Ordóñez, 2011). Their delineation has benefits in other fields like defence too and research continues in multi-dimension for improved delineation of these rut tracks passing through low contrast areas (Kalra et al., 2023).

Over a period of time, a number of edge detection algorithms have been developed, each of which has its own advantage. It is reported that the problem of edge detection has no generic technique which is applicable for all conditions. This is rather the motivation for the continued research to improve the methods of edge

detection (Sen and Pal, 2010; Orhei et al., 2021). Attempt is therefore made here to study the relevance of different edge detection algorithms for identification of the track impressions in the images and identify the most suitable edge detection method.

Most of the edge detection algorithms either use the first order derivative i.e. gradient filter or use a second order derivative i.e. a Laplacian filter (Marque, 2011). The gradient filter in the images is computed as below:

$$\nabla f = grad(f) = \begin{bmatrix} g_x \\ g_y \end{bmatrix} = \begin{bmatrix} \frac{\partial f}{\partial x} \\ \frac{\partial f}{\partial y} \end{bmatrix} \quad (5.1)$$

Here, g_x and g_y are the first derivative or gradients of the image $f(x,y)$ and show the pixel value changes in both x and y directions defined using a column vector ∇f . The second derivative-based edge filter that is used is computed using Laplacian of the image $f(x,y)$ by using a second-order differential equation as given below:

$$\nabla^2 f = \frac{\partial^2 f}{\partial^2 x} + \frac{\partial^2 f}{\partial^2 y} \quad (5.2)$$

Based on the above procedure, a study brings out the comparative analysis of various edge detection algorithms like Sobel, Prewitt, and Canny (Ahmad, 2018). The images processed for highlighting the edges use different high-frequency filters that de-emphasize the low-intensity features. All such operations make use of the convolution of images with filters representing different edges filters as given here:

$$conv(w, f) = w(s, t) * f(x, y) = \sum_{s=-u}^{s=u} \sum_{t=-v}^{t=v} w(s, t) f(x-s, y-t) \quad (5.3)$$

Here, $w(s, t)$ denotes a filter of dimension $(s \times t)$ that scans over the image $f(x, y)$. The symbol $(*)$ stands for convolution- $Conv(w, f)$ of image and filter. In these techniques, noise removal can be helpful.

A Laplacian filter is one of the edge detector used to compute the second spatial derivative of an image. It measures the rate of change of first derivative i.e. where pixel values change dramatically. It being sensitive to small changes and to noise, the Laplacian of Gaussian (*LoG*) was then evolved to reduce the noise in the images. In this approach, the image is first convoluted using a Gaussian filter to reduce the level of noise and then it is followed by a Laplacian convolution for highlighting the edges.

$$LoG(x, y) = \nabla^2 [g(x, y) * f(x, y)] \quad (5.4)$$

The Canny edge-detection algorithm which considers both these aspects is reported as a robust method for detection of edges in gray-scale images. It is widely used due to its short operation time and relatively simpler calculations. The traditional Canny algorithm uses certain steps. Firstly the image is smoothened using a Gaussian function, the first-order operator is applied. It is followed by non-maximum suppression of the magnitude of the gradient. Here, double threshold has been used for edge connections. Non-maximum suppression is employed to find the local maximum value of the pixels, and set the gray value corresponding to the non-maximum point to zero. This implemented so that a large part of non-edge points can be rejected.

Another method for detecting the edges is by using Marr–Hildreth algorithm which is based on zero-crossings. It is used in continuous curves that feature rapid and strong variations in the image brightness value. It is a simple algorithm and operates by convolving the image using Laplacian of Gaussian function, which is a fast approximation using difference of Gaussian. The edges are detected using Zero crossings which implies that at least two opposite neighboring pixels have different sign (Marr and Hildreth, 1980; Haralick, 1987).

Laplacian is used for emphasizing fine details while gradient highlight the edges (Gonzalez and Woods, 2008). Dagar and Dahiya, 2016 presented review of Soft computing techniques for edge detection problem. Gupta and Porwar, 2016 combined both Laplacian and Sobel filter to achieve increased sharpening of medical images that have less dynamic range of intensity values.

Baburaj and Dcruz, 2018 suggested using a distributed Canny edge detection algorithm. In this, the whole image is first classified into number of blocks and then the edge detection thresholds are adaptively computed based on block type. Barbu, 2021 presented the details about using a fourth-degree partial differential equation to remove the noise.

Orhei et al., 2021 worked on using the dilated convolution for improved edge detection in many of the cases. At lower threshold, the dilation is observed to be sensitive to artifacts while at higher threshold, the dilated filters discover new edge points. It is also reported that by dilating the kernels, one can get reduction in noise sensitivity too however, its benefits are high.

Considering the wide variation in the results by different edge detection algorithms, this study attempts to make a comparative analysis of standard edge detection algorithms with specific reference to the detection of linear track features.

The outcome of the results is given here.

5.2 Objective

To make a comparative analysis of different edge detection algorithms and try to identify the most suitable underlying algorithm for the detection of tracks with maximum accuracy and minimal noise.

5.3 Methodology

The study considered various edge detection algorithms like Sobel operator, Prewitt operator, Poberts Edges, Zero-cross, Laplacian of Gaussian (*LoG*), Hardy cross and Canny methods for comparative analysis. One more edge filter for detecting edges is also used for comparison. One of the alternate edge detection technique is also used by assigning higher weights for the edge filter. Hence, the new filter with weights as given below was also used for comparison of results.

$$w = [-4 \ 0 \ -4; -4 \ 24 \ -4; -4 \ 0 \ -4] \quad (5.5)$$

A general satellite image of terrain is taken from google map for further detection of edges. MATLAB software is used for the study.

Evaluation of effectiveness of Edge-detection algorithm is an important but a challenging task. Multiple solutions have been presented in the literature. These methods are grouped as subjective and objective methods. The subjective methods use human observation to evaluate the effectiveness of edge detection process. In objective methods, quantitative measures are defined based solely on the images and the edge-detection results. In the evaluation, the confusion matrix remains a key measure. In order to compare the results, different probability measures like precision (P), recall (R) and F-measure (F1) are computed, the details of which are given by Saski, 2007. Currently, the observation based criteria which is equally acceptable, is considered here for comparison of results.

5.4 Results and Discussion

Different edge detection algorithms are applied on the image of terrain containing various track features as shown in Fig. 5.1. The histogram of this image is given in Fig. 5.2. The dynamic range of pixels on horizontal axis in the histogram refers to the difference between the brightest and darkest pixel values, or the range of intensity values present in the image. The vertical axis of the image indicates the number of pixels in the image with corresponding brightness level in its 8-bit gray image having levels 0-255. This histogram forms the basis for enhancement of

relevant features in the image. The features of tracks shown in Fig 5.1, lying around the level of 190 are highlighted by employing suitable image processing techniques as presented in this chapter. The outcome of various edge detection algorithms computed using MATLAB was and superimposed over the original image for better perception of outcome which are indicated in Fig. 5.3-5.9.



Fig. 5.1 Original Image of the terrain around Chandigarh

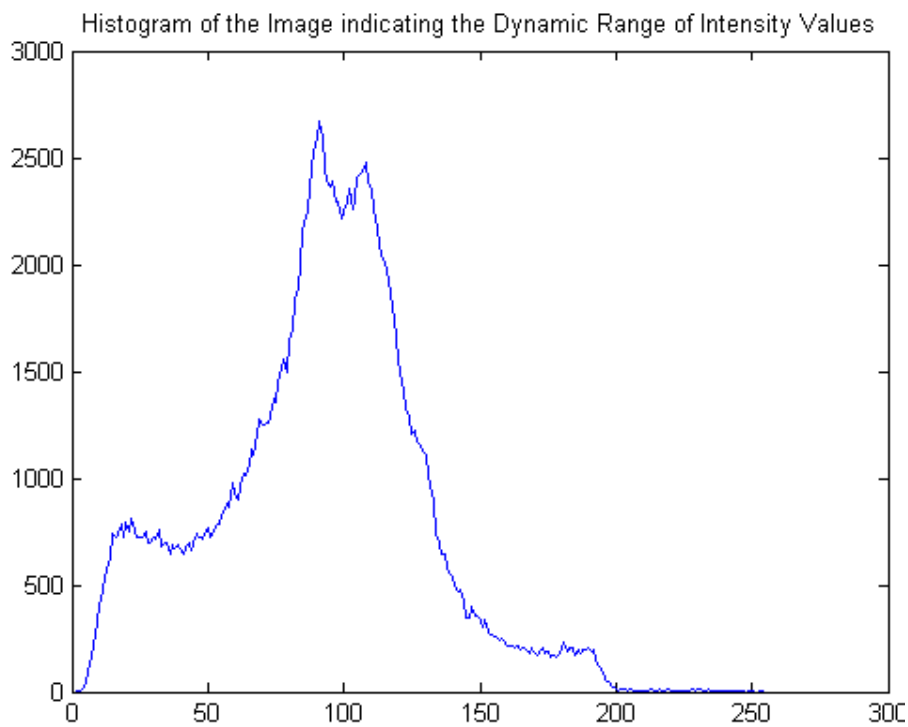


Fig. 5.2 Histogram of the image indicating the dynamic range of intensity values

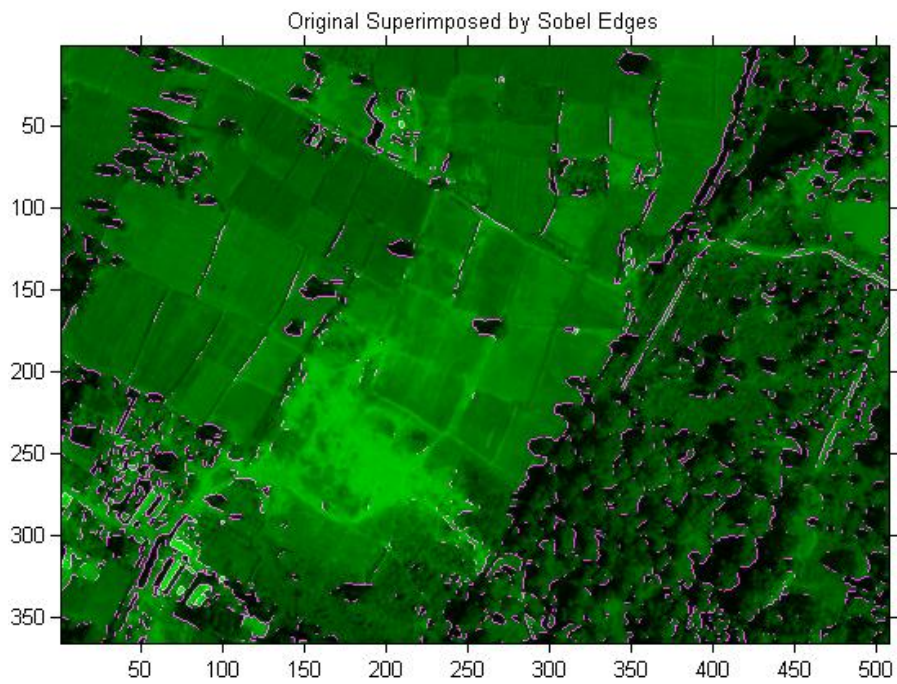


Fig. 5.3 Original image superimposed by Sobel edges

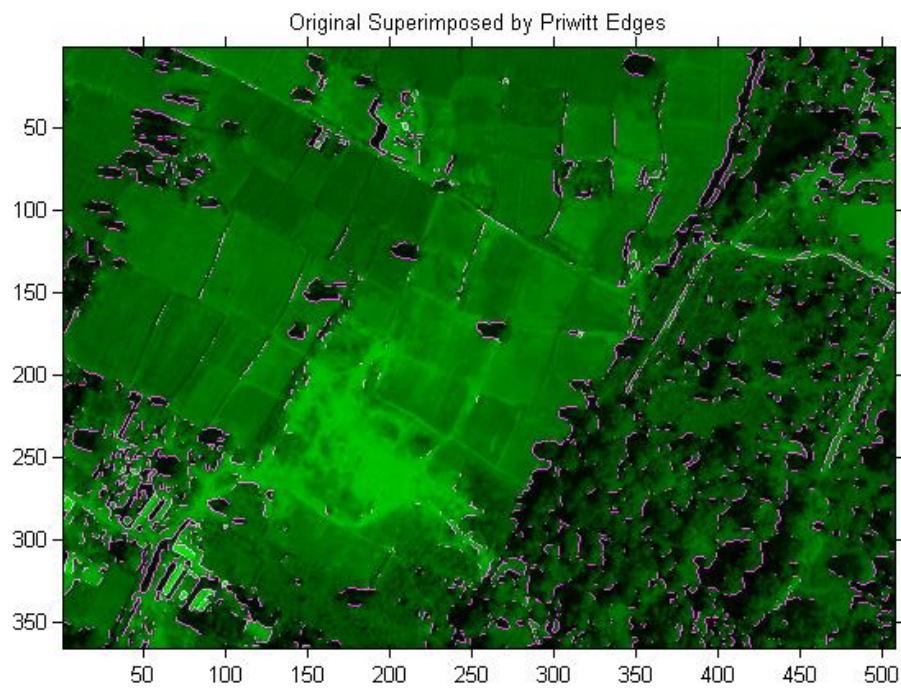


Fig. 5.4 Original image superimposed by Prewitt edges

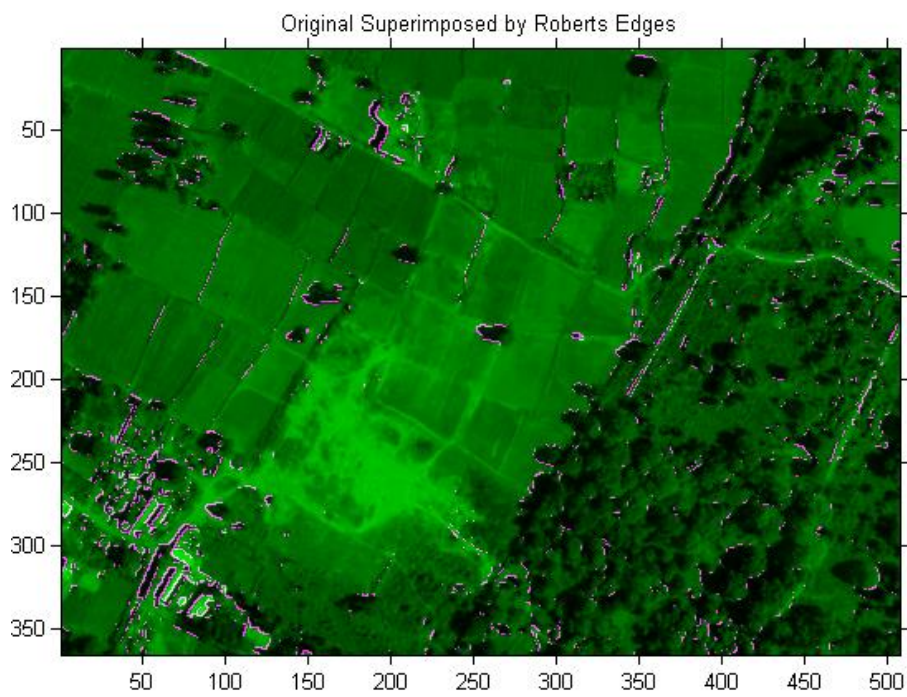


Fig. 5.5 Original image superimposed by Roberts edges

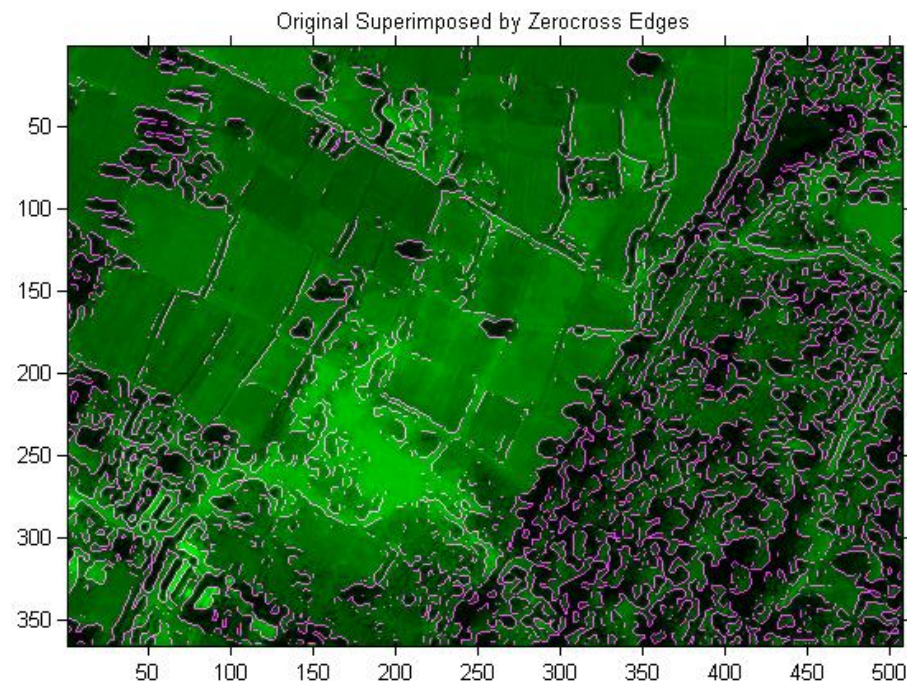


Fig. 5.6 Original image superimposed by Zerocross edges

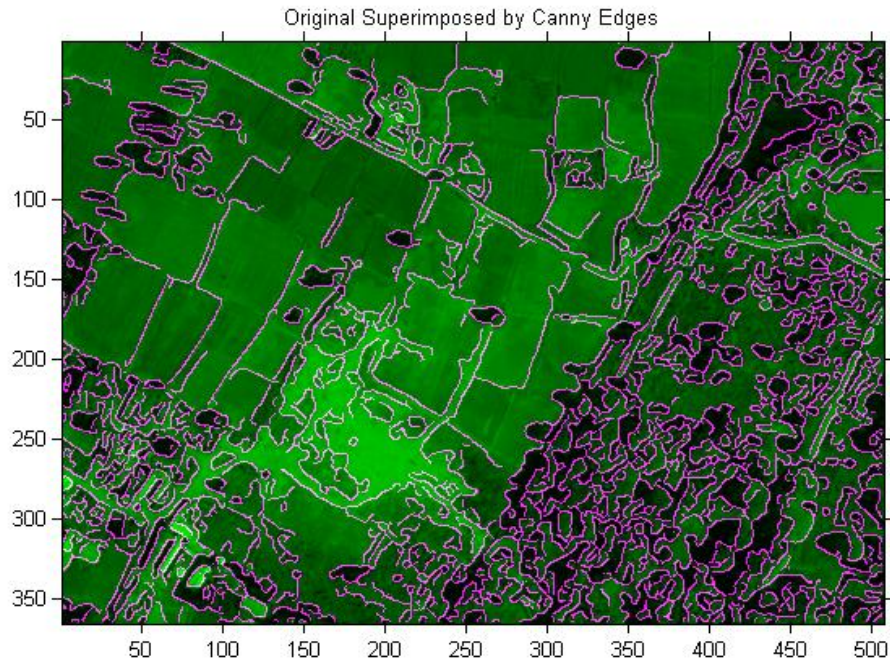


Fig. 5.7 Original image superimposed by Canny edges



Fig. 5.8 Original image superimposed by proposed edge filter

Based on the observation of results obtained after convolving the images with different edge detection filters, some useful inferences are drawn with specific reference to the study of tracks.

The comparative analysis brings out that vast difference between the outcomes from different edge detection filters. This puts in the need to confirm the suitability of edge detection algorithm before using them for further image processing. The gradient filters like Sobel picks up the boundaries quite well when sharp changes in intensity values are there. It de-emphasizes the lower levels of changes. This is the reason most of the tracks are not picked up in the image as shown in Fig. 5.3. The prewitt edge detection does not place specific emphasis on the pixels which are closer to the center of mask however it works on the similar principle. Therefore the results are not much improved as shown in Fig. 5.4. Both these algorithms are sensitive to noise. The results are not improved even with the gradient based another Roberts based filter as shown in Fig. 5.5.

On the other hand the Laplacian filter has been observed as more sensitive to highlighting the finer details, which can be seen by comparing the images. Laplacian however produces noisier image, therefore Laplacian over Gaussian (*LoG*) is preferred. Laplacian edge detector which calculates the second order derivatives in a single pass are approximating a second derivative measurement. These are very sensitive to the noise. Therefore, the image smoothening is first carried out using Gaussian filter before using the Laplacian filter. The method given by Zerocross method which is based on Laplacian over Gaussian (*LoG*) thus indicates improved result over Sobel and Prewitt algorithms as shown in Fig. 5.6.

Another most commonly used algorithm is the Canny edge detector however it is relatively much more complex. The noise reduction is first carried out using Gaussian filter, followed by computing first order derivatives. Non-maximum suppression which is an important step in the Canny algorithm is then performed. The purpose is to obtain the local maximum value of pixels and set the non-maximum point to zero, so that a large part of non-edge points can be eliminated. Hysteresis is then used for linking the broken lines found in the previous step. All the essential considerations are made in this algorithm, therefore the results appear to be much improved as shown in Fig. 5.7. The comparative analysis using visual appearance of the images clearly brings out that Canny Edge detection gives far better results in highlighting the edges.

Attempt was made to highlight the edges by retaining strong edge filter weights. The results indicate that it picked up the edges much sharply however when compared with Canny edges, more noise is seen to be picked up by this filter as shown in the lower part of image in Fig. 5.8.



Fig. 5.9 Original image compared with Canny Edges

Therefore, the Canny Edge detection is better suited for applications that need the automated detection of track features. The outcome of edge detection algorithms is also shown separately for the images as shown in Fig. 5.9. It is designed to be better than LoG filter by reduced sensitivity to noise. The benefits of underlying Canny Edge detection algorithm can be combined further with other techniques of improvement. Therefore in further attempts, one can consider combining Canny edge algorithm with other methods based on higher order derivatives or dilated filters etc. for improved accuracy of edge detection. The Canny edge detection algorithm is however widely used in computer vision for identifying the edge locations in the images. It's a multi-stage process that aims to detect the sharp and clean edges while minimizing the noise and false detections. The algorithm considers several key steps for addressing noise reduction, gradient calculation, double thresholding etc. The effectiveness of this algorithm in detecting the edge features is studied here for delineation of vehicle tracks in the images. The rut impressions on the ground are delineated by employing a number of techniques including that by optical cameras, photogrammetry and LiDAR sensors (Salmivaara et al., 2018). The width of rut profiles can be ascertained by delineation of its edges from surroundings. The technique finds direct utility in such situations.

5.5 Conclusions

From the observation of results and discussion thereon, the following key conclusions are drawn:

1. The edge detection filters highlight boundaries with specific application. The selection of suitable edge detection algorithm needs to be done carefully. In the study, various edge detection algorithms like Sobel operator, Prewitt operator, Poberts Edges, Zero-cross, Laplacian of Gaussian (*LoG*), Hardy cross and Canny methods are considered for comparative analysis. The current study leads to inference that the Canny Edge detection algorithm gives relatively better and

acceptable results for applications in linear track detection although further studies may lead to further improvement of edges detection.

2. A number of possible alternates can be explored to improve the edge detection algorithm further. The dilated filters could be one such alternative and the combination of two filters like Smoothed Sobel and Laplacian could be another approach. The higher degree of derivatives can also be employed usefully.

3. In further studies, one can consider combining the benefits of using Canny edge algorithm with other methods like higher order derivatives or dilated filters etc. for improved accuracy of edge detection.

5.6 References

1. Ahmed, A. S. (2018). Comparative study among Sobel, Prewitt and Canny edge detection operators used in image processing. *J. Theor. Appl. Inf. Technol.*, 96(19), 6517-6525.
2. Barbu, T. Mixed Noise Removal Framework Using a Nonlinear Fourth-Order PDE-Based Model. *Appl Math Optim*, 2021, 84 (Suppl 2), 1865–1876. doi: 10.1007/s00245-021-09813-4
3. Dagar, N. S., & Dahiya, P. K. (2016). Soft computing techniques for edge detection problem: a state-of-the-art review. *International Journal of Computer Applications*, 136(12).
4. Gonzalez, R. C. (2009). *Digital image processing*. Pearson Education India.
5. Gupta, S., & Porwal, R. (2016). Combining laplacian and sobel gradient for greater sharpening. *IJIVP*, 6, 1239-1243
6. Haralick, R. M. (1987). Digital step edges from zero crossing of second directional derivatives. In *Readings in computer vision* (pp. 216-226). Morgan Kaufmann.
7. Kalra, M. K., Shukla, S. K., & Trivedi, A. (2023). Track-Index-Guided Sustainable Off-Road Operations Using Visual Analytics, Image Intelligence and Optimal Delineation of Track Features. *Sustainability*, 15(10), 7914.
8. Kalra, M. K., Trivedi, A., & Shukla, S. K. (2023). Non-Linear Regression Analysis of Rut Profile Data for Optimal Data Storage and Efficient Terrain Condition Analysis. *IEEE Geoscience and Remote Sensing Letters*.
9. Marr, D., & Hildreth, E. (1980). Theory of edge detection. *Proceedings of the Royal Society of London. Series B. Biological Sciences*, 207(1167), 187-217.
10. Marques, O. (2011). *Practical image and video processing using MATLAB*. John Wiley & Sons.
11. Ordóñez, C., Chuy Jr, O. Y., Collins Jr, E. G., & Liu, X. (2011). Laser-based rut detection and following system for autonomous ground vehicles. *Journal of Field*

Robotics, 28(2), 158-179.

12. Orhei, C., Bogdan, V., Bonchis, C., & Vasiu, R. (2021). Dilated filters for edge-detection algorithms. *Applied Sciences*, 11(22), 10716.
13. Sasaki, Y. (2007) The Truth of the F-Measure; Technical Report; School of Computer Science, University of Manchester: Oxford, UK.
14. Sen, D., & Pal, S. K. (2010). Gradient histogram: Thresholding in a region of interest for edge detection. *Image and Vision Computing*, 28(4), 677-695.

CHAPTER - 6

EVALUATING THE POTENTIAL OF DIFFERENT TEXTURE MEASURES IN ENHANCING THE RUT TRACKS

The role of texture that becomes important in fine resolution images has been explored here. Specific studies have been conducted to evaluate the potential of different texture measures in enhancing the rut tracks.

6.1 Introduction

Vehicular movement in off-road unpaved areas is a common requirement for applications, particularly in defense, forestry, agriculture and unmanned ground vehicles. During operations, the vehicles at time need to pass through many of the soft ground conditions. The beaten tracks of leading vehicles, reported as being paths which are safe and suitable for guiding, are followed at times. At times, the track impressions of the leading vehicle need to be followed for strategic reasons (US Army FM 3-19, 1993). During night time operations, low-contrast conditions are common hindrances for these vehicles. Moreover, these days, visual-analytics-guided systems are seen to be replacing human efforts. Vision-based systems are increasingly being used in many such manned and autonomous ground vehicles (Graefe and Kuhnert, 1992).

Investigators conducted a study of the rut following robotic movement on unpaved terrain (Ordonez et al., 2011). Monocular-camera-based off-road track detection for the path following robot movement is proposed (Mei et al., 2018). In comparison to on-road surfaces or lane classification, off-road scenarios are shown to face many challenging situations. There are no well-defined edge cues and the tracks pass through a diversity of natural terrain surfaces. A review of the traversable path for autonomous ground vehicles in off-road detection is reported (Islam, 2022).

The vehicle tracks captured by these cameras have limited contrast. The changed illumination conditions, cluttered backgrounds, wetness and so forth bring about great challenges in the identification of tracks. In order to make these operations sustainable in such scenarios, it is important to look into alternate means too that can improve the track contrast in a given situation.

A deep-learning-based CNN method is presented for lane detection using vision cameras (Anbalagan et al., 2023). The use of the generative adversarial network (GAN) for addressing the issue of extracting road boundaries in complex

terrain scenarios is presented (Shamsolmoali et al., 2020). A framework has been given for combined tracking of paved and dirt roads (Forkel et al., 2021). In this work, a CNN-based measurement that utilized the self-similarity of (dirt) road areas is shown to be tracked using a look ahead length of 25 m. Although the machine learning aspect is important for track detection, even for these studies to accurately mark the vehicle tracks with feeble boundaries, a robust and accurate dataset is needed.

Furthermore, the role of traditional image processing and the computer vision techniques is important here. In the context of 3D robot vision, it has been observed that by combining both linear subspace methods and deep convolutional prediction leads to improved performance along with faster runtime performance compared to the state of the art techniques (Burchfiel and Konidaris, 2018). Ten different concerns for deep learning are observed and it is suggested that in order to reach artificial general intelligence, deep learning must be supplemented by other techniques (Marcus, 2018). In the study of microcirculation images, the limitations of deep learning are reported and a hybrid model to strike a balance between accuracy and speed by combining traditional computer vision algorithms and CNN is proposed (Helmy et al., 2022). Furthermore, for these advanced algorithms too, the correct delineation of tracks in different scenarios is required. This is where the traditional image enhancement techniques play a role.

Several techniques for image enhancement and better contrast are discussed (Gonzalez, 2009; Varshney and Arora, 2004). These techniques are primarily based on filters and histogram stretching. Several techniques of image enhancement have been compiled (Janani et al., 2015).

The unpaved track features which look like edges in low resolution images appear like elongated areas in the high resolution images. This additional aspect of comparative change in the texture of tracks with respect to their surroundings can reveal useful information for the improved interpretation of track features.

There are various techniques of texture estimation; however, the GLCM-based approach employing various statistical measures has shown very good results in a variety of applications (Mohanaiah et al., 2013). The relationship between the pixels in the image is characterized by using different statistical measures such as contrast, energy, entropy, homogeneity, etc. Texture analysis using GLCM is employed in the detection of road boundaries (Graovac and Goma, 2012). The contrast of tracks using texture based measures depends upon the surrounding terrain features. A study on various aspects influencing the texture is proposed (Zhang et al., 2017).

Considering various measures for an enhancement in track contrast, an attempt is made to quantify the effectiveness in a given surrounding track contrast using a new track index (TI) and to sort the images as per the track contrast. In this work, different aspects related to contrast enhancement and the optimization aspects are presented.

6.2 Review of Past Works

The vehicular movements in off-road areas pose many challenging situations which are essential to be addressed for sustainable operations. In places, the ground strength gives way in different environmental conditions, thereby needing some strengthening measures. Situations of low contrast are other issues which exert challenges on decision making for the track or rut following vehicular operations. Considerable efforts continue to make the off-road operations sustainable from varied perspectives. Improving the strength of unpaved terrain using geosynthetics (Singh et al., 2019) and its evaluation (Singh et al., 2022) for sustaining vehicular loads are a few such alternatives employed. Machine learning processes as employed in the crack detection of bridges and asphalt (Kumar et al., 2020) and the proposed self-attention-based U-net model (Gupta et al., 2022) can be extended for the autonomous detection of track features too. The delineation of track zones in spatially varying, low-contrast terrain is another important issue that requires attention for sustainable operations.

Tracks are seen to be distinguishable from their surroundings not only by the variation in tone but also by the pattern and texture which are differentiable with respect to their surroundings. Howard and Seraji, 2001 used a mobile robot with a vision system for real-time terrain characterization using an artificial neural network (ANN). An algorithm (Chowdhury et al., 2017) was introduced for a line follower robot to achieve the ability to autonomously follow a path that had straight lines.

Image stretching, power functions, low-high-pass filters, histogram stretching and its equalization are some of the well-known techniques employed for image enhancement (Gonzalez, 2009). A framework based on multipeak-mean-based optimized histogram modification was introduced to demonstrate the enhancement in contrast (Babu et al., 2015). Edge detection techniques have been used in preserving the high-frequency components and structural features for the detection of linear features. Broadly, the edge detection algorithms are grouped into two types on the basis of derivatives (Marques, 2011) which include: a) gradient-based operators which compute the first-order derivatives of an image and b) Laplacian-based operators which are based on the second-order derivatives of an image. Both gradient and Laplacian filters are used to highlight discontinuities in an image. Using these in the background, many variants of the edge detection algorithms have been developed; Sobel, Prewitt, Canny, LoG, etc., have been studied for a comparison of results, and each of them have been shown to have their own merits.

Texture representing the relation of the pixels with reference to their neighborhood reveals very useful information distinctive to the object. Texture-based analysis has been employed for image understanding and for different applications by various researchers. Various approaches have been used to describe the textures in the images which differ from each other mainly by the method used for extracting textural features. These approaches which are based on four methods, viz. statistical methods, structural methods, model-based methods and transform-based methods, have been compared (Bharti et al., 2004). Several applications make use of texture information for required feature extraction. A survey of texture feature extraction methods is given by Humeau-Heurtier, 2019.

In content-based image retrieval, a combination of edge information and texture information using co-occurrence matrix properties is used (Alsmadi, 2020). Texture features are used for evaluating the real-time distress conditions of roads (Doycheva et al., 2016). GLCM texture measures are used as feature descriptors for image retrieval in various applications (Sudha and Aji, 2019). A local second-order texture entropy has been employed to represent the nature of gray-scale variation and the authors, Liu et al., 2020 based on local texture entropy proposed an algorithm for better edge detection.

All of these studies are significant from the perspective of enhancing the track contrast, and related tasks are used in this study.

6.3 Tools and Methodology Used

In order to investigate the role of different resolutions, the images of Google Earth at different resolutions were taken as the basis in this study. The images taken for the analysis were from an area near Chandigarh. The test sites presented in this study were taken based on ground trials conducted in places with desertic terrain features near Suratgarh, Rajasthan, and with alluvial terrain features in Roorkee, Uttranchal, in India. In another set of images of tracks at ground level, vision cameras were used. The analysis was carried out using Sentinel Application Platform (SNAP) 8.0 and MATLAB 2020a software. The following points give details about the methodology used in this study:

6.3.1 Using Some Linear and Non-Linear Transformation Functions

Due to changed environmental conditions, many times, it is not possible to interpret features directly from images captured by cameras. Many features in the image become prominently clear when certain image processing techniques are applied on the images. There are various measures which can be used to enhance the track contrast, and some of which that are relevant to this study are described here.

The contrast between the two pixels is based on the difference between their gray levels. Many times, the full dynamic range is not used in the image, thereby making the image have reduced contrast. Contrast stretching tries to make use of the full dynamic range and improves the contrast uniformly for the whole image.

Contrast stretching as defined as improving the contrast by stretching the range of intensity values in a given range to the desired values. It is defined as follows:

$$g(x, y) = \frac{L - 1}{f_{\max} - f_{\min}} (f(x, y) - f_{\min}) \quad (6.1)$$

where, $g(x, y)$ is the array of pixels in the transformed image and $f(x, y)$ is that for the original image; f_{\max} and f_{\min} are the maximum and minimum gray values of the image pixels. L indicates the quantization levels, for instance, an 8-bit image contains $2^8 = 256$ levels. The transformation here can also be made for a given range of gray values using a piecewise linear stretching function.

There is a possibility of improving the image contrast in a specific range of gray levels using various non-linear transformation functions (Gonzalez, 2009; Varshney and Arora, 2004). Some of the transformation functions include logarithmic stretching, which enhances the contrast of pixels in a dark region, whereas the reverse function antilog enhances the contrast between bright pixels. Logarithmic stretching is defined using

$$s' = c_s \cdot \log(1 + r') \quad (6.2)$$

where, s' and r' are the output and input pixel values respectively. The parameter c_s is the scaling constant to obtain the output value in a desired dynamic range. The power or Gamma function can also be used to carry out the image stretching of the pixels to a varying degree using the following:

$$s' = c_s \cdot (r')^\gamma \quad (6.3)$$

In this transformation, the parameter c_s is the scaling constant and the value of $\gamma < 1$ is used when we are more sensitive to changes in the dark as compared to bright areas in the image. Similarly, $\gamma > 1$ is used when we are more sensitive to changes in bright areas than in dark areas. Another method of increasing image contrast is by manipulating the histogram of an image. A histogram is created by counting the number of times each gray-level value occurs in the image.

$$h(r_k) = n_k \quad (6.4)$$

where, r_k is the k^{th} gray level in the range $[0, L - 1]$ and n_k represents the number of pixels in the image with a gray level of r_k . The histogram is normalized to create a percentage distribution for each gray level in the image. The histogram equalization is the most common technique used for image contrast enhancement. It accomplishes this by stretching out the intensity range of the image. This allows for areas of a lower local contrast to gain. This method is usually seen to increase the global contrast of images, whereas another method of adaptive histogram equalization is used for contrast stretching over local areas. In this, the histograms are created for distinct sections of the image and the gray values are re-distributed.

6.3.2 Using Spatial Filters

Some spatial filtering methods have been used to sharpen the edges and remove much of the blur in images are quite relevant for enhancing image contrast. In all of these operations, the convolution of images with various filters is carried out using operations such as the following:

$$conv(w, f) = w(s, t) * f(x, y) = \sum_{s=-u}^{s=u} \sum_{t=-v}^{t=v} w(s, t) f(x - s, y - t) \quad (6.5)$$

where, $w(s, t)$ indicates the filter of size $s \times t$ dimension scanned over the image $f(x, y)$. The symbol (*) is used to indicate the convolution of the image and filter. Convolution computes the output based on the weighted average of brightness values of pixels located in a particular spatial frame. The filters or kernel used here was the matrix with values in a given spatial relation, which was used for highlighting a specific feature. The edge filters and various low-high frequency filters were designed based on the above concept.

The boundaries of the track areas represented by edges can be used to differentiate the track area using edge filters. Edges which are a set of connected pixels forming a boundary between two disjointed regions are considered as cues for track and road lane detection (Li et al., 2018). The vehicle tracks that are distinctive from the surroundings at the boundary and the role of edges representing boundaries were thus explored. Edge detection assists in preserving and highlighting the high-frequency components in the image. Edge detection usually depends upon the calculation of first or second derivatives of the image (Marques, 2011). The first-derivative-based edge filters were designed based on the gradient of the pixel values in the image and were computed as follows:

$$\nabla f = grad(f) = \begin{bmatrix} g_x \\ g_y \end{bmatrix} = \begin{bmatrix} \frac{\partial f}{\partial x} \\ \frac{\partial f}{\partial y} \end{bmatrix} \quad (6.6)$$

where, the gradients g_x and g_y are the first derivatives of image $f(x,y)$ indicating pixel value changes occurring in both the x and y direction and are represented as the column vector ∇f . The second-derivative-based edge filter was also defined using the Laplacian of the image $f(x,y)$, and was obtained using the second-order differential equation given below:

$$\nabla^2 f = \frac{\partial^2 f}{\partial^2 x} + \frac{\partial^2 f}{\partial^2 y} \quad (6.7)$$

However, the gradient-based filters were used to highlight the prominent edges, while the Laplacian filters brought out the finer details (Gupta and Porwal, 2016). Based on the above concept, many of the edge detection filters that are designed include Sobel, Prewitt, Roberts, Canny, etc. These are used to highlight the edges based on some varying concepts, and each of which has its own merits.

The contrast of linear features could also be highlighted by using other high-frequency filters, wherein the low-intensity features are deemphasized. These high-frequency filters which can be useful in differentiating the track and surrounding features based on the frequency of features were used in this study.

6.3.3 Using Texture Measures

The conventional techniques of image enhancement which are primarily based on the general understanding of brightness values in an image assist in highlighting the image features to an extent. When a group of pixels representing any feature is differentiable from its surroundings, the role of texture comes into place. The texture defines the spatial arrangement of these pixels in the feature. With the arrangement of pixels in the track zone being different from its surroundings, the role of texture is therefore explored in this study for improved image intelligence.

The GLCM-based texture measure which is considered as a good descriptor of features was used in this study. It considers the relation between two pixels at a time, named as the reference pixel and the neighbor pixel. The concept of measuring texture using GLCM by extracting various texture features is given by Haralick et al., 1973. The author introduced fourteen textural features that contain information about image texture characteristics. Later, Connors and Harlow, 1980 identified that only 5 of these 14 measures were sufficient, including energy, entropy, homogeneity, contrast and correlation. The key measures that were used in the current study are described here.

$$Energy = \sum_{i,j} p(i,j)^2 \quad (6.8)$$

$$Entropy = - \sum_{i,j} (p_{i,j}) \log_2(p_{i,j}) \quad (6.9)$$

$$Homogeneity = \sum_{i,j} \frac{p(i,j)}{1 + |i - j|} \quad (6.10)$$

$$Contrast = \sum_{i,j} |i - j|^2 p(i,j) \quad (6.11)$$

$$Correlation = \sum_{i,j} \frac{(i - \mu_i) \cdot (j - \mu_j) \cdot p(i,j)}{\sigma_i \cdot \sigma_j} \quad (6.12)$$

where, $p(i,j)$ is the probability value recorded for the co-occurrence of cells (i,j) in the *GLCM* matrix; μ_i and μ_j are the means while σ_i and σ_j are standard deviations. Here, different statistic measures have their own significance, and the details of which are given by the investigators (Haralick et al., 1973; Connors and Harlow, 1980). Energy, represented based on the angular second moment (*ASM*), measures the textural uniformity, indicating pixel pair repetitions. Entropy measures the disorder or complexity of an image. Homogeneity denotes the absence of intra-regional changes in the image. Contrast is indicative of the spatial frequency of an image and measures the extent of local variations present in the image. Correlation computes the linear dependency of the gray-level values in the *GLCM* matrix and indicates the relation of the reference pixel to its neighbor.

All of the above statistical measures were used in the analysis of texture over the images, as used in this study.

6.4 Results

In order to understand the effect of different measures in an enhancement in track contrast, images are enhanced using a number of techniques and some of these were used in this study. Since there could be several ways, only some significant measures influencing track contrast were considered here. In order to create the images using various techniques such as edge enhancement, high-pass filters and texture images, a filter of 5×5 size was convolved over the input images. In the study of texture, *GLCM* was created by downsizing the quantization levels as the computational complexity of this method is proportional to $O(G^2)$ (Clausi, 2002). More levels imply more accurate textural information, but with increased computational cost. Applying a large displacement value to a fine-texture image would yield a *GLCM* that does not capture detailed textural information (Gadkari, 2016). In order to compute image texture, a horizontal offset of 1 pixel and quantization level of 32 were used to create various texture images.

First of all, a comparison of various image enhancement measures was done on the images of different scales. So, the images of a road junction in an area near Chandigarh were captured at different resolutions, as given in Fig. 6.1a (source: Google Earth, Maxar Technologies).

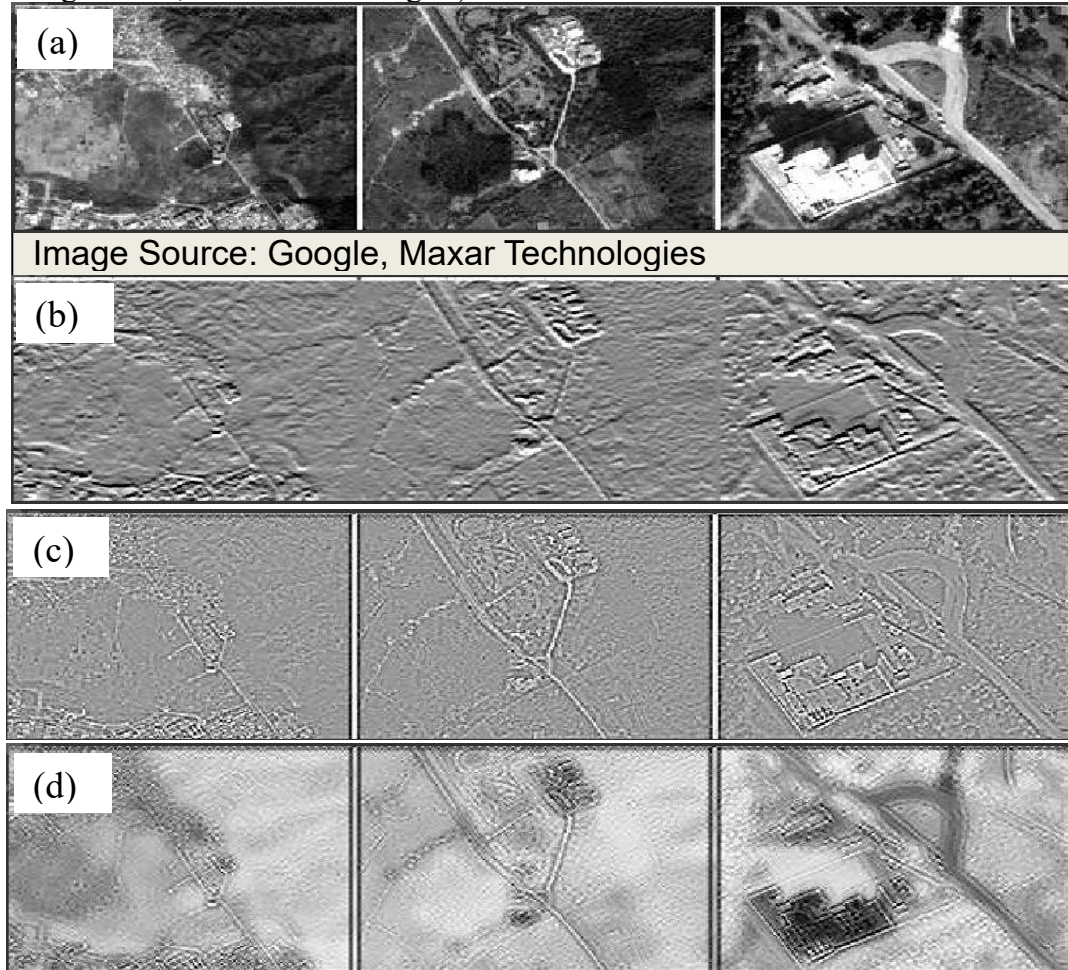


Fig. 6.1 Multiscale images of roads: (a) original in gray tone indicating coarse-, medium- and fine-scale images (source: Google Earth) enhanced using (b) Sobel edge detection filter, (c) Laplacian filter and (d) high-pass filter. (Images created using SNAP 8.0 software)

Among conventional methods, edge detection filters, using Sobel as the first-order and Laplacian as the second-order derivative, and high-pass filters were used and convolved over the images. The results of the analysis are shown in Fig. 6.1b–6.1d, respectively.

The texture analysis on the same images was also carried out using *GLCM*. The images representing different statistical measures of texture were created

as shown in Fig. 6.2.

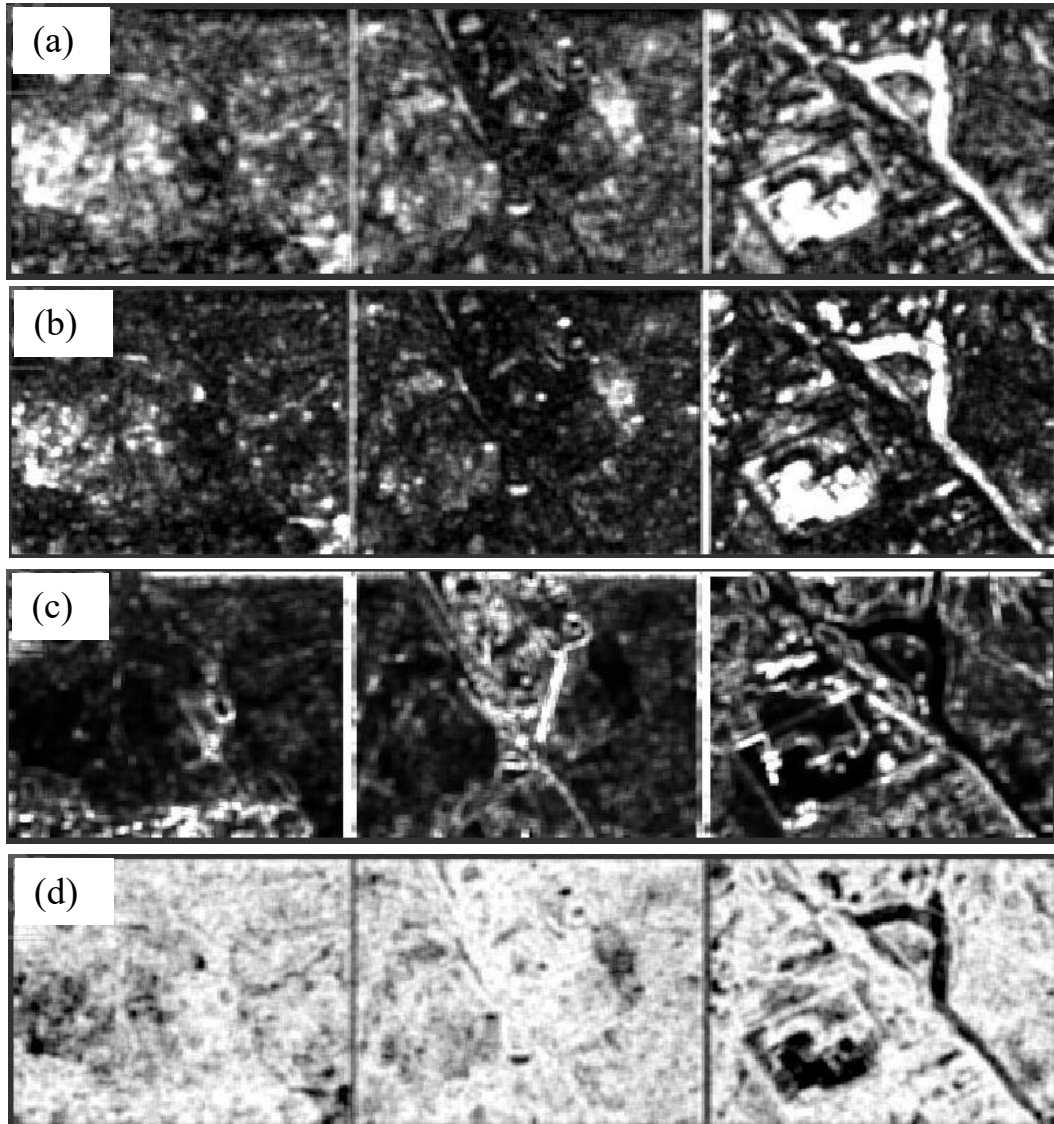


Fig. 6.2 Multiscale images of roads indicating coarse-, medium- and fine-scale images enhanced using (a) homogeneity, (b) energy, (c) contrast and (d) entropy as the texture measures. (Images created using SNAP 8.0 software)

Fig. 6.2 contains images that represent (a) homogeneity, (b) energy, (c) contrast and (d) entropy as the texture measures. An analysis of the images has been shown in Fig. 6.1, and Fig. 6.2 indicates one notable point that as the resolution increases, the role of enhancement measures using the non-linear filters and texture increases. This is because the pixels representing the track features as a group are prominently different to the surroundings.

The effect of various measures was investigated further to identify their role on the ground-scale images containing vehicle tracks. The results of the analysis carried out on the images of track impressions by the leading vehicle in desertic tracks are shown in Fig. 6.3.

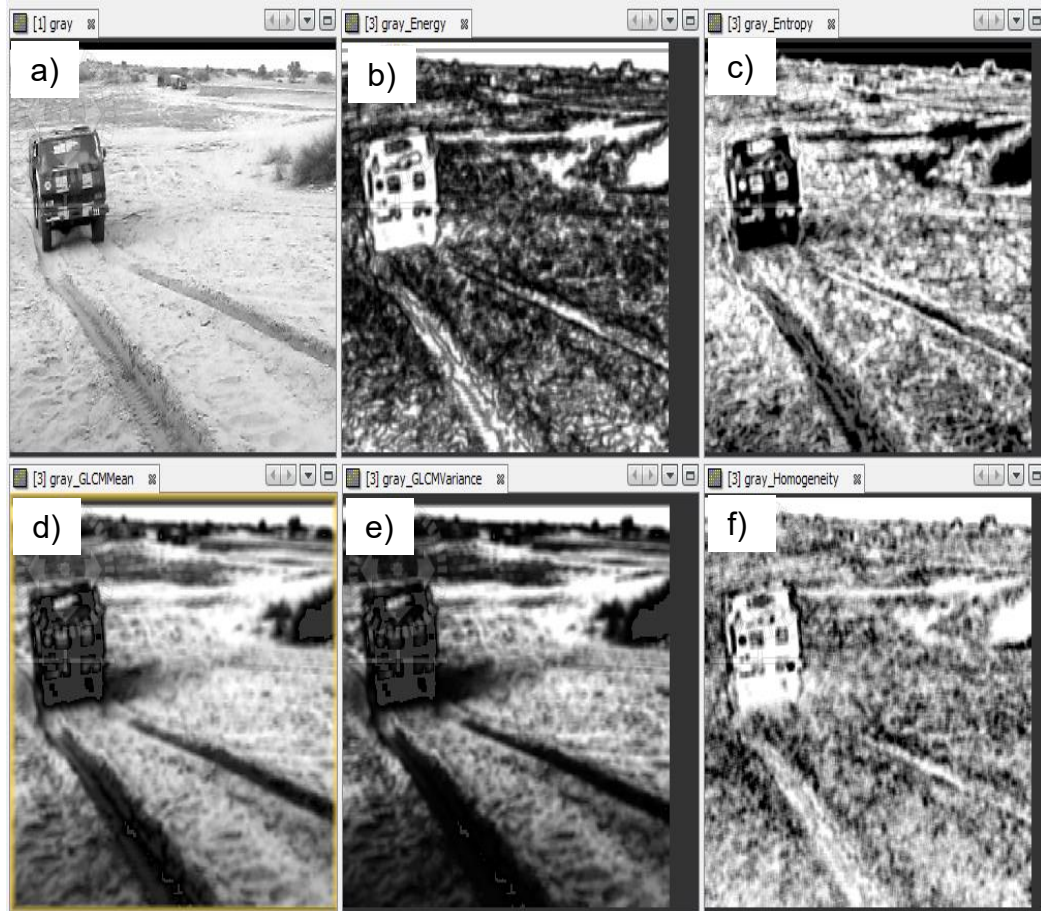


Fig. 6.3 Effect of different texture measures on tracks in desertic terrain: (a) original gray image and texture images created using filters of (b) energy, (c) entropy, (d) GLCM mean, (e) GLCM variance and (i) homogeneity image. (Images created using SNAP 8.0 software)

The influence of other texture measures such as *GLCM* mean and *GLCM* variance was also explored here. The visual appearance of the results reveals the importance of texture in delineating the tracks in a better way than the original gray image. These results, along with standard image enhancement measures, can be used in devising an improved way for differentiating the track zones.

6.4.1 Quantification of Track Contrast Using Proposed Track Indices

In order to compare the track contrast quantitatively, an index-based approach was proposed in this study. First of all, a cross sectional profile was drawn

across the track in each image as per the details marked on one of the texture images, as displayed in Fig. 6.4.

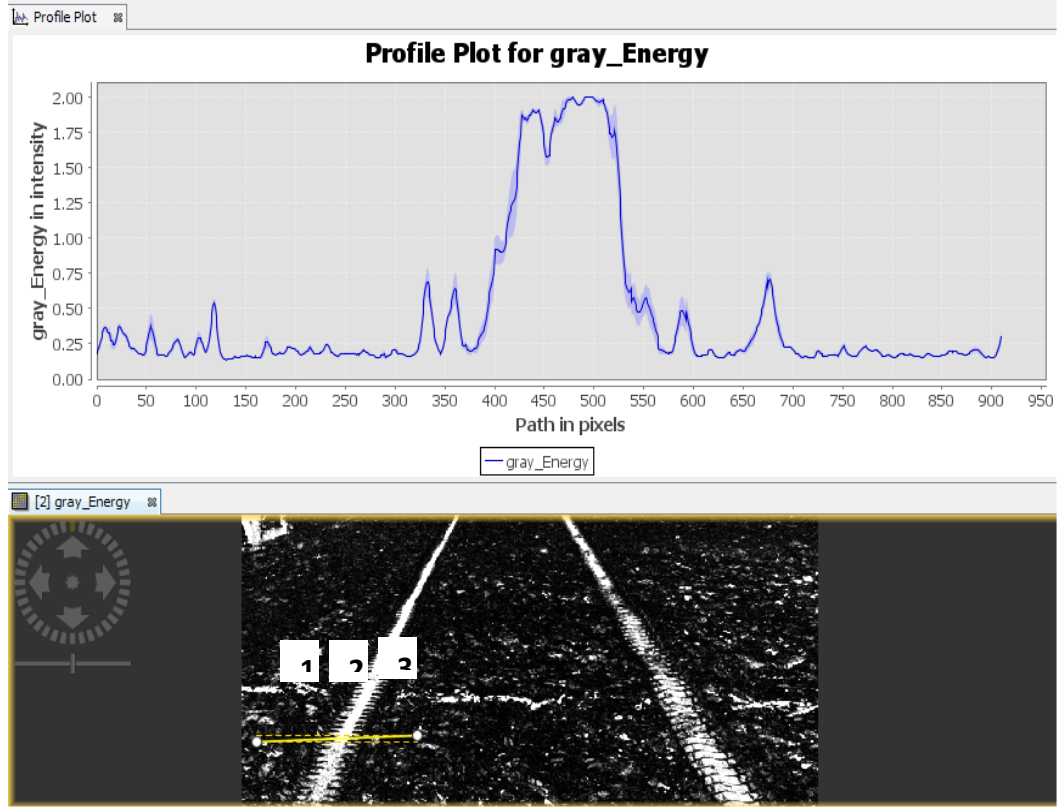


Fig. 6.4 Location of pixels chosen for comparing the contrast in track areas with reference to its surroundings (Image created using SNAP 8.0 software)

As the contrast of tracks needs to be considered with respect to its surrounding, for each of the image enhancement measures, areas representing pixels on-track (P_T) and pixels off-track (P_{OT}) were therefore considered. As local variation in the feature values was also expected, the mean value of the features value was taken. In this study, each measure was averaged over a rectangular area with a width of 11×100 pixels. In order to compare the contrast using various measures, the difference in the mean value of the statistical measure (X) on the pixels along the track (P_T) and in the pixels in the off-track (P_{OT}) areas were computed as shown below:

$$P_{OT} = \frac{N_1 X_1 + N_3 X_3}{N_1 + N_3} \quad (6.13)$$

$$P_T = \frac{N_2 X_2}{N_2} \quad (6.14)$$

Here, in a given enhancement measure, X_1 and X_3 are the values at the selected pixels

in the off-track zones located to the left and right of the track, respectively. Similarly, X_2 indicates the values for pixels on the track. As the range of values computed for different statistic measures shall be different, in order to compare the two measures, normalization was carried out, as shown below:

$$Y = \frac{X - X_{\min}}{X_{\max} - X_{\min}} \quad (6.15)$$

where, Y is the normalized value of X data representing the contrast enhancement measure and X_{\min} and X_{\max} give the minimum and maximum values of its range. Here, the range in the numeric values of data gets normalized between 0 and 1. A number of alternates were considered for defining the contrast quantitatively. The following four measures of track index as defined below were used in this study:

6.4.1.1 Based on Difference in Mean Values

The track index was defined on the basis of difference in the mean values of pixels on-track and located off-track. Depending upon the used statistic measure, the values of measure could be higher either on-track or off-track, and the absolute difference was thus taken as the measure, as described below:

$$TI(D) = \max(P_{OT}, P_T) - \min(P_{OT}, P_T) \quad (6.16)$$

6.4.1.2 Based on Ratio of Mean Values

The track index here was considered on the basis of the ratio of the mean values of pixels on-track and located off-track. Depending upon the used statistic measure, the values of measure could be higher either on-track or off-track; therefore, the ratio of maximum and minimum values was taken as the measure, as defined below:

$$TI(R) = \frac{\max(P_{OT}, P_T)}{\min(P_{OT}, P_T)} \quad (6.17)$$

6.4.1.3 Based on Normalized Difference in Mean Values

The track index here was considered by normalizing the difference in mean values of pixels on-track and located off-track. The measure was defined as follows:

$$TI(ND) = \frac{\max(P_{OT}, P_T) - \min(P_{OT}, P_T)}{\max(P_{OT}, P_T) + \min(P_{OT}, P_T)} * 100 \quad (6.18)$$

6.4.1.4 Based on the Ratio of Coefficient of Variance

The track index here considered the distinguishing feature of the track based on the standard deviation of the values of pixels on-track and located off-track. The co-efficient of variance (CV), which is the ratio of standard deviation to the mean value, was used here. Considering this measure, the variance-based index was then defined as below:

$$TI(CV) = \frac{\max(CV(P_{OT}, P_T)) - \min(CV(P_{OT}, P_T))}{\max(CV(P_{OT}, P_T)) + \min(CV(P_{OT}, P_T))} * 100 \quad (6.19)$$

All of the above track indices were evaluated for their effectiveness in this study. In order to do so, these indices were computed using data for different enhancement measures.

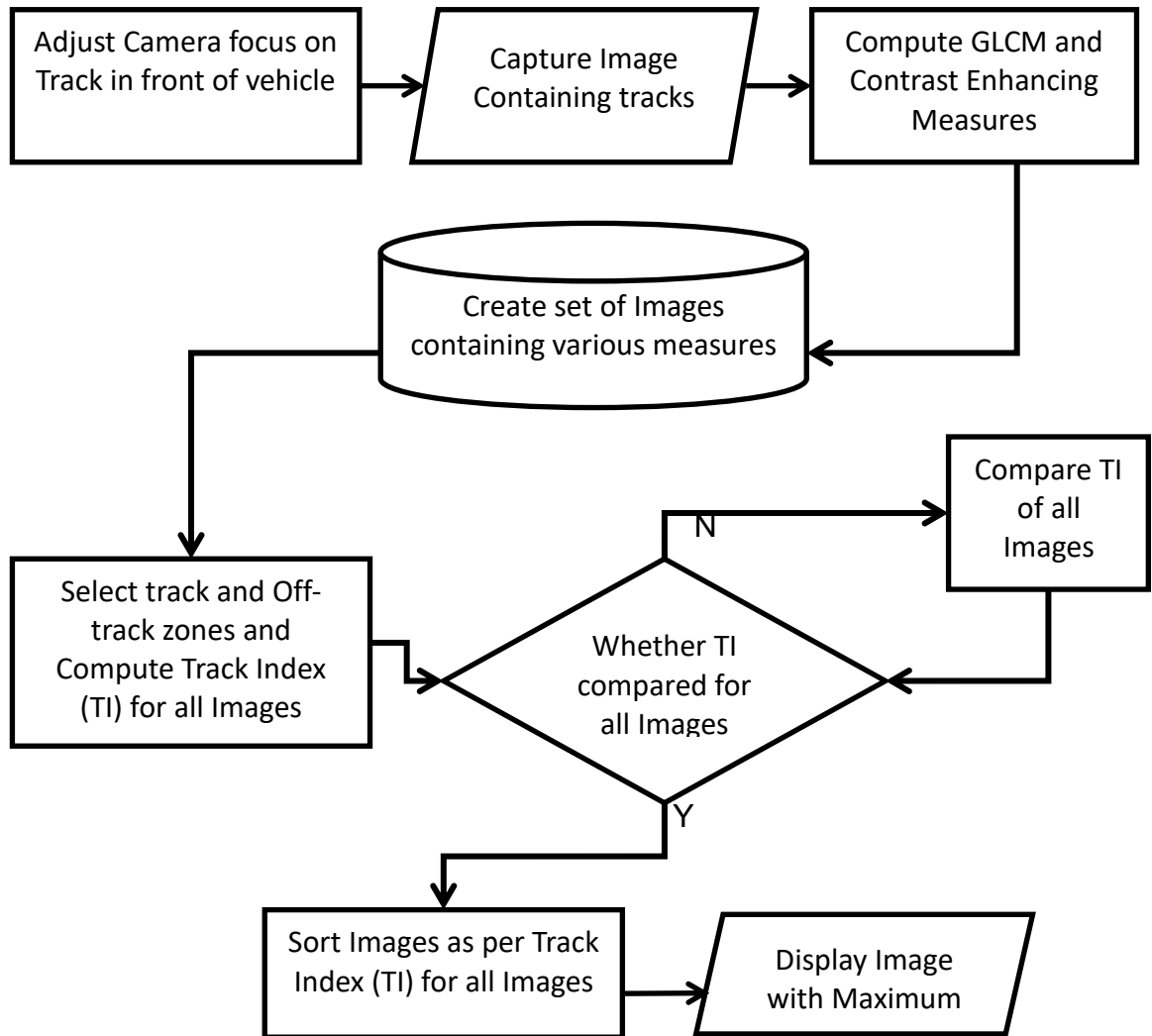


Fig. 6.5 Process flow to generate image with maximum track index outside of using various contrast enhancement measures.

6.4.2 Analysis of Track Contrast Data

The track impressions of the leading vehicle in the off-road terrain were used in this study. The track images were captured using vision cameras on board the vehicle. The procedure for obtaining the maximum contrast using different contrast enhancement measures is indicated in Fig. 6.5.

This procedure was applied for computing the track indices on various images created using different enhancement measures. The results of analysis using different measures are presented in a consolidated image in Fig. 6.6.

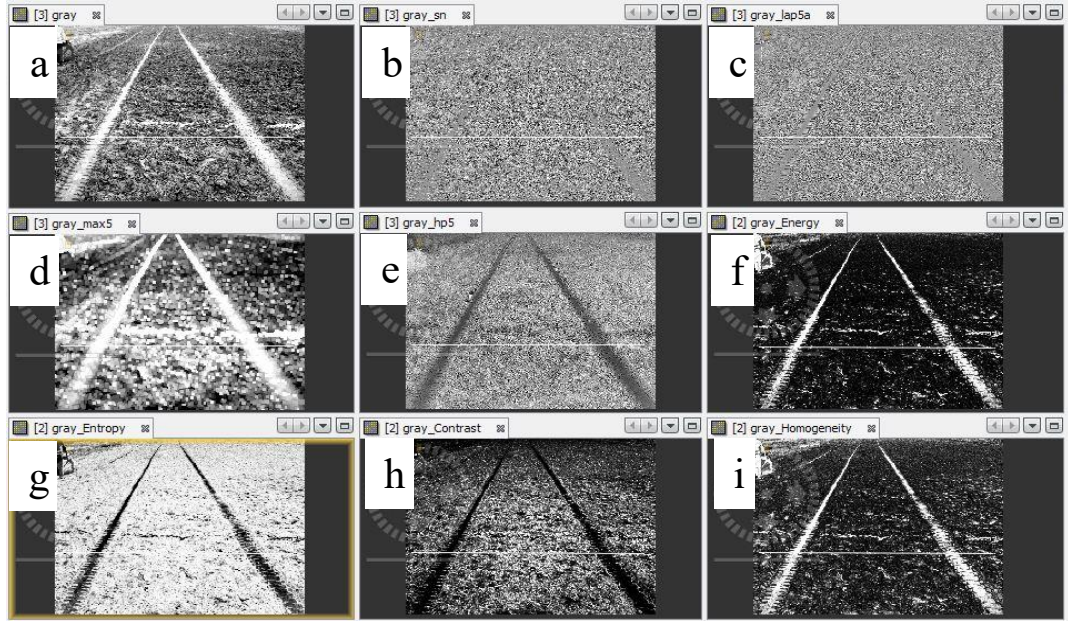


Fig. 6.6 Different contrast enhancement measures of leading vehicle tracks: (a) original gray image of the tracks and images created using (b) Sobel edge detection filter, (c) Laplacian edge filter, (d) Non-linear Max filter and (e) High-pass filter, and using texture measures of (f) Energy, (g) Entropy, (h) Contrast and (i) Homogeneity. (Images created using SNAP 8.0 software)

The visual appearance does create an enhancement in the track index via one or another measure. In order to make a comparative analysis, the pixel values were computed across the track area. The mean and standard deviation (σ) of the pixel values on-track and located off-track were also computed. Further computations were then carried out for evaluating different track indices. The analysis of data was consolidated, as shown in Table 6.1.

Table 6.1 Computation of track index (TI) for quantifying image contrast using different indices

Enhancement Measure	Computation of Track Index									
	Off-Track Mean	On-Track Mean	Off-Track Sigma	On-Track Sigma	Off-Track CV	On-Track CV	TI-Diff	TI Ratio	TI-Ratio-Normalized	TI-CV Diff
Gray	0.52	1.00	0.32	0.01	0.61	0.01	0.48	51.80	31.76	92.15
SobelE	0.47	0.47	0.30	0.05	0.65	0.10	0.00	99.97	0.01	51.98
Laplacian	0.50	0.51	0.35	0.02	0.70	0.04	0.00	99.08	0.46	79.81
Gray_Max	0.71	1.00	0.21	0.00	0.30	0.00	0.29	70.87	17.05	100.00
High-Pass Filter	0.50	0.03	0.33	0.02	0.65	0.54	0.47	1453.30	87.12	24.58
Energy	0.03	0.94	0.05	0.15	1.66	0.16	0.91	3.15	93.89	53.37
Entropy	0.91	0.04	0.14	0.10	0.16	2.52	0.87	2243.73	91.47	89.42
Contrast	0.34	0.00	0.25	0.00	0.73	2.27	0.34	131279.4	99.85	80.38
Homogeneity	0.10	0.97	0.15	0.09	1.49	0.10	0.87	10.61	80.81	23.15

Here, the mean values and standard difference for off-track and on-track pixel values were taken as the basis for evaluating various track indices. These indices indicated the comparative difference in track index values for different image enhancement measures. In order to evaluate the suitability of different measures, a new method was proposed. The images were first sorted and ranked based on the visual appearance. The ranking was then computed for each of the proposed track indexes and marked for each enhancement measure. The obtained details are summarized in Table 6.2.

Table 6.2 Computation of effectiveness of different track indices

Enhancement Measure	Visual vs. Computed Rank					Difference from Actual(>2 Ranks)			
	Vision-Based Ranking	TI-Diff_Rank	TI-Ratio_Rank	TI-Ratio-Normalized Rank	TI-CV-Diff Rank	TI-Diff Rank	TI-Ratio_Rank	TI-Ratio-Normalized Rank	TI-CV-Diff Rank
Gray	6	4	6	6	2	0	0	0	1
SobelE	9	9	9	9	8	0	0	0	0
Laplacian	8	8	8	8	5	0	0	0	1
Gray_Max	5	7	7	7	1	0	0	0	1
High-Pass Filter	7	5	4	4	11	0	1	1	1
Energy	3	1	2	2	7	0	0	0	1
Entropy	1	2	3	3	3	0	0	0	0
Contrast	2	6	1	1	4	1	0	0	0
Homogeneity	4	3	5	5	10	0	0	0	1
% Age Accuracy						88.9	88.9	88.9	33.3

The grading of each of the proposed track indexes was then compared with the visually graded rank of the images as per the track contrast. As the manually graded rank was subjected to some uncertainty in the correct ordering, a deviation of two ranks in computed rank from the manually graded rank was considered as acceptable. The table also indicates the results of the acceptable image ranking. The difference from the manual rank in the table is marked with *0* where the rank is within 2 images and marked as *1* where the difference is more than 2 images. The correctness of results was then computed and is given in the table above.

6.5 Discussion

The study about enhancing the track contrast using various contrast enhancement measures as consolidated in various Figures and tables demonstrates some important inferences. In the areas with low contrast, posing difficulty in the delineation of track areas, various image processing techniques (Gonzalez, 2009;

Varshney and Arora, 2004) can be used to complement the interpretation process. This can help vision-systems-based decision-making processes to be more robust in their interpretation.

It is observed from Fig. 6.1 and Fig. 6.2 that when a group of pixels representing any feature has a differentiable spatial arrangement from its surroundings, the role of texture assumes importance. The visual appearance of the contrast images demonstrates the role of texture in enhancing the track contrast in situations posing difficulty in the delineation of tracks. Further, the contrast images consolidated in Fig.6.1–Fig.6.3 indicate the role of GLCM in representing texture. Various statistic measures used here are seen as good indicators for delineating vehicle tracks. This supports the view expressed by Mohanaiah et al., 2013 that GLCM-based measures give very good results in many fields of applications.

Depending upon the surrounding features, the most optimal texture measures enhancing track features are seen to vary. The visual appearance of different contrast images in Fig. 6.6 demonstrates the varying role of different contrast enhancement measures in a given scenario. In order to make a comparative analysis, a quantitative method was proposed in this study. The pixel values computed at various locations across the track were used for this purpose. The mean and standard deviation of the pixel values on-track and located off-track were also computed and normalized to facilitate a comparison of all images with different ranges of contrast enhancement measures.

Different forms of track indices have been explored and presented in this study, as shown in Table 1. In order to compare the effectiveness of the track indices, the visual comparison was taken as the basis and the images were sorted based on each of the track indexes. The outcome of the comparison with visual perception as given in Table 6.2 demonstrates the effectiveness of the proposed track indices. The accuracy levels of the sorted images indicate that the proposed track-index-based approach is quite effective in sorting the contrast images based on the levels of contrast.

The proposed track-index-based approach can therefore be used for sorting the images of different enhancement measures based on track contrast. Although track indexes based on difference and ratio are both effective in sorting the images correctly, it is important that the influence of terrain features be considered here. For instance, in using the ratio-based track index, the Sobel- and Laplacian-based images, which have minimal variations in mean values of on-track and off-track areas, could lead to unexpected results. This kind of issue capped the overall accuracy of the results using the proposed track index, which in the present case could result in 88% accuracy. A separate study could shed more light on better understanding the influence of varying topography, the size of the kernel, the width of the interpretation channel, etc. However, on a comparative basis, the track index

based on the normalized ratio of difference is suggested to be used on preference, as it normalizes the comparison of different statistical measures rather than considering the absolute difference or ratio of the measures. An additional study could make this aspect even clearer for improving the result further. At this stage, machine learning tools could also be used to improve the accuracy levels of sorting the images even further based on inputs from all of these track indices.

While computing the track index, certain aspects need to be considered. The boundary areas of features in the track area influence the values of some enhancement measures, particularly in texture images. Therefore, for the computation of the track index, points in the track zone may thus be selected away from boundary areas for better inference of the track index.

Another study was carried out by the authors in desertic terrain to understand the influence of surrounding terrain features. Here, some additional parameters of GLCM were also considered and were related to GLCM mean and GLCM variance. The results shown in Fig. 6.3 indicate that the track could be delineated better than the original image by using one or another image enhancement measure as per the details given by Haralick, 1973 and Connors and Harlow, 1980. However, the most optimal measure in a given situation depends upon the surrounding terrain features. Therefore, the procedure given in Fig. 6.5 was adopted, which accounts for these variations and highlights the image with maximum track contrast.

Nowadays, machine learning is replacing human efforts. A number of attempts are being made in related studies of lane detection and its conditions, applying deep learning models. The accuracy of classification depends upon the accuracy and robustness of training sets. There are many cases when the vehicle tracks are there with feeble boundaries. This is where the proposed study of maximizing the track contrast could also be used for generating a robust and accurate dataset of track contrast.

The proposed study is seen to give a new method for making various tracks following off-road operations sustainable by improving decisions in low-contrast areas. This meets the requirements of both manual and autonomous navigation. Thus, the earlier works on the rut or track following vehicles as presented by Ordonez et al., 2011; Mei et al., 2018 and Chowdhury et al., 2017 can be improved even further. The proposed methodology can support making intelligent on-board decisions for delineating track zones.

6.6 Conclusions

Using visual analytics together with image intelligence and the optimal delineation of track features, a track-index-based contrast enhancement study was presented here leading to the following set of key conclusions:

1. In the locations posing difficulty due to low contrast in the delineation of track areas, various image processing techniques can be employed to complement the interpretation process.
2. In the context of identifying track zones with a significant dimension, texture measures play a vital role in enhancing track contrast for the improved delineation of vehicle tracks. Gray-level co-occurrence matrix (GLCM)-based statistic measures are used here to evaluate the track texture. These measures are seen to improve the contrast of vehicle tracks significantly.
3. A track-index-based quantitative measure could effectively be used for the comparative analysis of different contrast enhancement measures with a wide range of variations.
4. The proposed track-index-based technique can be usefully employed to sort out various images on the basis of track contrast with 88% accuracy, as seen in the current case. Further study to understand the influence of varying topography, the size of the kernel and the width of the interpretation channel, etc., could lead to an improvement in track index.
5. The proposed visual analytics and track-index-based approach leading to improved inference of track features could augment the decision-making process for improved autonomous decisions in low-contrast areas.

The proposed study is a novel way to make various tracks following off-road operations sustainable by improving decisions in low-contrast areas. The proposed methodology can support intelligent decisions in on-board vehicles for the better delineation of track zones.

6.7 References

1. Army, U. S. (1993). FM 3-19 FMFM 11-20 NBC Reconnaissance. Available online: <https://www.hsdl.org/?view&did=1049> (accessed on 30 July 2022).
2. Graefe, V., & Kuhnert, K. D. (1992). Vision-based autonomous road vehicles. In Vision-based vehicle guidance (pp. 1-29). New York, NY: Springer New York.

3. Ordonez, C., Chuy Jr, O. Y., Collins Jr, E. G., & Liu, X. (2011). Laser-based rut detection and following system for autonomous ground vehicles. *Journal of Field Robotics*, 28(2), 158-179.
4. Mei, J., Yu, Y., Zhao, H., & Zha, H. (2017). Scene-adaptive off-road detection using a monocular camera. *IEEE Transactions on Intelligent Transportation Systems*, 19(1), 242-253.
5. Islam, F., Nabi, M. M., & Ball, J. E. (2022). Off-road detection analysis for autonomous ground vehicles: A review. *Sensors*, 22(21), 8463.
6. Anbalagan, S., Srividya, P., Thilaksurya, B., Senthivel, S. G., Suganeshwari, G., & Raja, G. (2023). Vision-Based Ingenious Lane Departure Warning System for Autonomous Vehicles. *Sustainability*, 15(4), 3535.
7. Shamsolmoali, P., Zareapoor, M., Zhou, H., Wang, R., & Yang, J. (2020). Road segmentation for remote sensing images using adversarial spatial pyramid networks. *IEEE Transactions on Geoscience and Remote Sensing*, 59(6), 4673-4688.
8. Forkel, B., Kallwies, J., & Wuensche, H. J. (2021, July). Combined Road Tracking for Paved Roads and Dirt Roads: Framework and Image Measurements. In *2021 IEEE Intelligent Vehicles Symposium (IV)* (pp. 1326-1331). IEEE.
9. Burchfiel, B., & Konidaris, G. (2018, October). Hybrid bayesian eigenobjects: Combining linear subspace and deep network methods for 3D robot vision. In *2018 IEEE/RSJ International Conference on Intelligent Robots and Systems (IROS)* (pp. 6843-6850). IEEE.
10. Marcus, G. (2018). Deep learning: A critical appraisal. *arXiv preprint arXiv:1801.00631*.
11. Helmy, M., Truong, T. T., Jul, E., & Ferreira, P. (2023). Deep learning and computer vision techniques for microcirculation analysis: A review. *Patterns*, 4(1).
12. Gonzalez, R. C. (2009). *Digital image processing*. Pearson education india.
13. Varshney, P. K., & Arora, M. K. (2013). *Advanced image processing techniques for remotely sensed hyperspectral data*. Springer Science & Business Media.
14. Janani, P., Premaladha, J., & Ravichandran, K. S. (2015). Image enhancement techniques: A study. *Indian Journal of Science and Technology*, 8(22), 1-12.
15. Mohanaiah, P., Sathyanarayana, P., & GuruKumar, L. (2013). Image texture feature extraction using GLCM approach. *International journal of scientific and research publications*, 3(5), 1-5.
16. Graovac, S., & Goma, A. (2012). Detection of road image borders based on texture classification. *International Journal of Advanced Robotic Systems*, 9(6), 242.
17. Zhang, X., Cui, J., Wang, W., & Lin, C. (2017). A study for texture feature extraction of high-resolution satellite images based on a direction measure and gray level co-occurrence matrix fusion algorithm. *Sensors*, 17(7), 1474.

18. Singh, M., Trivedi, A., & Shukla, S. K. (2019). Strength enhancement of the subgrade soil of unpaved road with geosynthetic reinforcement layers. *Transportation Geotechnics*, 19, 54-60.
19. Singh, M., Trivedi, A., & Shukla, S. K. (2022). Evaluation of geosynthetic reinforcement in unpaved road using moving wheel load test. *Geotextiles and Geomembranes*, 50(4), 581-589.
20. Kalra, M. K., Shukla, S. K., & Trivedi, A. (2023). Track-Index-Guided Sustainable Off-Road Operations Using Visual Analytics, Image Intelligence and Optimal Delineation of Track Features. *Sustainability*, 15(10), 7914.
21. Gupta, S., Shrivastwa, S., Kumar, S., & Trivedi, A. (2023). Self-attention-Based Efficient U-Net for Crack Segmentation. In *Computer Vision and Robotics: Proceedings of CVR 2022* (pp. 103-114). Singapore: Springer Nature Singapore.
22. Howard, A., & Seraji, H. (2001). Vision-based terrain characterization and traversability assessment. *Journal of robotic systems*, 18(10), 577-587.
23. Chowdhury, N. H., Khushib, D., & Rashid, M. M. (2017). Algorithm for line follower robots to follow critical paths with minimum number of sensors. *International Journal of Computer*, 24(1), 13-22.
24. Babu, P., Rajamani, V., & Balasubramanian, K. (2015). Multi-peak mean based optimized histogram modification framework using swarm intelligence for image contrast enhancement. *Mathematical Problems in Engineering*, 2015(1), 265723.
25. Marques, O. (2011). *Practical image and video processing using MATLAB*. John Wiley & Sons.
26. Bharati, M. H., Liu, J. J., & MacGregor, J. F. (2004). Image texture analysis: methods and comparisons. *Chemometrics and intelligent laboratory systems*, 72(1), 57-71.
27. Humeau-Heurtier, A. (2019). Texture feature extraction methods: A survey. *IEEE access*, 7, 8975-9000.
28. Alsmadi, M. K. (2020). Content-based image retrieval using color, shape and texture descriptors and features. *Arabian Journal for Science and Engineering*, 45(4), 3317-3330.
29. Doycheva, K., Koch, C., & König, M. (2019). Implementing textural features on GPUs for improved real-time pavement distress detection. *Journal of Real-Time Image Processing*, 16, 1383-1394.
30. Sudha, S. K., & Aji, S. (2019). A review on recent advances in remote sensing image retrieval techniques. *Journal of the Indian Society of Remote Sensing*, 47(12), 2129-2139.
31. Liu, C., Xu, A., Hu, C., Zhang, F., Yan, F., & Cai, S. (2020, March). A New Texture Feature Based on GLCM and Its Application on Edge-detection. In *IOP Conference Series: Materials Science and Engineering* (Vol. 780, No. 3, p. 032042). IOP Publishing.
32. Li, M., Li, Y., & Jiang, M. (2018). Lane detection based on connection of various

- feature extraction methods. *Advances in Multimedia*, 2018(1), 8320207.
33. Gupta, S., & Porwal, R. (2016). Combining laplacian and sobel gradient for greater sharpening. *IJIVP*, 6, 1239-1243.
 34. Haralick, R. M., Shanmugam, K., & Dinstein, I. H. (1973). Textural features for image classification. *IEEE Transactions on systems, man, and cybernetics*, (6), 610-621.
 35. Connors, R. W., & Harlow, C. A. (1980). A theoretical comparison of texture algorithms. *IEEE transactions on pattern analysis and machine intelligence*, (3), 204-222.
 36. Clausi, D. A. (2002). An analysis of co-occurrence texture statistics as a function of grey level quantization. *Canadian Journal of remote sensing*, 28(1), 45-62.
 37. Gadkari, D. (2004). Image quality analysis using GLCM. Orlando (FL): University of Central Florida, 2004.

CHAPTER - 7

AN ADAPTIVE TECHNIQUE TO SELECT THE MOST EFFECTIVE RUT ENHANCEMENT MEASURE IN A GIVEN SURROUNDING

The suitable rut enhancement measures have been observed to vary as per the surrounding terrain. An adaptive technique has been explored that can select the most effective rut enhancement measure in a given surrounding.

7.1 Introduction

The movement of vehicles on unpaved terrain is quite common in agriculture, forestry, armed forces, robotics, Unmanned Ground Vehicles (UGV), night safari, etc. Many challenging operations like firefighting, search and rescue, and movement in snow-bound and loose desert soils for many combat missions utilize the unpaved off-road terrain during need. The trafficability condition of the area depends upon the spatial features and the ground state to support the movement of vehicles. Significant resources are available to infer the trafficability condition using spatial data resources. For instance, Pundir and Garg, 2021 worked on evaluating the impact of terrain features on trafficability employing spatial data resources. However, empirical and experimental models are there for precise evaluation of prevalent soil condition and their inference on trafficability conditions. Vehicles in many places get stuck due to these uncertainties.

Delineation of vehicle tracks on unpaved terrain reflects the wealth of information about trafficable off-road routes for these areas. Moreover, the rut formed by the earlier vehicular movement on unpaved terrain becomes the preferred route for applications like night safari and robotics-based operations for better stability (Ordonez et al., 2011). Tremendous work exists to study the rut formed by vehicles from different perspectives. For instance, Kalra et al., 2023 investigated the rut contrast improvement using various alternate indices. Liu et al., 2009 studied the variation in rut width on turnings using military vehicles. In another study, Vennik et al., 2019 investigated the impact of single and multiple passes of military vehicles. During strategic missions, vehicles move on unpaved terrain in low contrast dark conditions ((US Army FM 3-19, 1993). In such a scenario, the delineation of tracks or the rut impressions by leading vehicles plays an important role.

These days, many vehicular operations make use of vision-based systems. Pierzchala et al., 2016 used close-range photogrammetry to detect the rut. Salmivaara et al., 2018 worked on a vehicle-mounted LiDAR system for rut depth

detection and measurement. Digital image processing techniques are there to be employed to enhance the features of interest (Gonzalez et al., 2004). However, these techniques alone extend limited aid for delineating the tracks from their surroundings in an image. The pattern and texture of these tracks over tonal variation are some appropriate measures that enable the delineation of these tracks. The statistical measures of the GLCM-based texture analysis technique have shown reasonably good results in a wide range of applications (Mohanaiah et al., 2013). Fauji et al., 2020 presented one such study for improving the robustness of detection of road surfaces in varied environmental conditions using a combination of GLCM measures and local binary pattern (LBP).

In this work, the authors investigated conventional and texture-based analysis to delineate the tracks. The study used satellite images representing different resolutions and ground-based vehicle tracks formed by leading vehicles. A quantitative track index (TI) based approach is examined in this study to compare and find the most appropriate contrast measure for the delineation of tracks. The details of the study are presented here.

7.2 Related Work

Caraffi et al., 2007 used decision networks and the stereo vision technique for detecting the off-road path and obstacles. Howard and Seraji, 2001 used a vision system-based mobile robot for real-time terrain characterization by applying Artificial Neural Network (ANN). Ordonez et al., 2011 investigated the movement of robotic vehicles by tracking the rut in unpaved areas. Chowdhury et al., 2017 introduced an algorithm for a line-following robot to follow the straight-line path autonomously.

There are various techniques used for the enhancement of image contrast. These image-processing-based techniques primarily employ filters and histogram stretching. Janani et al., 2015 made a compilation of different image enhancement techniques. Babu et al., 2015 presented a framework for contrast enhancement. The edge detection techniques that preserve the structural features and the high-frequency components belong to either of the two groups based on the derivatives (Marque, 2011). The first one computes the Gradient or the first-order derivative of an image. The second one, based on the second-order derivative is a Laplacian operator. Both these filters highlight sharp changes or discontinuities in the picture. However, the gradient-based filters emphasize the prominent edges while Laplacian filters enhance the finer details (Gupta and Porwal, 2016). Based on these, researchers brought out several edge detection algorithms. Shrivakshan and Chandasekar, 2012 compared the prominent edge detection algorithms covering Sobel, Robert's cross gradient, Prewitt, Canny, Laplacian of Gaussian (LoG), etc. The goodness of edge detection algorithms depends upon measures such as the accuracy of edge detection, the localization of edges, and the minimal response. Canny's edge detection is a

computationally more expensive algorithm. However, it performs better than all these operators under almost all scenarios (Narendra and Hareesh, 2011).

The track features appear like an edge in the low resolution images. These features appear like elongated areas in high resolution images. In such a scenario, various high pass and edge detection filters are seen to give limited information for delineation of these tracks that pass through diverse surroundings. However, the distinctive pattern formed by these tracks gives rise to relative variation in its texture from the surroundings.

The relationship of pixels with neighboring pixels reveals worthwhile information distinctive to distinguish these objects. Various approaches exist that describe the texture in an image. Bharti et al., 2004 compared different approaches to describe the texture. Humeau-Heurtier, 2019 presented a survey of various methods of texture feature extraction. GLCM-based texture analysis could delineate well the road boundaries (Graovac and Goma, 2012). Measures like energy, homogeneity, entropy, contrast, etc. define the texture using this approach.

The most suitable texture measure that can distinguish the track area more prominently depends upon the surrounding. A study to enhance contrast enhancement using different alternate approaches is presented here. The proposed method of comparative analysis makes way for selecting the most optimal contrast enhancement measure.

7.3 Methodology Used

Suitable image processing techniques enhance the vehicle tracks and assist in their delineation in an image. The image background, resolution, and noise level in the image containing the tracks form the basis for selecting suitable measures.

7.4 Various Edge Enhancement and High-Frequency Filters

In some coarse-resolution imagery, the track impressions appear as linear features. In such cases, high-pass and edge-detection filters facilitate the detection of these features.

Edges that form a set of connected pixels create a boundary between two disjoint areas. Edge detection aids in highlighting the high-frequency components in an image. Edge detection usually depends upon the computation of the first or second derivatives of the image (Marque, 2011) and computed as below:

$$\nabla f = \text{grad}(f) = \begin{bmatrix} g_x \\ g_y \end{bmatrix} = \begin{bmatrix} \frac{\partial f}{\partial x} \\ \frac{\partial f}{\partial y} \end{bmatrix} \quad (7.1)$$

Here, g_x and g_y are the first derivative or gradients of the image $f(x,y)$ and show the pixel value changes in both x and y directions. It is defined using the column vector ∇f . The second derivative-based edge filter is also defined using Laplacian of the image $f(x,y)$ computed using a second-order differential equation as given below:

$$\nabla^2 f = \frac{\partial^2 f}{\partial^2 x} + \frac{\partial^2 f}{\partial^2 y} \quad (7.2)$$

Based on the above procedure, a study brings out the comparative analysis of various edge detection algorithms like Sobel, Canny, Prewitt, and *LoG*. The images processed for highlighting the edges use different high-frequency filters that de-emphasize the low-intensity features. All such operations make use of the convolution of images with filters for representing various edges or other high-frequency filters as given here:

$$\text{Conv}(w, f) = w(x, y) * f(x, y) = \sum_{s=-a}^a \sum_{t=-b}^b w(s, t) f(x-s, y-t) \quad (7.3)$$

here, $w(s,t)$ denotes a filter of dimension $(s \times t)$ that scans over the image $f(x,y)$. The symbol $(*)$ stands for convolution- $\text{Conv}(w,f)$ of image and filter. In these techniques, noise removal can be helpful. Barbu, 2021 presented the details about using a fourth-degree partial differential equation to remove the noise. Tavakkol et al., 2022 showed a spatially adaptive technique that performs when the directional texture is there.

7.5 Image Texture Measures

Most of the techniques mentioned above try to enhance the image contrast using primarily tone-based image classification, which gives limited understanding. This study uses texture measures as a descriptor of the spatial relation of pixels. Several applications employ texture for extracting the required features. Zhang et al., 2008 and Alsmadi, 2020 attempted content-based image retrieval by combining the edge detection and properties of a co-occurrence matrix. Pradhan et al., 2014 demonstrated the extraction of flooded areas using a *GLCM*-based texture analysis based program over TerraSAR- X satellite image. Micheal and Vani, 2015 employed texture features for automatic mountain detection using DTM data of lunar

images. Doycheva et al., 2019 used texture features for evaluating road distress conditions in real-time. Sudha and Aji, 2019 used *GLCM* texture features as the descriptors of features for image retrieval in varied applications. Liu et al., 2020 employed the local second-order entropy to characterize the variation in the grayscale. Winarno et al., 2021 applied edge detection with *GLCM* for fingerprint recognition even though the edges are predominant in such images. Here, the authors used edge detection for preprocessing. Feature extraction is based on the *GLCM* using measures like energy, contrast, homogeneity, and correlation to improve the results further. Singh et al., 2022 employed features of *GLCM* on Sentinel-2 imagery for the identification of avalanche debris areas. Kar and Banerjee, 2022 used *GLCM* texture features to evaluate the intensity of tropical cyclones.

This study used *GLCM*-based measures as a good descriptor of texture features. Haralick et al., 1973 proposed the *GLCM*-based concept of measuring texture by computing different texture measures. He introduced 14 features to represent the texture of an image. Subsequently, Conners and Harlow, 1980 presented that out of 14 parameters, only five are good enough to describe texture.

These parameters include Energy, homogeneity, entropy, correlation, and contrast. The following paragraphs provide details about the key measures used in the current study.

1) Energy: This parameter which reflects the uniformity and represents the angular second moment computes the uniformity of texture. This measure considers the pixel pair repetitions and detects the disorders in textures. A constant or periodic form shows high values of energy. The following equation defines this measure:

$$Energy = \sum_{i,j} p(i,j)^2 \quad (7.4)$$

where, $p(i,j)$ is the probability value recorded for the co-occurrence of cell i,j of the *GLCM* matrix.

2) Homogeneity: This statistic assumes larger values for the slight differences in the gray tone of pair elements and is more sensitive to near diagonal elements of the *GLCM*. It gives maximum value when all the image elements have same value. The following equation defines this measure:

$$Homogeneity = \sum_{i,j} \frac{p(i,j)}{1 + |i - j|} \quad (7.5)$$

3) Entropy: This statistic computes the complexity or disorderliness of the image. Complex texture typically has high entropy. The entropy is small for the image containing uniform texture whose GLCM elements have large values. The entropy correlates inversely with energy. The following equation defines this measure:

$$Entropy = - \sum_{i,j} (p_{i,j}) \log_2(p_{i,j}) \quad (7.6)$$

4) Correlation: It measures the linear dependency of gray level values in the GLCM matrix. It reflects the relation of the reference pixel with its neighbor. The following equation defines this measure:

$$Correlation = \sum_{i,j} \frac{(i - \mu_i) \cdot (j - \mu_j) \cdot p(i,j)}{\sigma_i \cdot \sigma_j} \quad (7.7)$$

where, μ_i , μ_j , σ_i , and σ_j are the means and standard deviations.

5) Contrast: This statistic represents the spatial frequency of an image and gives the difference-moment of *GLCM*. In the contiguous set of pixels, it evaluates the quantum of local variations by considering the difference between the highest and the lowest values pixels. The following equation defines this measure:

$$Contrast = \sum_{i,j} |i - j|^2 p(i,j) \quad (7.8)$$

GLCM contrast correlates inversely but strongly with homogeneity. Homogeneity decreases when the contrast increases while maintaining constant energy levels. This study presents the utility of all the above-computed texture measures over the track images. It computes these statistical measures and gives details for optimal selection reflecting maximum contrast.

7.6 Data and Tools Used

This study uses filters of suitable size representing different high-pass and edge enhancement filters and texture measures. It convolves them over the image to create the resulting filtered images. This study used *GLCM*-based measures to define the image texture. More levels imply higher accuracy but with increased computational cost. Clausi, 2002 provided details about the computational complexity using the *GLCM* method, which is proportional to $O(G^2)$. Suitable selection of displacement value in *GLCM* is a significant consideration as the large values result in missing the details of textural information (Gadkari, 2004). This

study uses a kernel of size 5×5 , a quantization level of 32, and a horizontal offset of 1 pixel to compute texture. It assigns the value to the center pixel of the filter, which then moves further to cover the whole image. This study used MATLAB and Sentinel Application Platform (SNAP) for further analysis. The google earth images of different resolutions, displaying track areas near Chandigarh given in Fig. 7.1a formed the basis for further study.

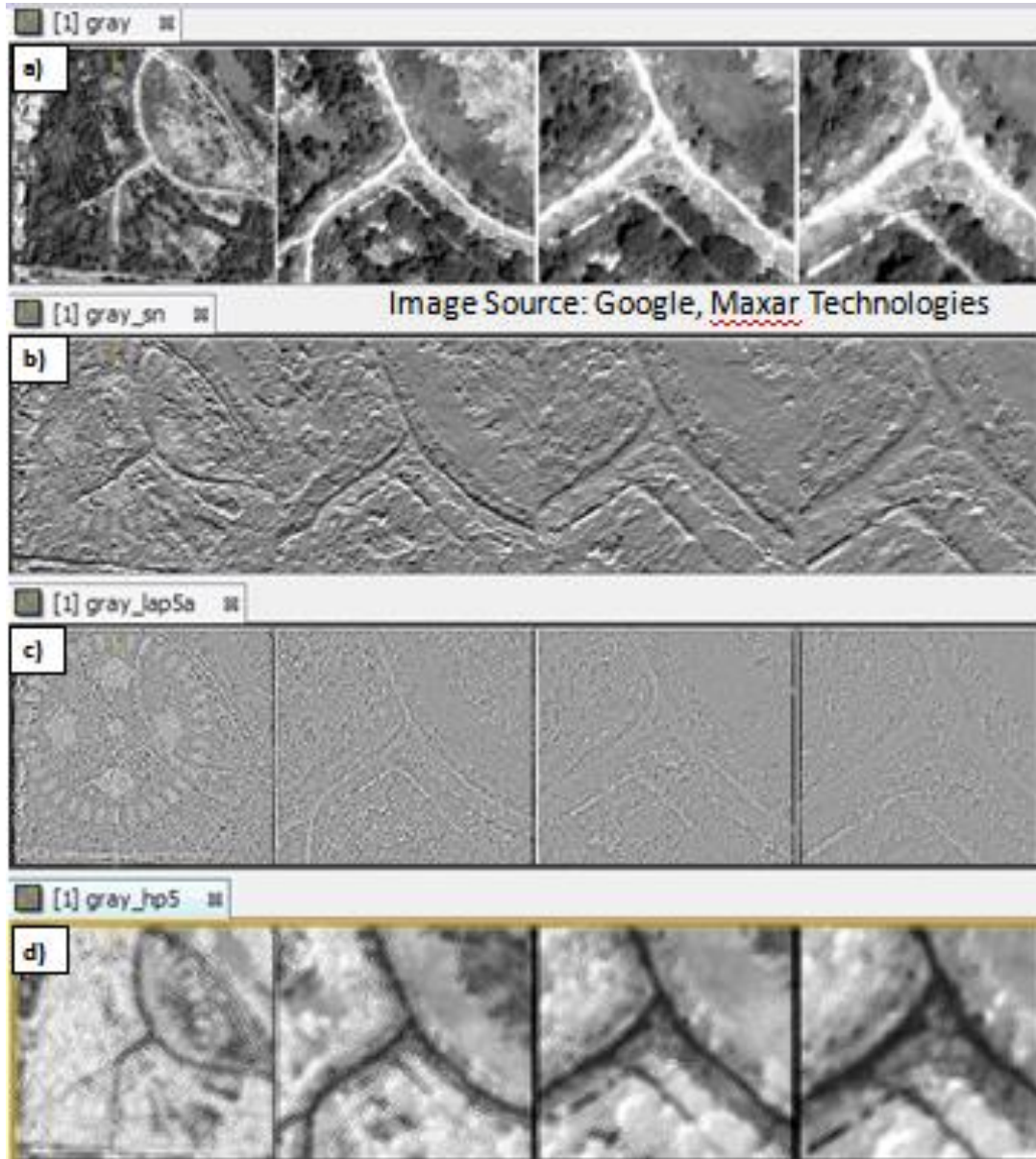


Fig. 7.1 a) Multi-resolution images of tracks (Source: Google, Maxar Technologies). Result after convolving images b) using Sobel edge detection filter c) using second-order Laplacian filter and d) using the high-pass filter.

7.7 Image Analysis and Results

Several conventional techniques can assist detection of various features in the image. Since the idea here is to highlight the linear track features and enhance their contrast, the authors analyzed the impact of edge detection and high-pass filters. The convolution using the Sobel gradient and Laplacian filter resulted in images as shown in Fig. 7.1b and Fig. 7.1c respectively. As the track boundaries are delineable using a high-pass filter, its convolution resulted in the image in Fig. 7.1d. The Fig. also shows a comparative effect of these techniques on three different resolutions. As the tracks have differentiable texture from the surroundings, the texture analysis using GLCM revealed meaningful results. Fig. 7.2 shows the outcome of various statistical measures on images of different resolutions.

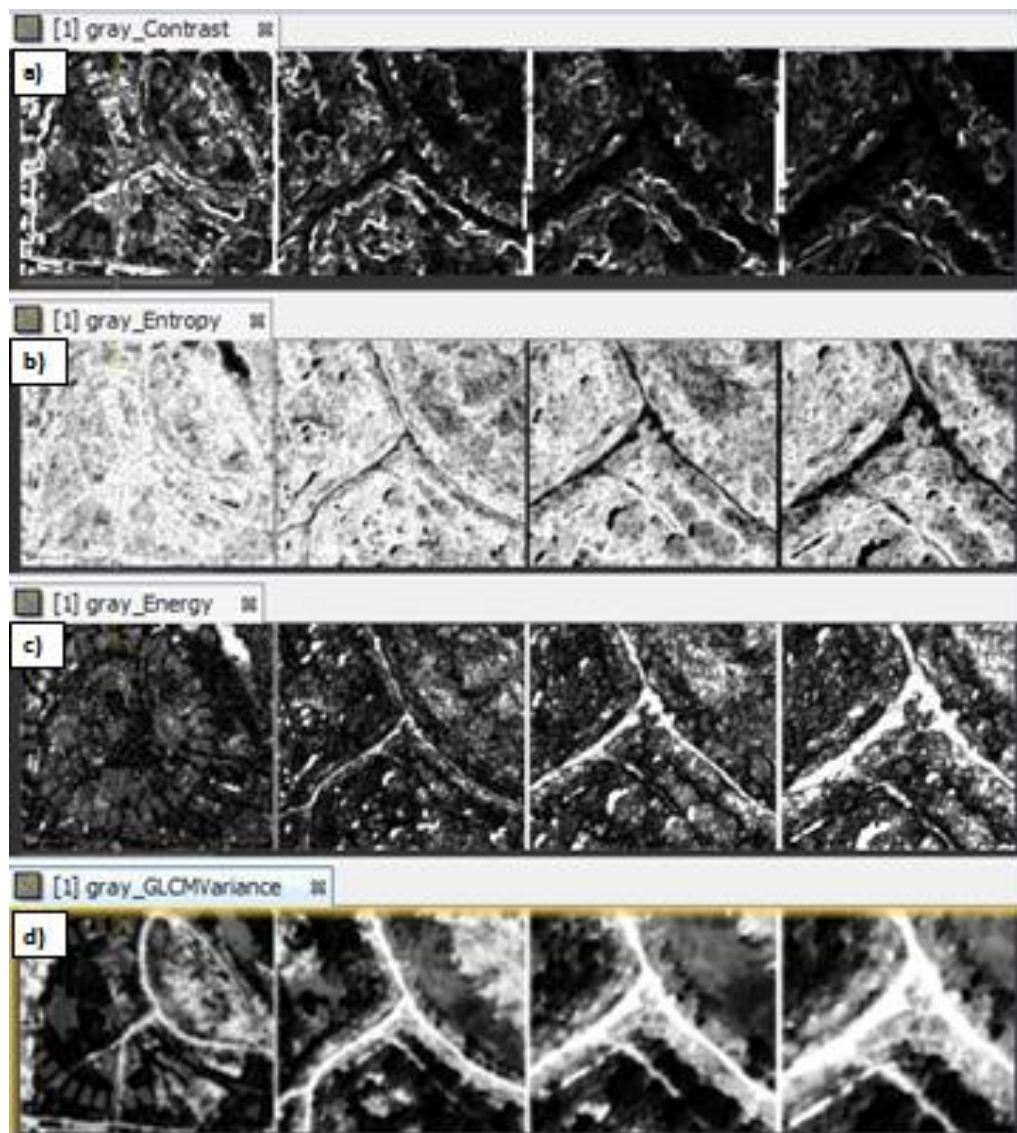


Fig. 7.2 Result of GLCM texture analysis on the multi-resolution images a) Contrast Image b) Entropy Image c) Energy Image and d) Variance Image

The visual appearance of the results at different resolution images brings out the importance of texture as the resolution improves. The texture analysis is carried further on the even finer resolution images captured using ground-level cameras. The illustration in Fig. 7.3 displays the track impressions of the leading vehicle. The contribution of texture increases as one moves toward the finer level of resolution.

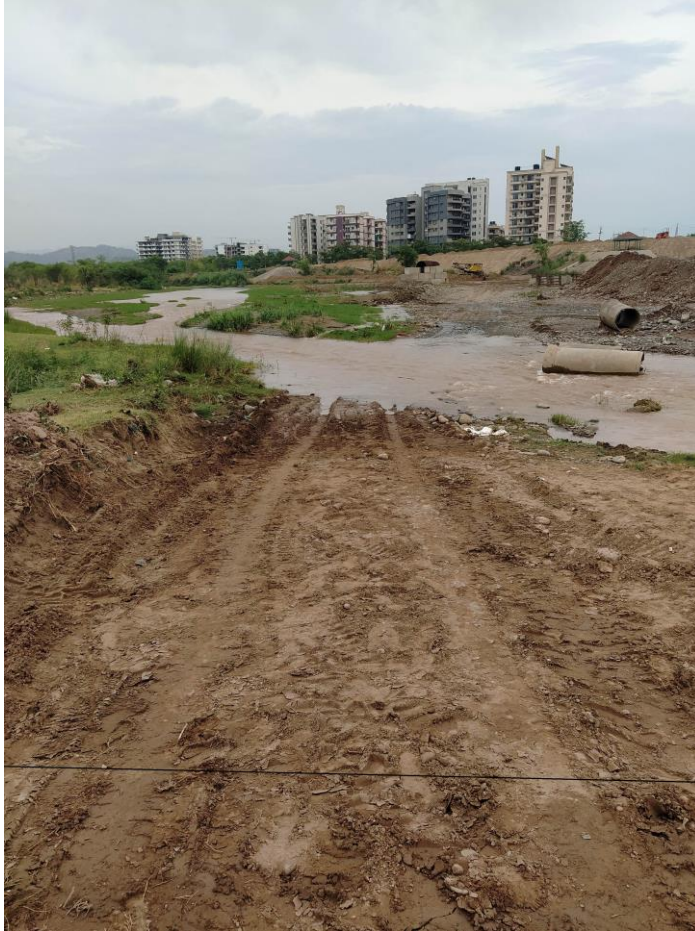


Fig. 7.3 Field Image of vehicle tracks impressions of leading vehicle

The Fig. 7.4 illustrates results of different contrast enhancement measures and texture analysis on the image of vehicle tracks, as observed in field running conditions.

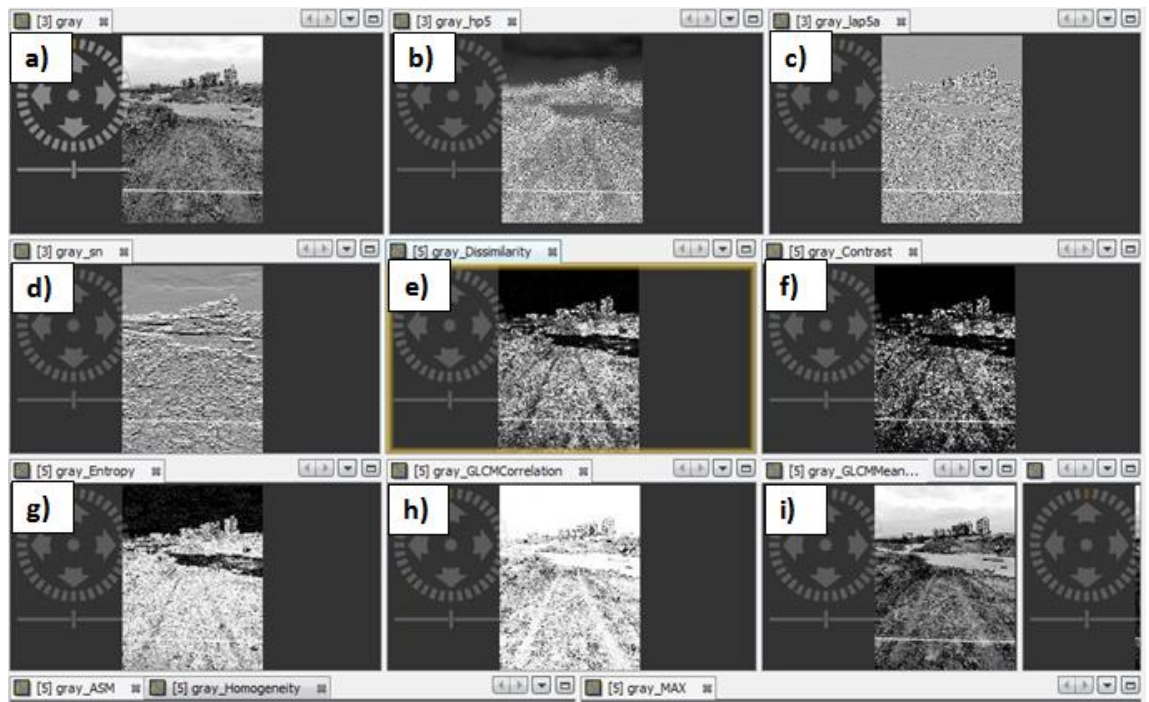


Fig. 7.4 a) Images of Vehicle Track impressions as observed in vehicle running condition a) In Original Gray tone and Using b) High-Pass filter c) Laplacian Filter d) Sobel Edge detection filter and GLCM measures of e) Dissimilarity f) Contrast g) Entropy h) Correlation i) Mean filter

These results exhibit the role of texture analysis for improved delineation of the vehicle tracks. The authors proposed a quantitative method of computing and comparing the track contrast here. This method considers the relative difference in contrast for on-track and off-track areas and computes the track index for arriving at the most optimal solution.

7.8 Track Index-based Optimal Selection

As illustrated in Fig. 7.5, the procedure comprises drawing a cross-sectional profile across the tracks on the image.

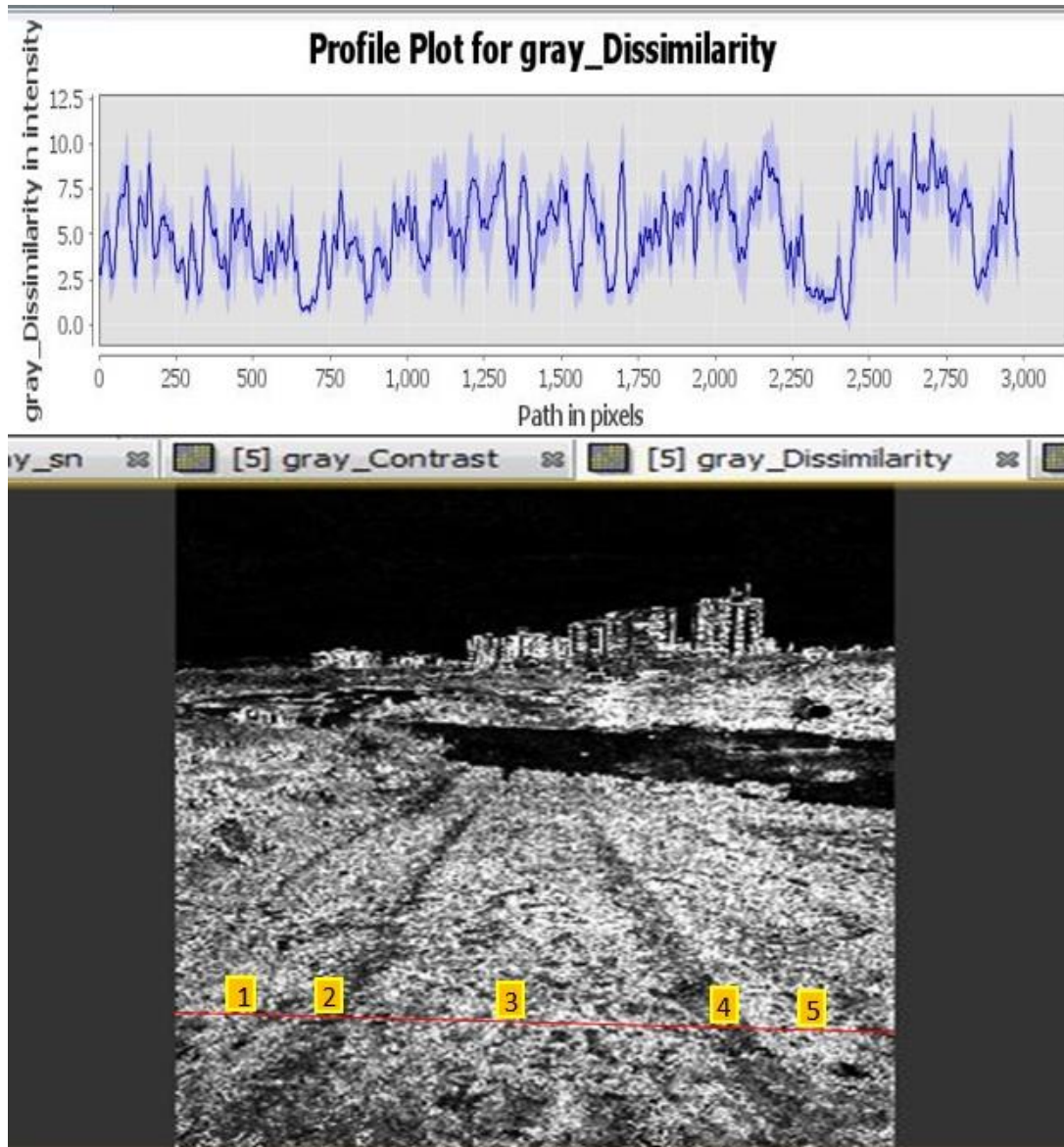


Fig. 7.5 Location of pixels chosen for comparing the contrast of track areas with reference to its surroundings

It selects the Pixels On-track (P_T) and Pixels Off-track (P_{OT}) in the image for each enhancement measure separately. It considers the average value of pixels in each area to account for the local variation. The authors considered this aspect by choosing a rectangular zone of 11x100 pixels. The average value of the statistical measure (x_i) is:

$$P_T = \frac{n_2 x_2 + n_4 x_4}{n_2 + n_4} \quad (7.9)$$

$$P_{OT} = \frac{n_1x_1 + n_3x_3 + n_5x_5}{n_1 + n_3 + n_5} \quad (7.10)$$

where, x_i , $i = [1:5]$ are the averaged statistical measure of areas around tracks. Here x_1 , x_3 , and x_5 are the averaged values for pixels in off-track areas left to the left Track, in-between Tracks, and right to the right Track, respectively. Similarly, the values x_2 and x_4 are the averaged values for pixels on the left and right Track, respectively.

If the focus is to highlight any single track, for instance, the Track by any two-wheeler, the computation for areas representing pixels on the Track is done for the points on one Track. Similarly, the mean value for the area representing Off-track makes the basis on the two zones surrounding the Track.

Data normalization is an important consideration here for a better comparison of the two measures having different ranges of values. Here, normalization considers the minimum and maximum values of the pixel value range for various contrast enhancement measures. The following equation explains this computation process:

$$Y = \frac{X - X_{\min}}{X_{\max} - X_{\min}} \quad (7.11)$$

where, Y is the normalized value of X data representing the contrast enhancement measure and X_{\min} and X_{\max} indicate the minimum and maximum values of its range. Here, the range in the numeric values of data gets normalized between 0 and 1.

The comparison of measures also needs to consider the variance in data for both off-track and on-track zones. Therefore, it uses the mean value and standard deviation to compute the coefficient of variation defined as:

$$CV = \frac{\sigma}{\mu} \quad (7.12)$$

where, CV is the coefficient of variation, and μ is the mean value of the Measure and σ is the standard deviation,. The lower the Coefficient of Variation, the better the reliability of the Measure, representing contrast based on normalized off-track and on-track pixel values. The Track Ratio (TR) for comparing the track contrast used here is:

$$TR = \frac{P_T}{P_{OT}} \quad (7.13)$$

Since the CV value for each image representing different contrast measures will be

different, the equation used for computing the normalized Track Index (TI) here includes:

$$TI = \frac{TR}{CV} \quad (7.14)$$

Table 7.1 gives the comparative details of the normalized track index as evaluated using various image enhancement measures.

Table 7.1 Computation of Track Index (TI) quantifying image contrast

Computation of Track Index						
Contrast Measure	Off_Track Mean	On_Track Mean	TrackRatio (TR)	Off_Tr_Sigma	Coeff of Variation	Track Index(TI)
Correlation	0.858	0.793	0.065	0.192	0.224	29.06
Dissimilarity	0.480	0.551	0.071	0.372	0.775	9.11
Contrast	0.291	0.379	0.088	0.294	1.010	8.72
Gray	0.681	0.632	0.049	0.429	0.630	7.83
Entropy	0.803	0.821	0.018	0.272	0.338	5.34
GLCM Mean	0.541	0.514	0.027	0.316	0.585	4.65
High Pass Filter	0.328	0.379	0.051	0.498	1.519	3.35
GLCM Homogeneity	0.243	0.219	0.024	0.311	1.281	1.86
SobelN	0.452	0.459	0.007	0.433	0.956	0.70
Laplacian	0.515	0.514	0.001	0.512	0.994	0.09
GLCM Variance	0.362	0.362	0.000	0.312	0.861	0.02

7.9 Discussion

Table 7.1 here presents the duly sorted values of the normalized track index. The same suggests that one can achieve better contrast than the original Gray Image using one or the other texture images of Contrast, Dissimilarity, Correlation, etc. The track index value for the original gray image increased from 7.83% to 29.06%. The comparative contrast of the Images shown in Fig. 7.4 confirms this view. It is noticeable that for testing this approach, the areas chosen in off-track and On-track zones are of size 100x11 pixels. By taking larger areas, the conclusions can improve even further.

The observation reveals that the GLCM texture-based technique effectively addresses the contrast enhancement issue. It also supports the view expressed by Mohanaiah et al., 2022 that GLCM-based measures give satisfying results in a large domain of applications. The track contrast enhancement achieved here verifies this point. The studies of the rut following robotic vehicles like the ones presented by Ordonez et al., 2011 and Chowdhury et al., 2017 can have improved decision-making about the track areas using the proposed technique.

Some related aspects are notable here. If a vehicle moves in a zig-zag fashion or during curves, Liu et al., 2009 reported in the study of movement on curves that the width of the track portion increases. The localization of the track zones is an important consideration here. The position of the camera capturing pixels data focus around the mid-portion of track zones may not give correct results always. The other way out could be to study the improved localization of the tracks by employing a deep-learning model. Already attempts are there by various researchers like Stewart et al., 2020 to identify the road network using CNN. These techniques can improvise the localization aspects of these tracks. The focus here is to highlight the relative contrast of the track zones w.r.t. the surroundings by quantified comparison.

As per the surrounding terrain, the Measure that shows better contrast could vary. There are some other aspects too which need consideration. For instance, the area around the tracks nearer to the vehicle gets captured with better resolution and usually has more variance of pixel values. However, the distant features around the tracks appear smooth to the image captured by the camera. These points may reveal different results at different sections along the track in the same image. This process considers various image enhancement measures, computes the track index in each case, compares, and displays the image with maximum contrast. The technique given in this study considers the effect of generating maximum track contrast and is thus adaptive to the changes in the surrounding terrain.

Further, the index-based computation at different sections along the track

shall vary as the vehicle moves. With this, the contrast-based ordered set of images shall also alter. One can apply the probabilistic approach to get the most optimal contrast image set. This aspect, however, demands more computational power from the onboard system. Alternatively, the contrast measure based on a suitably selected section can help to achieve reasonably good image ordering. A better measure of track contrast could also emerge by considering such additional inputs. This aspect, however, needs further study.

The images convolved using high-pass filters and edge detection like the one by Narendra and Hareesha, 2011 help highlight the boundaries of track areas w.r.t. its surroundings. However, there could also be many high-frequency features in the area that can bar distinguishing exactly the track areas. The role of texture in getting increased track contrast w.r.t. its surrounding becomes noticeable both visually and quantitatively. The GLCM texture-based results presented here support the views of Alsmadi, 2020 that these measures enrich the content for image retrieval.

An onboard decision-making tool can usefully employ the process given in this study for increased track contrast in both manual and autonomous navigation modes. It may extend as a vital support for the rut following vehicles, particularly those which operate in the low contrast areas. This study can help many industries like defence, autonomous ground vehicles, robotic vehicles, night safari, etc.

7.10 Conclusion

The contrast enhancement study presented here leads to drawing the following key conclusions:

The role of texture assumes importance and can reveal valuable information as the resolution increases. When the features of interest are of smaller dimensions, the texture analysis may not add much value in delineating the features. One can achieve better contrast than the original Gray Image using one or the other texture images of Contrast, Dissimilarity, Correlation, etc.

The track index value for the original gray image increased from 7.83% to 29.06%. The comparative contrast of the Images also confirms this view. It is noticeable that for testing this approach, the areas chosen in off-track and On-track zones are of size 100x11 pixels. By taking larger areas, the conclusions can improve even further. In the current study, the texture analysis of the image employs a kernel of size 5x5, horizontal displacement of 1 pixel, and 32 quantization levels. Considering other options of these associated parameters can give further insight into the dependence upon these parameters.

1. The statistical measures of GLCM-based texture analysis form a strong base for understanding the influence of texture in contrast enhancement. The suitable texture measure for maximizing the contrast could vary with the surrounding. The proposed track index-based technique can quantitatively bring out the variation in track contrast levels w.r.t. its surroundings. The proposed approach that brings out the image with optimal track contrast can thus prove vital for the on-board decision-making.

7.11 Scope for Further Studies

The current study used a kernel of fixed size 5x5, horizontal displacement of 1 pixel, and 32 quantization levels for the texture analysis of the image. Considering other options of these associated parameters can give further insight into the dependence upon these parameters.

The area around the tracks nearer to the vehicle gets captured with better resolution, while the distant features appear smooth in the image captured by the camera. This aspect needs further study for better insight and an improved decision on-board vehicle. Moreover, the track index-based study presented here considered images in the optical range. However, the comparative analysis of varied input source data could reveal some interesting results.

The proposed technique may also find application in areas like the detection of wake created by ocean-going vehicles. A wake, that causes instability to the vehicles operating in its surrounding can last long and impact other distant vehicles even. Depending upon the vehicle configuration, its speed, etc., the extent and time of wake may vary. A study on the detection of wakes using suitable sensors and various image analysis techniques could give better insight. The proposed track index that comparatively selects the images also seems to have good potential in detecting the most optimal image highlighting the wake.

7.12 References

1. Pundir, S. K., & Garg, R. D. (2021). Development of an empirical relation to assess soil spatial variability for off-road trafficability using terrain similarity analysis & geospatial data. *Remote Sensing Letters*, 12(3), 259-268.
2. Ordonez, C., Chuy Jr, O. Y., Collins Jr, E. G., & Liu, X. (2011). Laser-based rut detection and following system for autonomous ground vehicles. *Journal of Field Robotics*, 28(2), 158-179.
3. Kalra, M. K., Shukla, S. K., & Trivedi, A. (2023). Track-Index-Guided Sustainable Off-Road Operations Using Visual Analytics, Image Intelligence and Optimal Delineation of Track Features. *Sustainability*, 15(10), 7914.
4. Liu, K., Ayers, P., Howard, H., & Anderson, A. (2009). Influence of turning

- radius on wheeled military vehicle induced rut formation. *Journal of Terramechanics*, 46(2), 49-55.
5. Vennik, K., Kukk, P., Krebstein, K., Reintam, E., & Keller, T. (2019). Measurements and simulations of rut depth due to single and multiple passes of a military vehicle on different soil types. *Soil and Tillage Research*, 186, 120-127.
 6. Army, U. S. (1993). FM 3-19 FMFM 11-20 NBC Reconnaissance. Available online: <https://www.hsdl.org/?view&did=1049> (accessed on 30 July 2022).
 7. Pierzchała, M., Talbot, B., & Astrup, R. (2016). Measuring wheel ruts with close-range photogrammetry. *Forestry: An International Journal of Forest Research*, 89(4), 383-391.
 8. Salmivaara, A., Miettinen, M., Finér, L., Launiainen, S., Korpunen, H., Tuominen, S., Heikkonen, J., Nevalainen, P., Sirén, M., Ala-Ilomäki, J., & Uusitalo, J. (2018). Wheel rut measurements by forest machine-mounted LiDAR sensors—accuracy and potential for operational applications?. *International Journal of Forest Engineering*, 29(1), 41-52.
 9. Gonzalez, R. C. (2009). *Digital image processing*. Pearson education india.
 10. Mohanaiah, P., Sathyanarayana, P., & GuruKumar, L. (2013). Image texture feature extraction using GLCM approach. *International journal of scientific and research publications*, 3(5), 1-5.
 11. Fauzi, A. A., Utaminingrum, F., & Ramdani, F. (2020). Road surface classification based on LBP and GLCM features using kNN classifier. *Bulletin of Electrical Engineering and Informatics*, 9(4), 1446-1453.
 12. Caraffi, C., Cattani, S., & Grisleri, P. (2007). Off-road path and obstacle detection using decision networks and stereo vision. *IEEE Transactions on Intelligent Transportation Systems*, 8(4), 607-618.
 13. Howard, A., & Seraji, H. (2001). Vision-based terrain characterization and traversability assessment. *journal of robotic systems*, 18(10), 577-587.
 14. Chowdhury, N. H., Khushib, D., & Rashide, M. M. (2017). Algorithm for line follower robots to follow critical paths with minimum number of sensors. *International Journal of Computer*, 24(1), 13-22.
 15. Janani, P., Premaladha, J., & Ravichandran, K. S. (2015). Image enhancement techniques: A study. *Indian Journal of Science and Technology*, 8(22), 1-12.
 16. Babu, P., Rajamani, V., & Balasubramanian, K. (2015). Multipeak mean based optimized histogram modification framework using swarm intelligence for image contrast enhancement. *Mathematical Problems in Engineering*, 2015(1), 265723.
 17. Marques, O. (2011). *Practical image and video processing using MATLAB*. John Wiley & Sons.
 18. Gupta, S., & Porwal, R. (2016). Combining laplacian and sobel gradient for greater sharpening. *IJIVP*, 6, 1239-1243.
 19. Shrivakshan, G. T., & Chandrasekar, C. (2012). A comparison of various edge detection techniques used in image processing. *International Journal of Computer*

Science Issues (IJCSI), 9(5), 269.

20. Narendra, V. G., & Hareesh, K. S. (2011). Study and comparison of various image edge detection techniques used in quality inspection and evaluation of agricultural and food products by computer vision. *International Journal of Agricultural and Biological Engineering*, 4(2), 83-90.
21. Bharati, M. H., Liu, J. J., & MacGregor, J. F. (2004). Image texture analysis: methods and comparisons. *Chemometrics and intelligent laboratory systems*, 72(1), 57-71.
22. Humeau-Heurtier, A. (2019). Texture feature extraction methods: A survey. *IEEE access*, 7, 8975-9000.
23. Graovac, S., & Goma, A. (2012). Detection of road image borders based on texture classification. *International Journal of Advanced Robotic Systems*, 9(6), 242.
24. Barbu, T. (2021). Mixed noise removal framework using a nonlinear fourth-order PDE-based model. *Applied Mathematics & Optimization*, 84(Suppl 2), 1865-1876.
25. Tavakkol, E., Dong, Y., & Hosseini, S. M. (2022). Image denoising via spatially adaptive directional total generalized variation. *Iranian Journal of Science and Technology, Transactions A: Science*, 46(4), 1283-1294.
26. Zhang, J., Li, G. L., & He, S. W. (2008, September). Texture-based image retrieval by edge detection matching GLCM. In *2008 10th IEEE International Conference on High Performance Computing and Communications* (pp. 782-786). IEEE.
27. Alsmadi, M. K. (2020). Content-based image retrieval using color, shape and texture descriptors and features. *Arabian Journal for Science and Engineering*, 45(4), 3317-3330.
28. Pradhan, B., Hagemann, U., Tehrany, M. S., & Prechtel, N. (2014). An easy to use ArcMap based texture analysis program for extraction of flooded areas from TerraSAR-X satellite image. *Computers & geosciences*, 63, 34-43.
29. Micheal, A. A., & Vani, K. (2015). Automatic mountain detection in lunar images using texture of DTM data. *Computers & Geosciences*, 82, 130-138.
30. Doycheva, K., Koch, C., & König, M. (2019). Implementing textural features on GPUs for improved real-time pavement distress detection. *Journal of Real-Time Image Processing*, 16, 1383-1394.
31. Sudha, S. K., & Aji, S. (2019). A review on recent advances in remote sensing image retrieval techniques. *Journal of the Indian Society of Remote Sensing*, 47(12), 2129-2139.
32. Liu, C., Xu, A., Hu, C., Zhang, F., Yan, F., & Cai, S. (2020, March). A New Texture Feature Based on GLCM and Its Application on Edge-detection. In *IOP Conference Series: Materials Science and Engineering* (Vol. 780, No. 3, p. 032042). IOP Publishing.

33. Winarno, E., Hadikurniawati, W., Wibisono, S., & Septiarini, A. (2021, September). Edge detection and grey level co-occurrence matrix (glcm) algorithms for fingerprint identification. In 2021 2nd International Conference on Innovative and Creative Information Technology (ICITech) (pp. 30-34). IEEE.
34. Singh, K. K., Singh, D. K., Thakur, N. K., Dewali, S. K., Negi, H. S., Snehmani, & Mishra, V. D. (2022). Detection and mapping of snow avalanche debris from Western Himalaya, India using remote sensing satellite images. *Geocarto International*, 37(9), 2561-2579.
35. Kar, C., & Banerjee, S. (2022). Tropical cyclones intensity estimation by feature fusion and random forest classifier using satellite images. *Journal of the Indian Society of Remote Sensing*, 50(4), 689-700.
36. Haralick, R. M., Shanmugam, K., & Dinstein, I. H. (1973). Textural features for image classification. *IEEE Transactions on systems, man, and cybernetics*, (6), 610-621.
37. Conners, R. W., & Harlow, C. A. (1980). A theoretical comparison of texture algorithms. *IEEE transactions on pattern analysis and machine intelligence*, (3), 204-222.
38. Clausi, D. A. (2002). An analysis of co-occurrence texture statistics as a function of grey level quantization. *Canadian Journal of remote sensing*, 28(1), 45-62.
39. Gadkari, D. (2004). Image quality analysis using GLCM. University of Central Florida, Orlando, FL, 2004. (MS thesis) <https://stars.library.ucf.edu/etd/187> [Accessed on 30 Jul 2022]
40. Stewart, C., Lazzarini, M., Luna, A., & Albani, S. (2020). Deep learning with open data for desert road mapping. *Remote Sensing*, 12(14), 2274.

CHAPTER - 8

CONCLUSION, FUTURE SCOPE AND SOCIAL IMPACT

The important conclusions drawn from this research work have been presented in this chapter. The future aspects of the current study and its social impact have also been presented in detail.

The research work as outlined in preceding chapters has led to useful conclusions. The summary of work undertaken in this research, the conclusions drawn, the future scope and its social impact are given in following sections:

8.1 Summary of Work

Today a number of industrial applications need information about the potential of any unpaved terrain to support movement of vehicles. Today, it is a subject matter of study for many researchers in agricultural field, forestry, automobile industry, robotics, planetary explorations and defence among others. The movement of vehicles on any terrain is governed by surface topographical features like slopes, ruggedness, unevenness, landuse etc. and the underlying soil condition. Acquiring the spatial and temporal variation of soil condition by conventional means is laborious and cumbersome task. The alternative means have therefore been explored by various researchers. One of the most effective ways employed for analysing the prevalent soil condition is by monitoring the rut formed by vehicular movement on different soils. Many soil parameters like soil condition, its gradation, moisture content, soil strength etc. impact the shape of rut. Vehicle loading conditions like tyre size, vehicle weight, its speed, curvatures, and repeated passes also influence their shapes. Although many parametric studies are conducted to characterize and model the rut shapes based on different influencing parameters yet several aspects are still to be studied.

One aspect of the issues pertains to modelling and evaluation of rut depth. Most of the literature focuses on evaluating the rut depth. Certain issues are however typical in different scenarios which need to be addressed. The rut in desertic terrain has been observed to get filled by the sand pouring from sides. Similarly, the rut profile has been observed to become eccentric on the curves. This aspect demanded for mapping the shapes of rut profiles in different terrain-vehicle running conditions, the same has been studied in this research work. The tools for measurement of rut shapes too have been advanced from manual rut profiler to the advanced photogrammetric, Ultrasonic and laser profiler. Each of these tools has its

own merits and the suitability depends upon the purpose of study. Advanced laser-based systems are commonly used for mapping the rut profiles. However, the data acquired by these systems needs heavy resources for its storage, retrieval and analysis. The attempts for optimal storage and efficient solutions are therefore the need of time and have been addressed in this study.

It is also observed that during the rainy seasons and floods, the low-lying pockets, agricultural fields etc. are prone to water logging. In such a scenario, the trafficability potential of these unpaved areas gets impacted as per the condition of the soil. The identification of safe and trafficable zones considering the maximum possible soil distress by vehicular movement is another study area for bringing simpler decisions about movement. This aspect has been considered for detailed investigation of soil distress conditions in the field under varied dynamic conditions.

Another aspect of rutting research pertains to addressing the issues in wider spatial domain. While evolving suitable spatial models governing trafficability potential is an important aspect, the validation of interpreted information is another important area needing attention. Here, identification of track impressions that look like edges in coarse resolution images can provide useful information about identifying the trafficable zones. Identifying the tracks manually being tedious, alternate means need to be explored. Moreover, the rut tracks formed by the leading vehicle is said to provide useful information for the rut following robotic vehicles, defence, and forestry. The delineation of track impressions from surrounding terrain and visibility conditions is an important consideration needing attention. These aspects have been addressed in this research work.

Another important aspect that needs study for many applications pertains to delineation of rut tracks from the images. In the rut-following robotic vehicles employed for operational needs, the vehicles are preferred to follow the beaten tracks of the leading vehicle. This is considered as safe and guiding for the vehicles following it. During the operations in defence too, the movement decisions also consider the track impressions of the leading vehicle for guidance. These track impressions passing through varied kinds of surroundings pose poor contrast for their identification using on-board cameras. The decisions based on images acquired using satellite or aerial platform too face the similar problem. The effective means are therefore needed for improving the contrast in varied surroundings.

In this research work, rut is investigated from different perspectives. One aspect focuses on the experimental studies of rut profiles in different fields while the other one tries to address the issue of delineation of rut tracks by collating various image processing techniques. In the field based experimental studies, various shapes of rut profiles on different types of soil and vehicle running conditions are investigated. The most common rut shapes observed in field are identified and grouped in different categories. Attempt is then made to devise better ways for

optimal storage of most common rut profiles. In another experimental study, soil distress caused by movement of multiple vehicles is investigated for identifying and mapping the unpaved areas suitable for planning emergency support. Another part of study focuses on visual enhancement and detection of rut-based track impressions. Here various edge detection algorithms and texture analysis techniques are employed for better delineation of rut tracks. The conclusions drawn from these studies are given here.

8.2 Conclusions Drawn from Rut Studies

The conclusions drawn from the study of rut are enumerated below:

1. Vehicle immobilization condition is reported to be there when the rut depth is larger than the vehicle clearance height. However, the shape of rut is not uniform in all cases. The rut profile in loose sandy dunal soils of deserts takes a conical shape as the sand from the edges pours in as the rut profile. When the vehicle turns on curves, the rut shape becomes asymmetric due to lateral loads. Therefore, computing the profile of rut shape is seen as better measure than the rut depth.

2. Various tools are evolved that can be used for mapping the rut profiles. Manual profilometer is used to collect data for limited point locations however, it is not suitable for continuous measurements to monitor changes in terrain properties. In such cases, advanced systems like photogrammetric, ultrasonic and laser based scanners etc. are used.

3. Advanced laser-based systems are commonly used for mapping the rut profiles. However, the point cloud data generated by these systems demands for much higher memory for its storage and further analysis. The study revealed that a lot of data storage can be avoided by defining the rut profile mathematically with high accuracy using optimal number of parameters for efficient vehicular mobility decisions.

4. Various mathematical formulations are analyzed, and non-linear regression analysis is attempted on the commonly observed rut shapes. The proposed modified bell-shaped function could fetch compression of over 80% on straight patches and 71% on turnings while the accuracy level is maintained better than 99% in both cases. This also indicates that the proposal mathematical models to represent the rut shapes are well suited. Although complex scenarios could be dealt with separately, an optimal representation of the most common rut shapes can aid significant data saving for development of an efficient decision support system.

5. The road communication network is the lifeline for any area. The

flooding like situation can arise in plains, the foothills or any place in mountains wherein the excessive rainfall can disrupt the conventional routes. In such situations, in order to access the areas for the essential services, the unpaved off-road routes are sometimes followed. The soil conditions of such unpaved areas are however not always convenient for movement of vehicles. Under such scenarios, the use of information about maximum soil distress level of the area can be used to predict the suitability of terrain for different emergency scenarios.

6. In the current research work, rut-based investigation is carried out for ascertaining the maximum soil distress after multiple passes of vehicles on same track under different moisture levels. The rut depth is seen to increase as the soil moisture increased and it reached maximum when flooded. However, if the flooding continues for days in the depressions or low-lying areas, it is indicative of impermeable and compact strata below certain level. The effect of moisture on maximum distress level remained similar.

7. The water logged condition continued for days in this area reflects a string and impermeable strata below top depth. The effect of tillage practices is there but upto limited depth.

8. The outcome of this rut study can be the basis for creating maps with maximum soil distress level for planning emergency movement in the given area. As the saturation level in the area is the major contributing factor, the pockets could be identified which have relatively higher elevation in the area. The tracks prone to less moisture passing through such areas may be pre-marked and if possible pre-compacted to allow safe movement in the area during emergencies. The maps indicating maximum soil distress level in any area could provide basis for sustainable development of any social setup.

9. There are many applications where rut marks on soil play an important role. The beaten tracks of leading vehicles, being safe and suitable for guiding, are followed at times by the rut following robotic vehicles and operations in defence. These days, visual-analytics-guided systems are increasingly being used in many such manned and autonomous ground vehicles.

10. In the images of terrain containing rut impressions of vehicles, the identification of rut and the track passing through varied kinds of surroundings is a big challenge. The changed illumination conditions, cluttered backgrounds, wetness and so forth bring about great challenges in the identification of tracks. In order to make these rut following operations sustainable, it is important to evolve measures that can highlight better the vehicle track impressions in a given situation. In this research work, various image processing techniques that could be suitably applied here are investigated.

11. The path formed by vehicle rut looks like an edge on coarse resolution images. Over a period of time, a number of edge detection algorithms are developed, each of which has its own advantage. It is reported that the problem of edge finding has no universally accepted technique and this is rather the motivation for the continued research to improve the methods of edge detection. Attempt is therefore made here to study the relevance of different edge detection algorithms for identification of the track impressions in the images.

12. The selection of suitable edge detection algorithm needs to be done carefully. In this research work, various edge detection algorithms like Sobel operator, Prewitt operator, Pobelts Edges, Zero-cross, Laplacian of Gaussian (*LoG*), Hardy cross and Canny methods are considered for comparative analysis. The comparison of various edge detection algorithms led to inference that the Canny Edge detection algorithm gives relatively better and acceptable results for linear track detection.

13. Another aspect that is important in the study of rut impressions in the images is the relative size of the rut. The rut impressions forming tracks and appearing like edges in the coarse-resolution images take the shape of elongated areas in fine-resolution images. The surrounding terrain features play a big role in highlighting track impressions. The conventional tone based image processing techniques can highlight these tracks to a limited extent. The role of texture becomes important here as it can distinguish the features by considering a group of pixels having distinguishing features.

14. There are various techniques of texture estimation; however, the GLCM-based approach that is seen to give very good results in a variety of applications is used in the study. Here, the relationship between different pixels of the image is characterized by using various statistical measures such as contrast, energy, entropy, homogeneity, etc. Depending upon the terrain surrounding these tracks, the suitable measure for enhancement of tracks also varies.

15. In this study, various image processing techniques that can also be employed to enhance the track contrast are also used for comparative analysis. Considering various measures possible for enhancement of track contrast, an attempt is made to quantify the effectiveness in a given surrounding. A track index (TI) based quantitative approach is proposed to compare the images obtained after different enhancement measures and sort them. A track-index-based technique is proposed to sort various images as per their effectiveness in increasing the track contrast. Different forms of track indices are proposed and compared. The proposed track index is seen as effective in sorting 88.8% of contrast images correctly. The proposed technique of creating and sorting images based on the contrast level is seen as a useful tool for improved fidelity in many difficult situations for making the off-road operations sustainable.

16. An adaptive technique is also evolved that can select the most effective rut enhancement measure in a given surrounding. In the given case, the track index value for the original gray image increased from 7.83% to 29.06%. The comparative contrast of the Images also confirms this view. It is noticeable that for testing this approach, the areas chosen in off-track and On-track zones are of size 100x11 pixels. By taking larger areas, the conclusions can improve even further. Further study is however needed to understand the influence of varying topography, the size of the kernel, quantization level etc. All these aspects could lead to further improvement in the proposed track index.

8.3 Future Research Trajectories

Based on the research work carried out in this rut study, the following future research trajectories are suggested:

1. In current studies, research focused on defining the most common rut shapes mathematically optimally for efficient vehicular mobility decisions. An interesting analysis in the future would be to explore complex cases too. For instance, one may encounter a class wherein two separate rut profiles are blended to create a single rut class or cross each other. Here some additional mathematical representations may make the profile representation more generic and can address some more rut classes. In future activities, one can also explore the machine learning approach to train the system to auto detect the rut field boundaries for further optimization of data. It can also make predictive analysis about various terrain properties and classes in different field running conditions.

2. The maps indicating maximum soil distress level in any area could provide basis for sustainable development of any social setup by the Policy makers. Among some other benefits, the cultivation needs can be linked with rut depth attained by movement of given vehicle in the area. Suitable machinery can be selected to avoid excessive rutting on soil to avoid damage to roots of saplings. Rut depth formed by movement of vehicles on subgrade soils under different dynamic conditions can also provide valuable inputs for pavement design in deciding surface course layers.

3. The studies are needed for further improvement of edges detection for delineation of tracks in the images. A number of possible alternates can be explored to improve the edge detection algorithm further. The dilated filters could be one such alternative and the combination of two filters like Smoothed Sobel and Laplacian could be another approach. Using higher degree of derivatives can also be employed usefully. One can consider combining the benefits of using Canny-edge algorithm with other methods like higher order derivatives or dilated filters etc. for improved accuracy of edge detection. The machine learning techniques could also be an

interesting aspect to explore it further.

4. The proposed track index based computation is seen as very effective in bringing out the highest contrast using different techniques of image processing and texture analysis. However, with the movement of vehicle, the terrain surrounding shall change, and with this, the contrast-based ordered set of images shall also alter. Here, in future studies, one can apply the probabilistic approach to get the most optimal contrast image set. This will however demand for more computational power from the onboard system and thus needs further study. The machine learning approach could also be usefully employed here.

5. An adaptive technique for optimal track contrast in a given surrounding is also evolved in this study. Further study is however needed to understand the influence of varying topography, the size of the kernel, quantization level etc. All these aspects could lead to further improvement in the proposed track index. However, the proposed new methodology of using track index for enhancing the track contrast optimally in a given surrounding could be vital for the on-board vehicular mobility systems.

The research on the above points will bring state of the art solutions for the rut based systems aimed to interpret the ground response to movement of vehicles on any unpaved terrain.

8.4 Social Impact and Contributions to Knowledge

The following paragraphs bring out the social impact of the current research work and the contribution to the existing knowledge in this field:

1. The analysis of trafficability potential of any unpaved area is a common requirement for varied fields. The vehicles in industries like forestry, agriculture, and in defence frequently use the unpaved terrain for movement. Further, in many operations like firefighting, emergency response during peak traffic, alternate unpaved tracks are followed. The rut profile is seen as better means to reflect better the impact of vehicle running conditions. The advanced laser based tools employed for mapping these profiles need huge storage for its point cloud data. The suggested mathematical models to optimise the storage of data for these profiles are to make the on-board mobility evaluation systems more efficient.

2. In the current research work, rut based investigation is carried out for ascertaining the maximum soil distress by multiple passes of vehicles on same track under different moisture levels. The outcome of this rut study can be the basis for creating maps with maximum soil distress level for planning emergency movement

in the given area. As the saturation level in the area is the major contributing factor, the pockets could be identified which have relatively higher elevation in the area. The tracks prone to less moisture passing through such areas may be pre-marked and if possible pre-compacted to allow safe movement in the area during emergencies. The maps indicating maximum soil distress level in any area could provide basis for sustainable development of any social setup. There are other societal benefits too of this study.

3. In the agriculture field, the rut study as presented here can provide many benefits. The agricultural industry needs the information about the prevalent state of compaction level, moisture level and tillage need. The information about rut depth can provide useful insight of the prevalent terrain condition. Rut is reflective of cultivation state and moisture levels in the field. The need for further irrigation may be directly correlated by observing the rut formed by vehicular movement.

4. Higher levels of rut depth by vehicular movement impacts the roots adversely. So the information about rut depth can be useful in restricting the movement to protect the roots. Excessive rut in any agricultural field impacts adversely the movement of farm machinery and payload levels of vehicles carrying agriculture produce/crop.

5. Higher levels of rut depth in any field indicate more the requirement of power for the forwarder vehicles. Studies have shown that rutted areas can experience significant yield reductions.

6. The cultivation needs can be linked with rut depth attained by movement of given vehicle in the area. Suitable machinery can be selected to avoid excessive rutting on soil to avoid damage to roots of saplings. Rut depth formed by movement of vehicles on subgrade soils under different dynamic conditions can also provide valuable inputs for pavement design in deciding surface course layers.

7. The edge detection study for delineation of track like features has many advantages. It helps in delineation of rut tracks formed on unpaved terrain by vehicular movement. These tracks provide wealth of information about terrain strength, ground distress level, and preferred routes for futuristic developments. The tracks identification from the images acquired by satellite and aerial platform can also be useful for surveillance purpose by extracting information about any movements in the area.

8. The proposed visual analytics and track-index-based approach leading to improved inference of track features could augment the decision-making process for improved autonomous decisions in low-contrast areas. The study can assist in making intelligent decisions leading to the tracks following off-road operations

sustainable by improving decisions in low-contrast areas. This meets the requirements of both manual and autonomous navigation.

9. To select the most optimal contrast enhancement measure in a given scenario, authors proposed a quantified measure of track index. An onboard decision-making tool can usefully employ the proposed track-based approach for increased track contrast in both manual and autonomous operations. This study can help many industries like defence, autonomous ground vehicles, robotic vehicles, night safari, etc. where the track impressions of previous vehicles extend a vital support, particularly in the low contrast areas.

The benefits of the presented research work on rut study both at experimental and image processing level as above bring out the utility of the presented research work. On one hand the outcome paves way for making on-board mobility decisions more efficient while on the other hand, it sets the base for better fidelity by improved delineation of rut tracks. The soil distress level mapping is also seen as important from sustainable developments in any area.

DELHI TECHNOLOGICAL UNIVERSITY
(Formerly Delhi College of Engineering)
Shahbad Daulatpur, Main Bawana Road, Delhi-42

PLAGIARISM VERIFICATION

Title of the Thesis: Investigation of Rut Patterns in Different Terrain Conditions for Vehicular Movements **Total Pages** 135# **Name of Scholar:** Manoj Kumar Kalra

Supervisor (s)

1. Prof A. Trivedi, DTU, Delhi and
2. Dr S. K. Shukla, ECU, Australia

Department of Civil Engineering

This is to report that the above thesis was scanned for similarity detection. Process and outcome is given below:

Software used: Turnitin **Similarity Index:** 10%* **Total word Count:** 39,568

Excluding Plagiarism verification report, and brief profile

* As per Turnitin report

Date: 9 June 2025

Candidate's Signature

(Manoj Kumar Kalra)

Signature of Supervisor(s)

(Dr S. K. Shukla)


ECU, Australia

(Prof A. Trivedi)

DTU, Delhi

MK Kalra

Thesis_MKKalra_2K16PHDCE01_10 Jun 2025_CInd.doc

 Delhi Technological University

Document Details

Submission ID
trn:oid::27535:100049238

Submission Date
Jun 9, 2025, 9:54 PM GMT+5:30

Download Date
Jun 9, 2025, 10:19 PM GMT+5:30

File Name
Thesis_MKKalra_2K16PHDCE01_10 Jun 2025_CInd.doc

File Size
11.2 MB

135 Pages

39,568 Words

218,533 Characters



Page 2 of 149 - Integrity Overview

Submission ID trn:oid::27535:100049238

10% Overall Similarity

The combined total of all matches, including overlapping sources, for each database.





Filtered from the Report

- ▶ Bibliography
- ▶ Cited Text
- ▶ Small Matches (less than 8 words)
- ▶ Submitted works




Exclusions

- ▶ 7 Excluded Sources
- ▶ 2 Excluded Matches

Match Groups

-  **284** Not Cited or Quoted 10%
Matches with neither in-text citation nor quotation marks
-  **0** Missing Quotations 0%
Matches that are still very similar to source material
-  **1** Missing Citation 0%
Matches that have quotation marks, but no in-text citation
-  **0** Cited and Quoted 0%
Matches with in-text citation present, but no quotation marks

Top Sources

- 9%  Internet sources
- 7%  Publications
- 0%  Submitted works (Student Papers)

Integrity Flags

2 Integrity Flags for Review

-  **Replaced Characters**
59 suspect characters on 27 pages
Letters are swapped with similar characters from another alphabet.
-  **Hidden Text**
569 suspect characters on 1 page
Text is altered to blend into the white background of the document.

Our system's algorithms look deeply at a document for any inconsistencies that would set it apart from a normal submission. If we notice something strange, we flag it for you to review.

A Flag is not necessarily an indicator of a problem. However, we'd recommend you focus your attention there for further review.

BRIEF PROFILE

Shri Manoj Kumar Kalra is with Civil engineering background from Thapar University, Patiala. He has been serving DRDO for over 30 years and he has addressed a number of technical requirements related to the defence forces.

He has experience in the fields of risk assessment and control of various hazards. He has expertise in the fields of terramechanics, geoinformatics and image processing. He has worked on various applications for the armed forces that involved different technical domains. His interest areas include bringing an integrated solution to various operational issues by interfacing the domain science, instrumentation and image analysis.

He has contributed several research papers in the international journals of repute, conferences and technical reports. He has brought out some novel systems that led to development of products, creation of IPRs and patents for DRDO.

The current research work is focused on movement of vehicles on unpaved terrain by characterizing the rut impressions formed by the vehicles. This work has applications in variety of fields including agriculture, robotics, forestry, defence and automotive industry. The outcome shall pave the way for making an efficient system for the off-road movement.



DELHI TECHNOLOGICAL UNIVERSITY

(Formerly Delhi College of Engineering)
Shahbad Daultapur, Main Bawana Road, Delhi-42

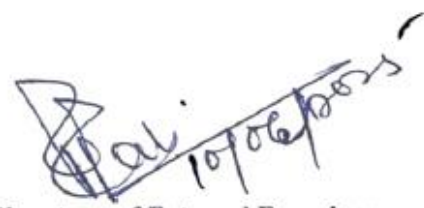
CANDIDATE'S DECLARATION

I **Manoj Kumar Kalra** hereby certify that the work which is being presented in the thesis entitled "**Investigation of Rut Patterns in Different Terrain Conditions for Vehicular Movements**" in partial fulfillment of the requirements for the award of the Degree of Doctor of Philosophy, submitted in the Department of **Civil Engineering**, Delhi Technological University is an authentic record of my own work carried out initially during the period from **12/08/2016** to **10/6/2025** under the supervision of **Prof. A. Trivedi, DTU Delhi and Dr. Sanjay Kumar Shukla, ECU Australia**.

The matter presented in the thesis has not been submitted by me for the award of any other degree of this or any other Institute.


Candidate's Signature

This is to certify that the student has incorporated all the corrections suggested by the examiners in the thesis, and the statement made by the candidate is correct to the best of our knowledge.


Signature of Supervisor
Signature of External Examiner